

Detection of Monoamine Mediated Immune Cell Communication by Nanosensors

Dissertation

for the award of the degree

“Doctor rerum naturalium”

of the Georg-August-Universität Göttingen

within the doctoral program

“IMPRS Physics of Biological and Complex Systems”

of the Göttingen Graduate Center for Neurosciences, Biophysics and

Molecular Biosciences (GGNB)

Submitted by

Meshkat Dinarvand

from Manchester, United Kingdom

Göttingen 2021

Thesis Committee

Prof. Dr. Sebastian Kruss

Physical Chemistry II, Ruhr-University Bochum

Prof. Dr. Jörg Enderlein

Third Institute of Physics, Biophysics, University of Göttingen,

Prof. Dr. Nils Brose

Department of Molecular Neurobiology, Max Planck Institute of Experimental Medicine

Members of the Examination Board

Referee: Prof. Dr. Sebastian Kruss

Physical Chemistry II, Bochum University

2nd Referee: Prof. Dr. Jörg Enderlein

Third Institute of Physics, Biophysics, University of Göttingen,

Further members of the Examination Board

Prof. Dr. Tiago F. Outeiro

Department of Experimental Neurodegeneration, Center for Biostructural Imaging of Neurodegeneration, University Medical Center Göttingen

Prof. Dr. Timo Betz

Third Institute of Physics, Biophysics, University of Göttingen,

Prof. Dr. Silvio O. Rizzoli

Department of Neuro- and Sensory Physiology, University Medical Center Göttingen

Date of the oral examination: 15.11.2021

Affidavit

I hereby declare that the doctoral thesis “*Detection of Monoamine Mediated Immune Cell Communication by Nanosensors*” is written independently without any unauthorized support, all sources and aids are quoted.

Göttingen, 2021

Table of Contents

Table of Contents	I
Abstract	IV
Motivation and Outline	1
Chapter Summary	2
Chapter 1. Scientific Background	2
Chapter 2. Results	2
Section 2.1, Detection of Serotonin Exocytosis from Platelets:	3
Section 2.2, Detection of Dopamine Exocytosis from Neutrophils:	3
Chapter 3. Discussion.....	4
1 Scientific Background	5
1.1 The Immune System.....	5
1.1.1 The Adaptive Immune Response.....	5
1.1.2 The Innate Immune Response	6
1.2 Neutrophils	7
1.2.1 Neutrophil Degranulation	9
1.2.2 Neutrophil Phagocytosis.....	11
1.2.3 NETosis	12
1.3 Platelets	13
1.4 Platelet and Neutrophil Interaction	16
1.5 Neurotransmitters in The Immune System.....	17
1.5.1 Autocrine/Paracrine Regulatory Role of Platelet Serotonin.....	17
1.5.2 Autocrine/Paracrine Regulatory Role of Neutrophil Dopamine	20
1.6 Detection of Monoamine Mediated Immune Cell Communication.....	23
1.6.1 Manuscript	26
2 Results	43
2.1 Detection of Serotonin Exocytosis from Platelets.....	43
2.1.1 Manuscript	43
2.1.2 Supplementary Material	52
2.2 Detection of Dopamine Exocytosis from Neutrophils	67

2.2.1 Manuscript	67
2.2.2 Supplementary Material	94
3 Discussion	108
3.1 Nanosensor Design.....	108
3.2 Detection of Serotonin Exocytosis from Platelets.....	111
3.2 Detection of Dopamine Exocytosis from Neutrophils	114
Conclusion	119
References	120
Acknowledgement	133

Table of figures

Figure 1	Main host defense mechanisms of neutrophils.....	9
Figure 2	Platelet undergoes morphological changes upon activation	14
Figure 3	Neutrophil-platelet interaction	17
Figure 4	Serotonin modulates the function of various immune cells	19
Figure 5	The dopaminergic system in neutrophils.....	22
Figure 6	The structure of single-walled carbon nanotubes.....	25
Figure 7	NIRDA detection strategy.....	117

Abstract

The immune system comprises many organs, organ systems, cell types and secretory components that together form an intricate host defense network encompassing physical, biological and chemical barriers. Secretory components of the immune system play an important role in modulating the immune response. In this dissertation, I focus on monoamine mediators, predominantly involved in the nervous and endocrine systems, as modulators of the immune system. Immune cells do not function independently and homogeneously; their activity is modulated by their microenvironment which is controlled by the composition of the inflammatory mediators. Therefore, immune cells tune their activity according to their spatial condition. The complexity and flexibility of the immune response compels researchers to investigate dynamics of exocytosis from immune cells with novel detection systems. Conventional analytical tools often lack spatial resolution to detect release events from cells simultaneously and identify localized regions where exocytosis occurs. In this dissertation, a novel fluorescent nanosensor based on single-walled carbon nanotubes (SWCNTs) is designed to detect release of monoamines from neutrophils and platelets with high spatiotemporal resolution in the near infrared (980 nm) region. This study provides new information regarding monoamine exocytosis from immune cells. Initially, a near infrared SWCNT sensor was designed to detect exocytosis of serotonin from human platelets. The selectivity, specificity and reversibility of the sensor was demonstrated. The nanosensor had a K_d value of $301 \text{ nM} \pm 138 \text{ nM}$. Then, a paracrine immune modulation involving platelet-derived serotonin and dopamine exocytosis from neutrophils was discovered. We observe that the entire dopaminergic machinery (tyrosine hydroxylase, dopamine transporter, dopamine receptors, vesicular monoamine transporter) is expressed and functionally active in neutrophils. Exocytosis was investigated with fluorescent false neurotransmitters. Serotonin induced dopamine exocytosis following Ca^{2+} mobilization in neutrophils. Dopamine exocytosis was detected with our nanosensors and we showed that upon neutrophil-platelet interaction, stimulated platelets induced dopamine release from neutrophils. Finally, the immunomodulatory role of dopamine was studied and we discovered dopamine suppressed NETosis, an important host defense strategy of neutrophils, in a receptor-mediated and concentration dependent manner. In summary, the development of novel fluorescent probes/sensors for neurotransmitters enabled imaging with unprecedented spatiotemporal resolution and identification of a new role of neurotransmitters in the immune system.

Motivation and Outline

Complex biological functions such as the way cells propagate signal to each other and communicate, are governed by multiple factors. Therefore, studying such communications requires investigative methods that can record cellular behavior within a cell's specific spatial and temporal context. Monoamines mediate cellular communication in the nervous system (known as neurotransmitters) and the endocrine system (known as hormones). There is increasing evidence that monoamines also play an important role in cell-cell communication in the immune system. Some immune cells have been known to create "immune synapses". In this dissertation, I aimed to apply a novel fluorescent nanosensor to study monoamine exocytosis in human neutrophils and platelets. We also discovered a new link that mediates platelet-neutrophil interaction. In the first part of the dissertation, a fluorescent nanosensor with high spatio-temporal resolution is designed to visualize exocytosis of serotonin from human platelets. We uncovered new information about serotonin exocytosis from platelets due to sub-cellular spatial resolution of our novel nanosensor (named NIRSer). In the second part of the thesis, I focus on the dopaminergic signaling in human neutrophils. First, with conventional analytical tools, we establish that human neutrophils are capable of synthesis, storage and release of dopamine. These data confirmed and expanded previous studies. Then, for the first time, I report that serotonin is a stimulator of dopamine exocytosis in neutrophils. This finding was confirmed by investigating the molecular signaling pathway. We designed a nanosensor platform (named NIRDA) based on near infrared single-walled carbon nanotubes to detect exocytosis with a microscopic setup. Platelet-derived serotonin mediated dopamine release from neutrophils which was visualized by our nanosensor platform providing the first visualization of dopamine exocytosis in neutrophils upon interaction with platelets. Finally, we report that dopamine acts as an autocrine/paracrine modulator of neutrophil behavior by reducing the rate of neutrophil extracellular trap formation (NETosis). We believe this nanosensor platform is a powerful tool in biological studies as it can be tailored to detect different biogenic molecules *in situ* with high spatiotemporal resolution. The synthesis of the nanosensors did not require complicated chemical reactions and a relatively simple fluorescent microscopic setup was used for imaging of the nanosensors.

Chapter Summary

This dissertation covers the following main topics; **a**, High spatio-temporal detection of monoamine exocytosis from neutrophils and platelets with a novel nanosensor. **b**, Studying dopaminergic machinery in neutrophils and the immunomodulatory role of dopamine on neutrophils. **c**, A new cell communication pathway between platelets and neutrophils in which platelet-derived serotonin induces exocytosis of dopamine from neutrophils.

Chapter 1. Scientific Background

In the first chapter, I start with the scientific background on the function of immune cells in the immune system.

Section 1.1 includes a general overview of the immune system. Sections 1.2 and 1.3, cover the role of neutrophils and platelets in immunity. This dissertation investigates a new platelet-neutrophil communication involving monoamine mediators. Subsequently, Section 1.4, outlines the present knowledge on platelet-neutrophil interactions within an immune response. Section 1.5, outlines the role of monoamine mediators (serotonin and dopamine) in immune modulation. Monoamines are better known in the context of the nervous and endocrine systems. But our knowledge on their role in the immune system is increasing. I will cover the effect of serotonin and dopamine as immune mediators since detection of these two molecules is the subject of this dissertation. In section 1.6, I outline the importance of designing novel detection methods that allow for studying immune cell exocytosis within their spatial context, as cellular behavior is tuned by the microenvironment of the immune cells. In section 1.6.1, I include a mini-review (own contribution) that covers novel sensors for detection of dynamic monoamine exocytosis with a special focus on carbon-nanotube based nanosensor.

Chapter 2. Results

In chapter 2, I present the results of my dissertation. which includes one published manuscript and one unpublished manuscript.

Section 2.1, Detection of Serotonin Exocytosis from Platelets:

Section 2.1., is a published research article (own contribution) on detection of serotonin exocytosis from human platelets by fluorescent nanosensors based on single-walled carbon nanotubes (SWCNT) functionalized with serotonin specific aptamers. We named the nanosensor NIRSer. Section 2.1.1 includes the main manuscript and section 2.1.2, includes the supplementary material (includes experimental methods and additional results). This manuscript covers the design and synthesis of NIRSer. NIRSer characterization is carried out to study the selectivity and sensitivity of the nanosensor for serotonin. We show that NIRSer's response to serotonin is reversible which makes it a suitable detector as opposed to a serotonin label. The dose-response curve of NIRSer is plotted to measure the dissociation constant of the sensor. Finally, we immobilize NIRSers on glass surfaces and seed human platelets on top to record release events from platelets. Comparing the fluorescent signal of serotonin-depleted platelets with control platelets indicated that NIRSers could successfully record localized release of serotonin from platelets.

Section 2.2, Detection of Dopamine Exocytosis from Neutrophils:

Section 2.2, is an unpublished research article (own contribution) on discovering dopaminergic machinery in human neutrophils induced by platelet-derived serotonin. In section 2.2.1, I include the main manuscript and in section 2.2.2, I include the supplementary material (experimental methods and additional results). We employed SWCNTs functionalized with (GT)10 ssDNA molecules as nanosensors which had been previously shown to detect dopamine. The nanosensor was named NIRDA. First, we studied the dopaminergic system in neutrophils and confirmed the findings of previous studies on this topic. However, exocytosis of dopamine from neutrophils hasn't been explored previously. Therefore, we studied the kinetics of exocytosis with fluorescent dopamine analogs (FFNs). We discovered serotonin induced exocytosis of dopamine from neutrophils. Then, we employed our nanosensors to visualize the release of dopamine. We discovered Ca^{2+} mobilization is an important step in dopamine exocytosis in neutrophils. We were able to image intracellular Ca^{2+} increase and dopamine exocytosis simultaneously. Then we visualized dopamine exocytosis events with serotonin receptor

agonists and antagonists and discovered that exocytosis is receptor-mediated. We also compared the fluorescent signal of NIRDA in response to neutrophils depleted from dopamine and control groups and confirmed that the fluorescence response is indeed from dopamine and not interfering molecules or mechanical forces applied to NIRDA surface. Then, platelet-neutrophil interactions were studied by seeding both platelets and neutrophils on NIRDA surfaces and stimulating platelets to release serotonin. We observed the stimulation of platelets caused dopamine exocytosis by neutrophils which was recorded by the NIRDA sensors. Finally, we studied the role of dopamine as an autocrine/paracrine immunomodulator in neutrophils. We discovered that D2-like receptors were expressed in neutrophils and dopamine reduced the rate of NETosis in neutrophils.

Chapter 3. Discussion

In chapter 3., I discuss the results of my PhD projects. Chapter 3 is divided in 3 sections. In section 3.1, I discuss the design of the nanosensors. The advantage of designing SWCNT based nanosensors for detecting cellular communication is discussed and compared to conventional analytical methods. In section 3.2., I discuss the results of the first project which was designing NIRSer nanosensors for detection of serotonin release from human platelets. In section 3.3., I discuss the results of the second project which was exocytosis of dopamine from neutrophils induced by serotonin.

1 Scientific Background

1.1 The Immune System

The immune system in mammals comprises a collective of cells, their secretory components, organs and organ systems (lymphatic system, the spleen, the thymus, and the bone marrow) that protect an organism against harm. All the immune cells originate from the same progenitor stem cell that is hematopoietic stem cells in the fetal liver and adult bone marrow.¹ In a simplistic model, when certain cell types (epithelial/endothelial cells, mast cells, macrophages, neutrophils and platelets) encounter a harmful foreign (pathogen) or endogenous (tissue injury) substance, they produce signals which activate, recruit and program themselves and other cells of the immune system to the site of action. A second level of protection is activated when antigen presenting cells (APCs) provide lymphocytes with necessary information to attack specific targets.² This cooperation between immune cells requires regulated flow of information in an intricate communication network by the immune system. cells in this complex network constantly communicate and interact with each other to recognize and produce a response against any threat to the body. Based on the type of response, immunity is broadly classified to two groups of innate and acquired (or adaptive) immune response. It is important to point out that the two immune responses are not distinctively separated by the cells involved or by the chronology of the events, rather elements of each group, regulate the action of the other and they cooperate to effectuate an immune response.

1.1.1 The Adaptive Immune Response

As the name implies, the adaptive immune response is acquired over time and improves through repeated exposure to the same entity. This line of defense includes the B cells and T cells. These cells initiate a response by binding to antigens and proliferating to antigen specific T cells or B cells.²

Presentation of endogenous antigens with major histocompatibility complex (MHC) class I, by normal cells activates CD8⁺ cytotoxic T cells.³

1 Scientific Background

Presentation of exogenous antigens by professional antigen presenting cells with MHC class II activates naïve CD4⁺ T helper cell (Th cell).⁴

B cells are antibody producing immune cells. B cells also present antigens to T cells. T cells produce cytokines that in turn induce B cell maturation to antibody secreting B cells and later development of memory B cells.⁵ Antibodies enhance innate immunity by opsonizing antigens and facilitating phagocytosis, attracting killer cells to produce Antibody-dependent cellular cytotoxicity and activating the complement system.⁶

The nature of the interactions between immune cells which leads to differentiation to antigen specific cells and subsequently an efficient immune response is highly complex and influenced by the microenvironment and the specific balance between various secretory components of the immune system.

1.1.2 The Innate Immune Response

The innate immune response is an evolutionary conserved host defense system which shares elements with the simplest animals and even plants.⁷ It encompasses physical and physiological barriers. Here, we only cover cells and secretory components of the immune system that produce a rapid response against pathogens. Innate immunity is typically characterized by a lack of specificity and memory. However, it is critical to host defense because of its broad and rapid response.⁸ The cells involved in this type of immunity include; phagocytic cells like macrophages, monocytes and neutrophils, secretory cells like basophils, eosinophils and mast cells, and natural killer cells.⁹ This grouping is not mutually exclusive since the cells in each group are classified by their most distinctive feature. For example, phagocytes also secrete cytokines.¹⁰ Eosinophils typically secrete leukotrienes, prostaglandins and cytokines but they are also phagocytic.¹¹ Basophils and mast cells are mainly involved in allergic reactions.^{12,13} Professional phagocytes recognize non-host cells through surface receptors, internalize them and either directly kill them or present antigens to T cells to cooperate with adaptive immunity.¹⁴

The secretory components play an important role in regulating the innate immune response by mediating interaction between the immune cells. These molecules are called inflammatory mediators and include complements (most complements are secreted from

1 Scientific Background

hepatocytes), cytokines, acute phase proteins and eicosanoids.^{15,16} Complements bind to pathogens and aid phagocytosis. They can stimulate mast cells to release inflammatory mediators like histamine and serotonin. And act as chemoattractant for neutrophils. Certain complements independently kill organisms by binding to their surface and permeating their membrane.¹⁷

The role of platelet and neutrophils in the immune system will be discussed further in the next sections

1.2 Neutrophils

Neutrophils are the most abundant white blood cells (~70% of all leukocytes) and therefore, the main driver of innate immunity. Approximately 1 to 2×10^{11} neutrophils are generated daily.¹⁸ Neutrophils were originally perceived to be homogenous terminally differentiated cell population¹⁹ which after extravasation to tissue are cleared by macrophages within a few hours of generation (half-life of 18.5 hours²⁰).²¹ At first glance, it's easy to dismiss neutrophils as non-specific propagators of inflammation and tissue damage with basic abilities such as crawling, phagocytosis, degranulation and production of oxygen reactive species (ROS) or proteases. However, the behavior of neutrophils is more nuanced and specific than originally perceived. Neutrophils can be primed to distinct subpopulations with different surface markers and activities.²² The microenvironment of neutrophils greatly influence generation of neutrophils with specific phenotypes.²³

Classical neutrophil behavior following an acute inflammatory response includes three main activities; phagocytosis, degranulation, and formation of neutrophil extracellular traps (NETs) which is termed NETosis (Figure 1).²⁴

After pathogen invasion, damaged host cells (e.g. endothelial cells) release signals to alert innate immune cells. In addition, patrolling cells of the innate immunity have pattern recognition receptors (PRR) which bind to pathogen-associate molecular patterns (PAMP) or damaged-associated molecular patterns (DAMP). Tissue resident immune cells (mainly macrophages) release inflammatory cytokines and chemoattractants that produce the first

1 Scientific Background

signs of inflammation²⁵ and trigger activation and recruitment of mast cells, macrophages, platelets and neutrophils.

Initially, contraction of the smooth muscle and increased permeability of the vasculature occurs. Adhesion molecules (E-selectin, P-selectin) on the endothelium are upregulated. Binding of selectins to their ligands on neutrophils (PSGL-1) and neutrophil L-selectin to its ligand on the endothelium induces rolling of neutrophils on the endothelium. In the next step, β 2-integrins are activated which promote firm adhesion, arrest of neutrophils and extravasation. Neutrophils are then guided to the site of infection by chemokines where they eliminate the source of infection by phagocytosis.²⁶

Beyond broad microbicidal effect, neutrophils are implicated in cancer and autoimmune diseases.²⁷ They also modulate the immune response of other immune cells. This is because a single neutrophil produces less cytokine than a single macrophage or lymphocyte^{28,29}, but neutrophils are more abundant than all other immune cells. As a result, neutrophil cytokines are important drivers of the immune response.³⁰ For instance, chemoattractants secreted from neutrophils recruit monocytes and DCs.^{31,32} Neutrophil cytokines promote macrophage reprogramming to pro- or anti- inflammatory state.^{33,34} Secretory components from neutrophils contribute to B cell proliferation, maturation and antibody production.³⁵ Interferon- γ from neutrophils contribute to T cell differentiation.^{36,37} Through feedback loops, neutrophils suppress their own aggregation and activation and even induce their own cell death.³⁸

1 Scientific Background

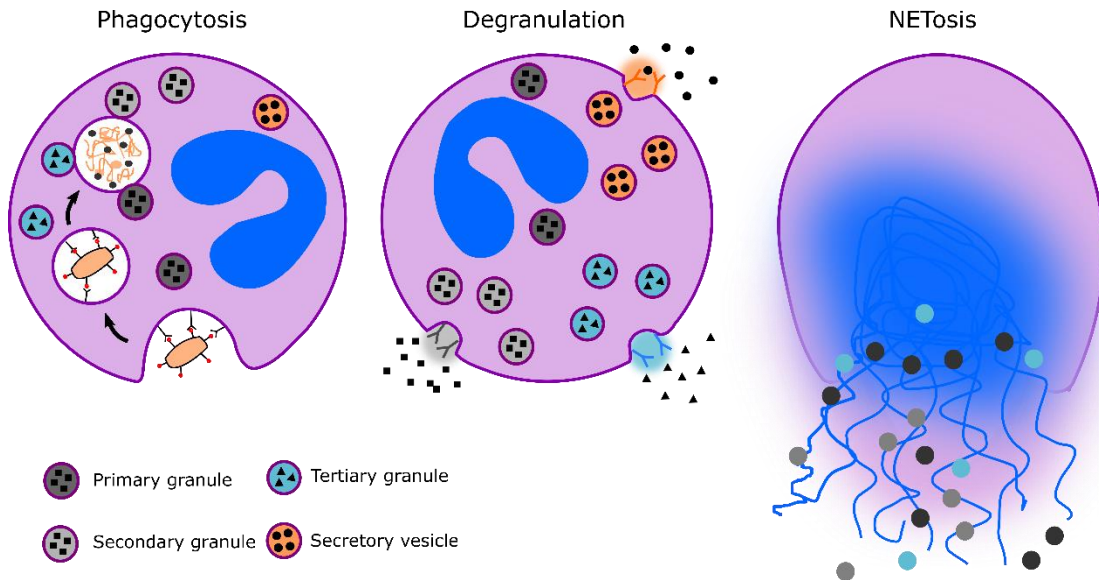


Figure 1. Main host defense mechanisms of neutrophils; Phagocytosis of mainly tertiary, secondary and primary granules, in that order. Degranulation of mainly secretory vesicles, tertiary and secondary granules, in that order. NET formation which is characterized by expulsion of chromatin, histones and antibacterial peptides from neutrophils.

1.2.1 Neutrophil Degranulation

An important host defense strategy of neutrophils is degranulation which involves receptor-mediated fusion of neutrophil granules with plasma membrane and releasing their content in the extracellular space or phagosomes to neutralize and digest pathogens. Neutrophil granules are a reservoir of antimicrobial proteins, proteases, components to produce reactive oxygen species (ROS), extracellular matrix proteins, adhesion receptors and cytokines. As the content of the granules are highly damaging to the host tissue, neutrophil degranulation is tightly regulated.³⁹

Neutrophils contain at least four distinct types of granules which are formed sequentially during myeloid cell differentiation. Each granule type contains cell components produced at that specific differentiation stage. Primary (also called azurophilic) granules store elastase, myeloperoxidase (MPO), cathepsin and defensin. As MPO production stops at early stages of differentiation, all other granules are MPO negative. Secondary (also called specific) granules store lactoferrin and lower content of gelatinase. Tertiary granules store high content of matrix metalloprotease 9 (gelatinase B). Secretory vesicles contain plasma

1 Scientific Background

proteins such as serum albumin, suggesting their origin as endocytosed vesicles from the plasma membrane containing extracellular components.⁴⁰

Degranulation can be divided to extracellular release and phagosomal release.⁴¹ Extracellular release is favored by Secretory vesicles followed by tertiary granules, secondary granules, and primary granules.⁴² Inflammatory mediators such as N-Formylmethionyl-leucyl-phenylalanine (fMLP) result in secretory exocytosis, almost exclusively;⁴³ however, powerful stimulators such as Phorbol myristate acetate (PMA) lead to high level exocytosis of tertiary granules, moderate secondary, and low level of primary granules.^{44,45} The signaling pathway that leads to specific granule exocytosis is not completely understood. But we know that Ca^{2+} mobilization plays an important role in all types of granule trafficking and exocytosis.³⁹ It is suggested that gradual increase in intracellular Ca^{2+} dictates hierarchical release of granules from secretory to primary granules.⁴² G protein-coupled receptor (GPCR) ligation in neutrophils causes signal propagation by phosphorylation of a range of proteins and ultimately Ca^{2+} mobilization. Granules are guided toward the plasma membrane by microtubules after cytoskeleton remodeling. Then, the granule/vesicle is tethered to the membrane leading to granule fusion. Reversible pores are created enabling release of the granular content.⁴⁰

Increase in intracellular Ca^{2+} as a prominent signaling molecule, induces exocytosis of many granules. Different signaling pathways might induce distinct granule exocytosis. For instance, phospholipase D (PLD) signaling has been involved in degranulation of primary and secondary granules.⁴⁶

β -arrestins are another class of proteins involved in exocytosis of primary and secondary granules.⁴⁷ GTPases are involved in granule exocytosis. A family of GTPases called Rho GTPase is involved in remodeling of the actin cytoskeleton required for several neutrophil functions such as cell motility (chemotaxis), phagocytosis, and exocytosis. Rac2 Rho GTPase is selectively involved in primary granule release.⁴⁸

Granule/vesicle fusion to plasma membrane is controlled by SNAP receptor (SNARE) proteins, soluble N-ethylmaleimide sensitive factor (NSF) and the soluble NSF-attaching proteins (SNAPs).⁴⁹ The mechanisms of vesicle docking and fusion are extensively studied in neurons. The components of the fusion complex include SNAREs on vesicle membrane

1 Scientific Background

(v-SNAREs) that engage with SNAREs on target membrane (t-SNAREs) facilitated by NSF, SNAP, Ca^{2+} and calcium-binding proteins. In exocytosis of neurotransmitters, syntaxin 1 and SNAP-25 on cell membrane and synaptobrevin 1 (also known as VAMP-1) on vesicle membrane form the SNARE complex. Neutrophils express various SNARE isoforms. For instance, syntaxins 1A, 3, 4, 5, 6, 7, 9, 11, and 16 have been observed in human neutrophils.⁵⁰ SNAP-23 and syntaxin 6 was associated with secondary granule exocytosis.⁵¹ VAMP-2 was associated with secretory vesicles, secondary and tertiary.⁵² VAMP-7 was highly expressed in all types of neutrophil granules.⁵³

In section 2.2, we investigate secretion of dopamine from neutrophils induced by serotonin and the role of intracellular Ca^{2+} .

1.2.2 Neutrophil Phagocytosis

Phagocytosis is a host defense mechanism in which neutrophils recognize particles through a receptor-mediated process, engulf them by their plasma membrane and take them up into early phagosomes. Then, granules fuse with phagosomes and release their content including the nicotinamide adenine dinucleotide phosphate (NADPH) oxidase complex Nox2 which generates superoxide anions to neutralize and digest particle with the help of other microbicide components of granules.⁵⁴

Neutrophils can phagocytose both opsonized and non-opsonized particles. Neutrophils have Fc receptors that bind to immunoglobulin and β 2-integrins that bind to complement-coated particles.⁵⁵ The main Fc receptors in human neutrophils are Fc γ receptors such as Fc γ RIIA (CD32) and Fc γ RIIIb (CD16) in resting, and Fc γ RI (CD64) in interferon primed neutrophils.⁵⁶

After engagement of an Fc γ receptor with its ligand, a phosphorylation cascade occurs which activates phosphatidylinositol 3-kinase (PI3K), that converts phosphatidylinositol 4,5-bisphosphate (PI4,5P2) to mainly phosphatidylinositol 3,4,5-trisphosphate (PI3,4,5P3) and also diacylglycerol (DAG) by phospholipase C (PLC).⁵⁷ These downstream effector proteins induce actin polymerization and membrane remodeling required for phagocytosis.

1 Scientific Background

Rac1 is required for actin assembly in immunoglobulin mediated phagocytosis while Rho for complement mediated phagocytosis.^{58,59} PI3,4,5P3 also stimulates myosin X, Rho GTPases are involved in delivery of endomembranes to the site of phagocytosis.⁶⁰ As a result, a phagosome cup is formed around the particle. In the next step, after the phagosome is sealed, the phagosome undergoes maturation by acquiring microbicidal enzymes, vacuolar (V) ATPases and the NADPH oxidase complex.

Phagocytosis trafficking in neutrophils is not similar to endocytosis where vesicles are trafficked through early/late endosomes to end up in lysosomes. Instead of the traditional lysosome, secretory vesicles and granules take part in phagocytosis. Localized fusion and secretion of granules to phagosomes and generalized degranulation and secretion of neutrophils follow the same pattern as discussed in neutrophil degranulation section. Ca^{2+} mobilization plays an important role in both granule fusion and extracellular secretion. Another class of important molecules are PKC isoforms which translocate to the membrane upon phagocytosis.⁶¹ Src-family kinases are also involved in degranulation to phagosomes. For instance, Hck protein kinases seem to be localized to azurophilic granules.⁶²

Although Ca^{2+} and protein kinases play critical role in both degranulation and phagocytosis, their specific target are less known. As a result, it is less known how neutrophils discriminate between different granule types during degranulation.

SNARE family proteins are involved in granule fusion with phagosome. Even less is known about the specific SNAREs involved in phagocytosis compared to general degranulation. Many isoforms of SNARE proteins have been identified in neutrophils; however, whether these isoforms can afford specificity in the type of granule fusion is not completely understood. A family of Rab GTPases are highly involved in membrane fusion and phagosome maturation and directional movement of phagosomes along microtubules. The activity of Rab GTPase mainly results in generation of phosphatidylinositol3-phosphate (PI3P).⁵⁵

1.2.3 NETosis

The third line of defense by neutrophils is formation of web-like structures composed of decondensed chromatin, histones and numerous proteins. This process is called NETosis.

1 Scientific Background

Since NETosis results in cell death, it is not known whether NETosis is simply a consequence of pathogen attack that leads to cell death like other cell death processes such as apoptosis, necrosis, phagocytosis-induced cell death or an active host defense strategy by neutrophils. NETs, “web structures”, predominantly capture pathogens and prevent spreading of the infection.⁶³ They also contain microbicide proteins to neutralize pathogens. NET is formed through distinct stages of chromatin decondensation, nuclear swelling, nucleoplasm spreading into the cytoplasm, and finally membrane perforation.⁶⁴ NET-induced neutrophil suicide was first observed by PMA stimulation and was considered to be NADPH oxidase–dependent. However, later studies showed that pathogen induced NETosis *in vivo* does not necessarily lead to cell death and the term vital NETosis was coined, further explaining that rather than suicidal cell death, NETosis might be an active host defense strategy.⁶⁵

NETosis is highly regulated and dysregulation of NETosis has been implicated in several autoimmune diseases and vasculitis.⁶⁶

In chapter 2.2, we investigate the role of dopamine in modulating NETosis in neutrophils.

1.3 Platelets

Platelets, also called thrombocytes, are anucleated fragments of megakaryocytes of the bone marrow released in the circulation system. Platelets play an important role in hemostasis, wound healing and thrombosis (pathological clotting).⁶⁷ They are also part of the innate immune response. The impact of platelets in immunity is sometimes understated. There is an evolutionary link between hemostasis and immune response.^{68,69} And platelets sit at the interface of these two important phenomena.^{70,71} This is possibly because clot formation (a result of hemostasis) is also an important host defense strategy by sequestering the infectious agent and preventing it from spreading to other regions of the body.

In this section, the classical role of platelets in hemostasis is briefly discussed. Then, we will focus on platelet’s role in immunity. As discussed earlier, similar to other leucocytes, the specific response of platelet in different situations is dependent on the spatial context

1 Scientific Background

of the cells. This includes the endothelium cells, other leukocytes at the site and the secretory components (cytokines, chemokines and eicosanoids).

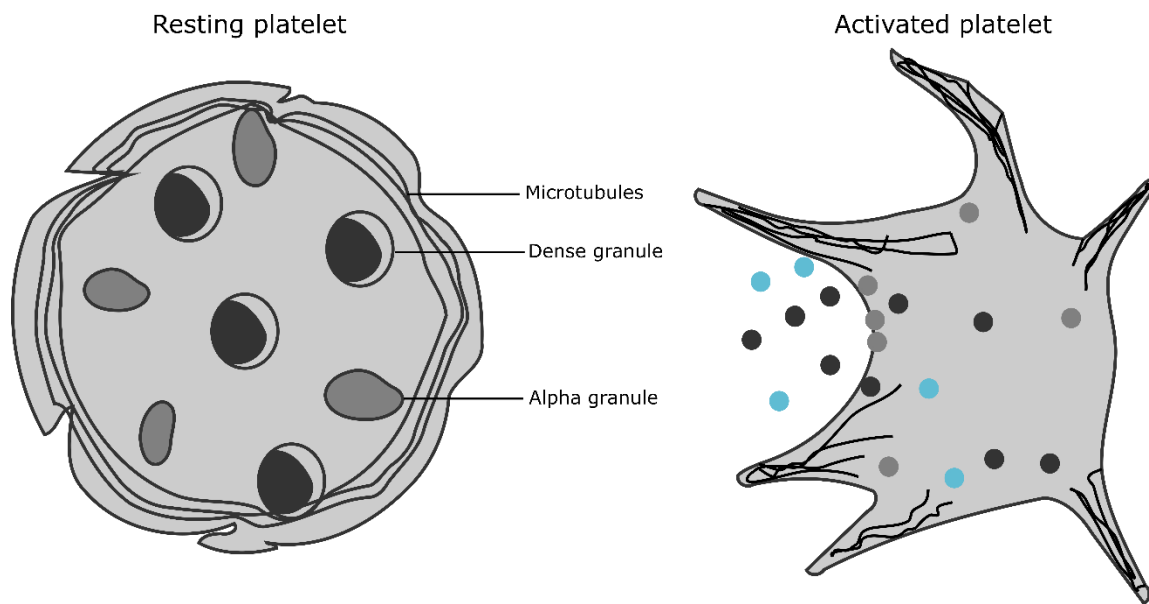


Figure 2. Platelet undergoes morphological changes upon activation. Microtubules dictate the morphological change from discoid to star-shape upon platelet activation.

The classical role of platelets in hemostasis consists of a few distinct steps starting from activation of circulating platelets through receptor-mediated signaling. Platelets have many unique receptors and also receptors shared by other blood cells. The receptors include the following:

Integrins, leucine-rich repeated receptors (glycoprotein GPIb/V/IX and Toll-like receptors), G-protein coupled proteins (protease activates receptors (PAR-1, PAR-4 thrombin receptors), P₂Y₁, P₂Y₁₂ ADP receptors, TP α and TP β thromboxane A₂ receptors), receptors for immunoglobulins (GPVI, Fc γ RIIA), C-type lectin receptors (P-selectin) tyrosine kinase receptors (thrombopoietin receptor, Gas-6, ephrins and Eph kinases) and other receptors (CD63, CD36, P-selectin ligand 1, TNF receptor type).⁷²

Platelets also contain glycogen granules, dense granules and α -granules.⁷³ α -granules contain proteins important in hemostasis,⁷⁴ such as; vWF, fibrinogen, P-selectin, PECAM-1, CD40 ligand, platelet factor-4, β -thromboglobulin, thrombospondin, platelet-derived growth factor, FV and $\alpha_{IIb}\beta_3$. Dense granule store nucleotides (ADP, ATP), proinflammatory mediators (serotonin, histamine), pyrophosphate and calcium.⁷⁵

1 Scientific Background

Vascular damage triggers; a) platelet activation and adhesion on the surface of endothelium b) activatory components secreted from the site of platelet arrest triggers further platelet activation and recruitment to the damaged site c) a platelet aggregate is formed which aids wound healing and prevents blood loss.⁷⁶

Similar to neutrophil rolling on activated endothelium, platelets also engage with activated endothelium via binding of GPIb-IX-V to VWF and P-selectin to PSGL-1. Next, integrins such as $\alpha v \beta 3$ mediate firm adhesion.⁷⁷ As soon as a layer of activated platelets adhere on the surface of damaged endothelium, degranulation occurs. Activated platelets release many secreting molecules that have activatory effects on platelets, other blood cells and the endothelium. They also modulate the function of blood components.⁷⁸

Resting platelets are discoid shaped in the circulating system. As soon as they are activated through receptor-mediated signaling, (mainly activation of $\alpha_{IIb} \beta_3$ integrin) the platelets undergo significant morphological change and formation of pseudopodia (Figure 2). Platelet agonists that are produced by platelets and other leukocytes contribute to release of intracellular Ca^{2+} , protein phosphorylation, degranulation, shape change and adhesion of platelets.⁷⁹

Beyond the classical role, platelets have immune receptors, allowing them to interact with molecular components of the immune system as well as other immune cells. Platelets recruit immune cells by secreting mediators of inflammation, and by acting as an adhesion site for leucocytes. They can directly interact with other leucocytes by forming receptor ligand bonds. Platelets have several Toll-like receptors. Through TLR 2/6 and 1/2 signaling, platelets become activated and increase expression of P-selectin, and induce degranulation and aggregation. TLR4 signaling also induces platelet aggregation and interaction with other leukocytes.⁸⁰ Platelets also secrete antimicrobial peptides. As a result, they play an important role in the innate immune response, especially through their interaction with neutrophils.

In the next section, I will discuss the interactions between neutrophils and platelets and their impact on immune response. In section 2.1, the release of serotonin from platelets is investigated with NIRSer nanosensors.

1.4 Platelet and Neutrophil Interaction

Platelets and neutrophils interact with each other through receptor-ligand engagement and release of mediators (Figure 3). Activated platelets bind to neutrophils through P-selectin (on platelets) and P-selectin glycoprotein ligand-1 (PSGL-1 on neutrophils).⁸¹ Platelets release hundreds of secreting molecules when activated. Platelet-derived serotonin promotes platelet dependent neutrophil recruitment.⁷⁸ Platelets also promote extravasation of neutrophils to tissue in response to infection.⁸² As discussed earlier, there is a link between the innate immune response propagated by neutrophils and hemostatic activity of platelets. This link is especially highlighted in sepsis induced coagulation. In this bi-directional link, Platelets can directly stimulate NET formation by binding to neutrophils and creating an anchor for neutrophil sequestration. Platelet agonists such as thrombin, ADP, collagen and arachidonic acid all induce platelet dependent NETosis. NET formation also activates platelets and induces coagulation and thrombosis.⁸³ Platelet-dependent NETosis isn't always mediated through direct receptor-ligand signaling (mainly through P-selectin and PSGL-1). It had been observed that thromboxane A2 (TXA2) released from activated platelets also mediated NETosis. On the other hand, NET components such as elastases and cathepsin G, activate platelets through PAR-1 and PAR-2 signaling. Histones released during NETosis can also directly activate platelets. Platelets then, bind to NETs and promote additional platelet aggregates on the NET scaffold.⁸⁴ Histone H4 which is released during NETosis is a thrombin activator by stimulating release of PolpyP from platelets which in turn activates thrombin.⁸⁵ NETs also promote formation of thrombin dependent on engagement of TLR2 and TLR4 receptors. This vicious cycle induced by the tight coordination of platelets and neutrophils originally evolved to fight infection by mediating coagulation at the site of infection and preventing dissemination of infection. However, it is responsible for sepsis induced disseminated vascular coagulation in extreme pathological events.

In section 1.5, I will explain further the role of neurotransmitters in immune cell communication and autocrine/paracrine modulation of activity.

In section 2.2, platelet0neutrophil interaction in the context of dopamine exocytosis is explored.

1 Scientific Background

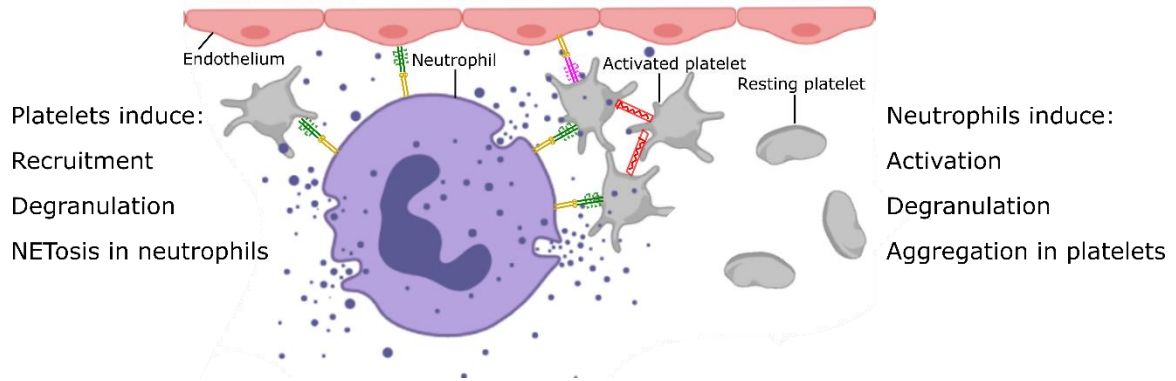


Figure 3. Neutrophil-platelet interaction. The link between neutrophils and platelets is bidirectional as platelets activate and recruit neutrophils while, neutrophils also activate platelets. These cell communication with each other by secreting inflammatory mediators and receptor-ligand binding. Figure created with BioRender.com

1.5 Neurotransmitters in The Immune System

1.5.1 Autocrine/Paracrine Regulatory Role of Platelet Serotonin

Serotonin (5-hydroxytryptamine, 5-HT) is a messenger molecule that is mostly associated with the nervous system as an important monoamine neurotransmitter that in the central nervous system (CNS) is produced by the Raphe nucleus in the brainstem.⁸⁶ Serotonin modulates various CNS functions such as; appetite, mood, anxiety and sleep.⁸⁷ However, other cell types also produce serotonin. Nearly 90% of all the serotonin in the body is produced by the enterochromaffin cells (EC) in the gastrointestinal (GI) tract.⁸⁸ Serotonin released from ECs acts on the neurons of the enteric nervous system and affects motility of the GI tract by modulating constriction of the smooth muscle and secretion of secretory glands. Afterwards serotonin is taken up by platelets. Since significant amount of serotonin circulates the body through platelets, it stands to reason to assume serotonin plays an important role in all platelet functions from its role in hemostasis to immune response.

5HT is synthesized from the essential amino acid, tryptophan, by the enzyme Tph1 in the EC cells⁸⁹ and Tph2 in the CNS neurons.⁹⁰ Platelets uptake serotonin through serotonin transporters (SERT). Inside the cytosol, 5HT is stored in specialized vesicles by the action of vesicular monoamine transporters (VMAT-2 in neurons and platelets⁹¹ and VMAT-1 in endocrines⁹²). When 5HT is secreted, it binds to 5HT receptor family which contains seven

1 Scientific Background

distinct subclasses (5-HT₁, 5-HT₂, 5-HT₃, 5-HT₄, 5-HT₅, 5-HT₆, and 5-HT₇). All these receptors are GPCR receptors except for 5-HT₃ which is a ligand-gated ion channel.⁹³ 5HT receptors are expressed on immune cells⁹⁴, the vascular smooth muscle⁹⁵ and endothelium.⁹⁶ This shows the broad effect of platelet-derived serotonin on hemostasis and immunity. The first group of platelets upon activation, release serotonin from dense granules. Serotonin activates other circulating platelets through 5-HT_{2A} signaling. Agonistic binding to this receptor leads to activation of phospholipase C (PLC), an important signal transduction pathway. PLC cleaves phosphatidylinositol 4,5-bisphosphate (PIP₂) in to diacylglycerol (DAG) and inositol 1,4,5-triphosphate (IP₃). These important secondary messengers induce increase of intracellular Ca²⁺ which mediates a cascade of cellular activities including motility, shape change, degranulation, adhesion and aggregation of platelets.⁹⁷

Serotonin as a platelet activator, plays a central role in promoting hemostasis and thrombosis. However, many cell types have receptors for serotonin which shows serotonin plays other roles beyond hemostasis. Platelet-derived serotonin promotes cellular growth and proliferation and have a role in cancer propagation⁹⁸ which is outside the scope of this study. They also promote growth in smooth muscles and endothelium.⁹⁹ Serotonin is a powerful vasoconstrictor.¹⁰⁰ Serotonin under pathological conditions increase permeation and leakiness of vasculature, promoting inflammation and vascular damage.¹⁰¹ In the same vein, a link between fibrosis and serotonin has been observed.¹⁰² Platelet-derived serotonin modulates the function of both innate and adaptive immune response (Figure 4). 5HT mediates differentiation of DC cells. Activates naïve T cells and promotes growth of T cells and induces cytokine production in those cells. It also promotes growth and activation in B cells and NK cells. 5HT promotes recruitment, migration and cytokine production in immune cells. In previous sections, I discussed how platelets recruit neutrophils to the site of inflammation, induce rolling, adhesion and extravasation of neutrophils. Among other mediators, serotonin also plays a role by activating the surface of endothelium and bringing P-selectins to the surface.⁹⁷ To investigate whether non-neuronal serotonin (mainly platelet-derived) directly promotes leukocyte adhesion and recruitment and neutrophil extravasation, Tph-1 deficient mice were employed. In knockout mice, 50% less leukocyte rolling was observed. Moreover, less selectin engagement was observed. As a result, there

1 Scientific Background

were less firm leukocyte adhesion events. Neutrophil extravasation in tissue was also diminished.⁷⁸

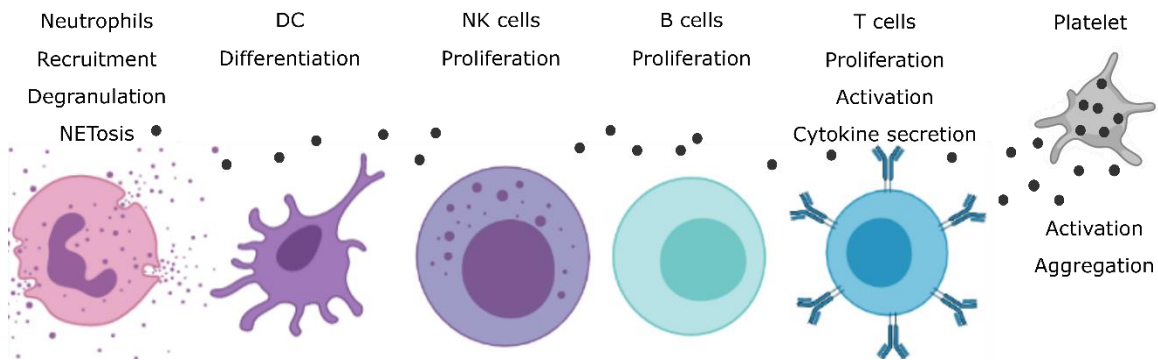


Figure 4. Serotonin modulates the function of various immune cells. Figure was created with BioRender.com

In another study¹⁰³, the role of platelet serotonin on propagation of reperfusion damage and prognosis of myocardial infarction (MI) was studied. Excessive recruitment of leucocytes especially neutrophils to the site of myocardial damage is one of the harmful events during reperfusion after myocardial infarction. As discussed earlier, platelet serotonin recruited neutrophils to the site of inflammation. In this study, it was further observed that serotonin also induced neutrophil degranulation, promoted increased surface expression of CD11b which mediated neutrophil adhesion to platelets or endothelium and induced release of MPO and oxygen reactive species, all exacerbating tissue damage. Long-term administration of selective serotonin reuptake inhibitors, SSRIs, in animal models reduced risk of myocardial ischemia/reperfusion injury (which is related to platelet depletion of serotonin).¹⁰³ Interestingly, previous clinical studies also supported this hypothesis. In one study, it was observed that SSRI antidepressant use correlated with reduced MI and that the protection against MI was directly related to the affinity of the SSRI for serotonin transporter.¹⁰⁴

As discussed, platelet serotonin plays an important role in regulating the immune response especially the function of neutrophils. In section 2.1, I will demonstrate my work on designing a nanosensor based on fluorescent single-walled carbon nanotubes (SWCNTs) to detect release of serotonin from platelets with high spatio-temporal resolution. With this novel tool, we were able to highlight new information about the kinetics of release from platelets, the hotspots of release as well as the intercellular variations for the first time.

1 Scientific Background

1.5.2 Autocrine/Paracrine Regulatory Role of Neutrophil Dopamine

Dopamine is mainly synthesized by dopaminergic neurons. Resident or transmigrated immune cells can “meet” dopamine in the CNS, lymphoid organs which are heavily innervated, and in the circulation where low concentrations of dopamine exist.¹⁰⁵ All immune cells express various dopamine receptors (DR).¹⁰⁶ DRs are G protein coupled receptors. Five subtypes (D1, D2, D3, D4, and D5) of dopamine receptors have been identified. These receptors are classified in two groups based on their signaling pathway. D1 and D5 are called D1-like family and D2, D3 and D4 are called D₂-like receptors.¹⁰⁷ As immune cells are regularly exposed to dopamine and they express DRs, the effects of dopamine on the function of immune cells have been investigated.^{108–112} The immunoregulatory role of dopamine on immune cells is highly dynamic. The type of response that dopamine exerts, is dependent on many factors such as the concentration of dopamine, the type and pattern of DR expression, the type of immune cell, and the activation state of the immune cell. Because the role of dopamine is context dependent, studying its effects is challenging. Most studies to this date have investigated the dopaminergic system in T cells. Stimulation of cytokine secretion, adhesion, migration were observed in T cells as a result of dopamine receptor mediated interaction.¹¹³ Dopamine stimulated naïve T cells but suppressed activated T cells.¹¹⁴ Dopamine suppressed proliferation and cytokine secretion in activated T cells.^{115–122} Dopamine induced migration in naïve CD8⁺ cells via D3 receptors.¹²³ And activated resting Teff cell via D2 and D3 and suppresses Tregs via D1.¹²⁴ In resting T cells, dopamine could selectively induce secretion of TNF α via D3 or IL-10 via D2 or both via D1-like receptors.¹²⁵ At low concentrations (0.1-5 μ M), dopamine via D1-like receptors, reduced intracellular ROS production and apoptosis in lymphocytes but at high concentrations (100-500 μ M) it had the reverse effect.¹²⁶

There are less studies on the immunomodulatory role of dopamine in other immune cells. For instance, dopamine suppressed secretion of INF- γ , TNF- α and IL-1 β in NK cells and TNF- α in neutrophils and monocytes and increased secretion of IL-10 in neutrophils, monocytes, B cells, macrophages (peritoneal M ϕ s) and marrow-derived DCs. Dopamine also increased secretion of CXCL1 in NK cells and peritoneal M ϕ s. The response to

1 Scientific Background

dopamine was observed to be dopamine receptor mediated by testing several dopamine receptor agonists and antagonists. In addition to regulating cytokine production, dopamine also affected (mainly inhibitory) adhesion and chemotaxis of immune cells.¹¹²

In neutrophils, dopamine attenuated proinflammatory activation, adhesion on endothelium and migration in response to chemoattractants.¹²⁷

Agonist binding to D1-like receptors activates adenylate cyclase enzyme to increase intracellular levels of cAMP. cAMP (a secondary messenger) mediates a broad range of cellular functions, mainly but not exclusively, by activating protein kinase A (PKA). One of the many downstream proteins affected in this signaling pathway is NFκB protein complex. NFκB is a rapid-acting transcription factor that regulates important cellular responses related to a broad range of (mainly extracellular) stimuli. This cellular response includes cytokine production, transcription and cell survival. In B cells, activation of PKA through cAMP, suppressed NFκB activation.¹²⁸ Therefore we can assume that dopamine through activation of D₁-like receptors increases the intracellular cAMP and activates PKA leading to inaction of NFκB. This could explain the attenuating effect of dopamine on secretion of proinflammatory cytokines.¹²⁹ In the immune cells, in addition to DRs, many receptors signal to NFκB activity; such as T-cell receptors (TCRs), B-cell receptors (BCRs), TNFR, CD40, BAFFR, LTβR, and the Toll/IL-1R family.¹³⁰

Immune cells in addition to expressing DRs, are capable of endogenous catecholamine synthesis.^{122,124,131–136} As such, these cells, upon activation, release dopamine which then as an autocrine/paracrine modulator, can regulate the function of immune cells.¹³⁷ Again, most studies to this date, focus on the autocrine/paracrine role of the dopaminergic system in lymphocytes, mainly T cells. for instance, a subset of follicular helper T cells (T_{FH} cell) synthesized significant amounts of dopamine and stored them in dense-core granules containing chromogranin B. when T_{FH} cells interacted with their cognate B cells, dopamine was released and caused upregulation and rapid translocation of ICOSL to the surface of B cells. The increased ICOSL in turn increased surface presentation of CD40l on T cells, improving T cell B cell interaction. Mathematical models showed that dopamine-mediated rapid translocation of ICOSL, increased B cell output from germinal centers.¹³⁸

1 Scientific Background

Human DC cells stored dopamine in their secretory vesicles. Antigen specific interaction with naïve CD4+ T cells stimulated dopamine release from DC cells. In turn, dopamine induced T-cell differentiation to Th2 subtype. inhibition of dopamine release shifted T-cell differentiation to Th1 subtype.¹³⁹

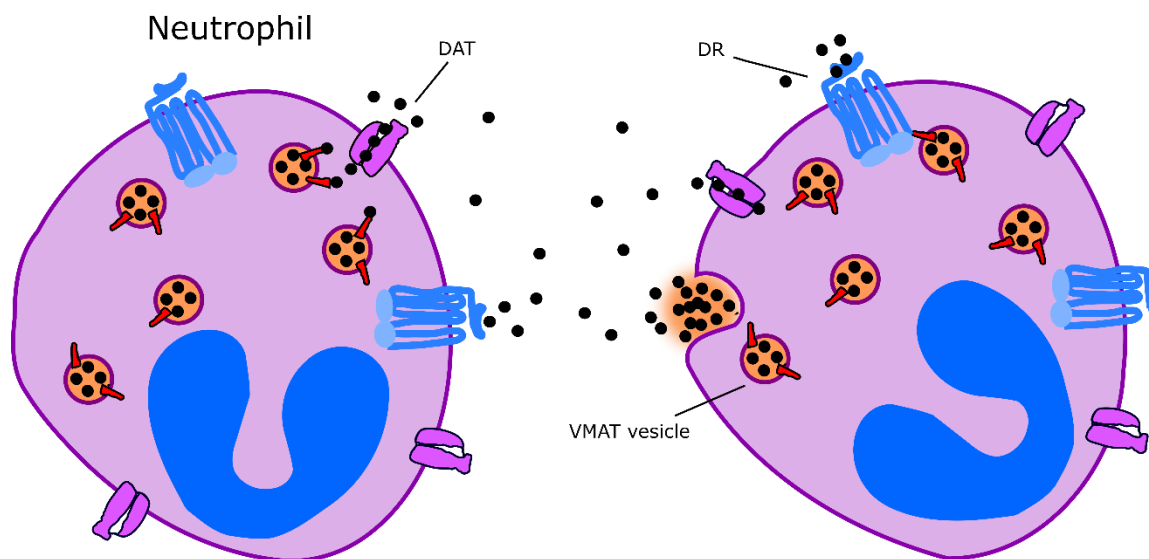


Figure 5. The dopaminergic system in neutrophils; an autocrine/paracrine immunomodulator.

There is limited information about dopaminergic machinery in neutrophils (Figure 5). In one of the first studies on this subject *Cosentino et al.*¹⁴⁰, detected catecholamines (norepinephrine (NE), epinephrine (E), dopamine (DA)) and their metabolites in neutrophils by HPLC with an electrochemical detector. Alpha-methyl-p-tyrosine (a TH inhibitor) reduced DA and NE, pargyline (MAO inhibitor) reduced DA metabolites, reserpine (VMAT inhibitor) reduced DA and NE and desipramine (NE reuptake inhibitor) reduced NE content. These observations showed that neutrophils expressed the enzymes to produce, store and metabolize these molecules. More recently, studies have emerged that further prove the existence and functional role of dopaminergic machinery in neutrophils and its implication for the immune response. When phagocytes (neutrophils and macrophages) were exposed to lipopolysaccharides (LPS), they released catecholamines (E and NE). It was also observed that LPS stimulation increased the expression of enzymes involved in catecholamine biosynthesis (TH and dopamine β -hydroxylase). The implications of catecholamine release from phagocytes in acute lung

1 Scientific Background

injury in animal models was studied. An inhibition of catecholamine production in phagocytes reduced inflammation. This effect is contradictory to other studies that claimed dopamine attenuated proinflammatory response in neutrophils.¹⁴¹ However, their study was limited to investigating the effect of phagocyte derived catecholamines on inflammation in general and they did not study the specific effect of catecholamines as modulatory molecules on the phagocytes function or other immune cells. In another study, the effect of phagocyte-derived catecholamines on macrophages were investigated.¹⁴² To distinguish between phagocyte-derived catecholamines and catecholamines released from the adrenal glands they tested adrenalectomized animal models. And reported a link between enhanced inflammation in acute lung injury and the level of catecholamines released from phagocytes. Interestingly, they observed a compensatory increase in expression of TH and DBH in adrenalectomized rats. In this study, catecholamines (E and NE) activated NF κ B action in macrophages. This protein complex regulates important cellular responses related to stimuli. They reported an increase in proinflammatory cytokines as result of NF κ B activation. Note that this conclusion is in contradiction with other studies that claimed dopamine at least through D1 receptors predominantly inactivates NF κ B action and thus suppresses proinflammatory response.¹²⁹ This shows that the effect of dopamine in immune cells is highly dynamic and non-monolithic. The net result of activation of several dopamine receptors types and the spatial context of the cells highly influence how the cells response to dopamine.

1.6 Detection of Monoamine Mediated Immune Cell Communication

As discussed in previous sections, the immune response is mediated by very specific and intricate interactions between various immune cell types and the chemical balance between their secretory components in the immediate microenvironment of the cells. The cells don't function in isolation and the type of response is controlled by the spatial context of the cells. Therefore, it is important to study cellular behavior of the immune cells with high spatio-temporal resolution. So far, most studies about monoamines can be classified in two general groups. First, the effect of monoamines on the function of immune cells. In these types of studies, normally a monoamine is added to a specific cell type *in vitro* and its effect on cytokine production, chemotaxis or other cellular functions is studied. In these

1 Scientific Background

types of studies, the limitation is that the spatial context of the monoamine is eliminated. A purified cell suspension is exposed to a static concentration of a monoamine which does not mimic a physiological situation. Normally these monoamines, as I discussed earlier are transiently released upon receptor-mediated signaling events in small localized regions at the site of interaction between cells (immune synapse). Second type of studies involve studying the monoamine machinery by the expression level of proteins and enzymes involved in receptor signaling, storage, uptake, metabolism and release of monoamines. these types of studies often focus less on the functionality of the proteins.

A detection method should be sensitive, not only to temporal changes but also to spatial changes at a subcellular level. In this chapter, a mini-review article is included that will first discuss our current understanding of monoamine detection, the conventional methods of detection and current research highlights in the field. Note that most of the methods discussed are extensively employed in neuroscience rather than immunology since monoamines are an important class of neurotransmitters with huge implication for the function of the nervous system. Then, the limitations of the conventional methods and the advantages of using single-walled carbon nanotubes (SWCNTs) as nanosensors for live detection of monoamines in discuss. Currently there is a huge interest in designing sensors with the ability to study these intricate cellular communications *in situ*. SWCNTs have interesting and unique properties that can be manipulated to design such sensors. I will focus on SWCNTs as an interesting sensor strategy in the next session.

SWCNTs can be pictured as single layers of rolled up graphene sheets.¹⁴³ As shown in Figure 1A., the perimeter of the tube and the angle of rolling creates distinct lattice structures that are characterized by chiral indices. Each SWCNT chiral species exhibits unique optical properties and have unique fluorescence emission peaks. All semiconducting SWCNTs fluoresce in the near infrared (nIR) region (>850 nm) which is beneficial for biomedical imaging as this range fall within the biological transparency window (Figure 6C). As organic fluorophores, SWCNTs are superior to most fluorophores because of minimal photobleaching or blinking.¹⁴⁴ Furthermore, SWCNTs can be easily functionalized with biological macromolecules such as oligonucleotides to manipulate their fluorescence properties (Figure 6B).

1 Scientific Background

In the following manuscript (section 1.6.1) the properties of SWCNTs as nanosensors for monoamines detection is discussed extensively.

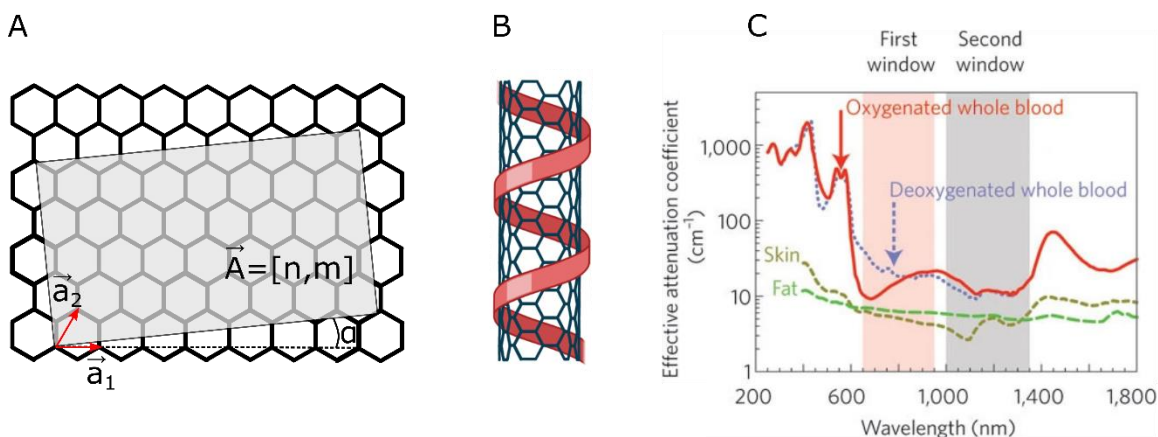


Figure 6. The structure of single-walled carbon nanotubes. A. The lattice structure of a SWCNT, the chirality of the SWCNT is determined by the perimeter of the tube and the angle of rolling. B. A SWCNT functionalized with a ssDNA strand. C. The biological transparency window, the maximum absorbance of (6,5) SWCNTs at $\sim 950\text{-}1000\text{ nm}$ falls in the biological transparency window which is characterized by low absorbance of water and tissue. (C) was Reprinted by permission from Springer Nature Customer Service Centre GmbH: Springer Nature, Nature Nanotechnology (Bioimaging: second window for in vivo imaging, Andrew M. Smith et. al)¹⁴⁵, COPYRIGHT (1996)

1 Scientific Background

1.6.1 Manuscript

Imaging of Monoamine Neurotransmitters with Fluorescent Nanoscale Sensors

Meshkat Dinarvand¹, Sofia Elizarova², Dr. James Daniel², Dr. Sebastian Kruss^{1*}

¹Institute of Physical Chemistry, Göttingen University, Tammannstrasse 2, 37077 Göttingen, Germany

² Department of Molecular Neurobiology, Max Planck Institute of Experimental Medicine, 37077 Göttingen, Germany

Publication Date: June 11, 2020

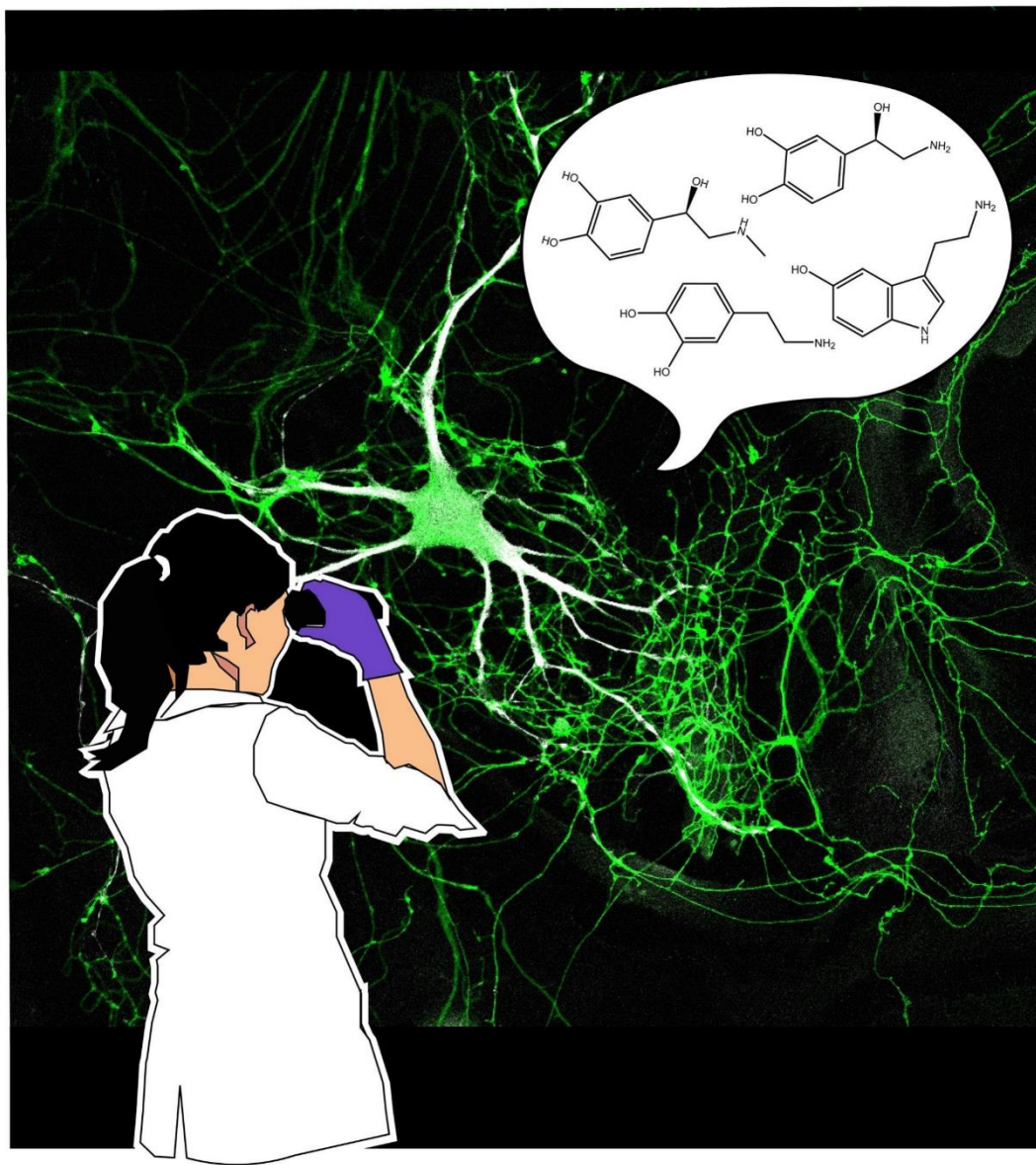
<https://doi.org/10.1002/cplu.202000248>

This manuscript was published in ChemPlusChem by European Chemical Societies Publishing

This is an open access article distributed under the terms of the Creative Commons CC BY license, which permits unrestricted use, distribution, and reproduction in any medium, provided the original work is properly cited.

Imaging of Monoamine Neurotransmitters with Fluorescent Nanoscale Sensors

Meshkat Dinarvand,^[a] Sofia Elizarova,^[b] James Daniel,^[b] and Sebastian Kruss^{*,[a]}



1 Scientific Background

Cells use biomolecules to convey information. For instance, neurons communicate by releasing chemicals called neurotransmitters, including several monoamines. The information transmitted by neurons is, in part, coded in the type and amount of neurotransmitter released, the spatial distribution of release sites, the frequency of release events, and the diffusion range of the neurotransmitter. Therefore, quantitative information about neurotransmitters at the (sub)cellular level with high spatiotemporal resolution is needed to understand how complex cellular networks function. So far, various analytical methods have been developed and used to detect neuro-

transmitter secretion from cells. However, each method has limitations with respect to chemical, temporal and spatial resolution. In this review, we focus on emerging methods for optical detection of neurotransmitter release and discuss fluorescent sensors/probes for monoamine neurotransmitters such as dopamine and serotonin. We focus on the latest advances in near infrared fluorescent carbon nanotube-based sensors and engineered fluorescent proteins for monoamine imaging, which provide high spatial and temporal resolution suitable for examining the release of monoamines from cells in cellular networks.

1. Biological background and motivation

Intercellular communication is a vital mechanism by which biological signals are transmitted between cells of a multicellular organism. The nervous system in particular is an example of complex intercellular communication and uses specialized structures to receive, process and send signals throughout an organism. Signals are propagated both within the nervous system, between specialized cells called neurons, and from the nervous system to cells in peripheral tissues such as skeletal muscle. The transmission of signals from a neuron to another cell is referred to as neurotransmission. Neurotransmission generally involves the secretion of a specific biomolecule, a 'neurotransmitter', from a stimulated neuron into the extracellular space (Figure 1a). The neurotransmitter then diffuses and activates postsynaptic receptors, communicating a chemical message from one neuron to its target cell. Classically, neurotransmission occurs at specialized structures called synapses, comprising a presynaptic bouton from which the neurotransmitter is released and a postsynaptic structure on the target neuron at which receptor proteins are concentrated (Figure 1a).

Within a neuronal presynaptic structure, neurotransmitters are stored in tens to thousands of highly concentrated small vesicles (in the 0.1 mol/L range) from which they are released through exocytosis milliseconds after stimulation of the neuron.^[1,2] Neurons can form up to 350,000 individual synapses with other cells,^[3,4] constructing complex neuronal circuits that give rise to the central nervous system and are capable of transmitting and computing huge volumes of information. These highly dynamic networks facilitate the function of the nervous system as the master controller and computer of the organism.

There are hundreds of identified chemical transmitters in the central nervous system. Glutamate and GABA are the predominant fast-acting neurotransmitters, rapidly activating or inhibiting target neurons respectively. The majority of other neurotransmitters are modulatory, acting to modify neuronal activity on a slower timescale and exerting either excitatory or inhibitory effects on neurons in a context-dependent manner. One notable family of modulatory neurotransmitters is the monoamines, which includes dopamine, serotonin, norepinephrine, epinephrine and histamine. Monoamines also play an important role as hormones. For instance, epinephrine is secreted from adrenal medulla in response to sympathetic innervation and mediates a wide range of physiological response, broadly called fight or flight response.^[5] Serotonin is secreted by enterochromaffin cells in the gastrointestinal tract and regulates intestinal motility and digestion.^[6] Researchers have also reported the production and release of these molecules from cells even without neuronal innervation (Figure 1a). For instance, some immune cells are capable of production and release of neurotransmitters such as dopamine, to self-regulate or possibly communicate with other immune cells through autocrine and paracrine signalling to modulate immune responses.^[7,8]

The mechanisms that control release and diffusion of neurotransmitters in the extracellular space are critical in intercellular communication. Thus, understanding the dynamics of neurotransmitter release has been an intense area of research over the last several decades. There are various factors regarding monoamine exocytosis that complicate studying the dynamics of release compared to other signalling chemicals. In the following section we will discuss some of those challenges and why they necessitate unique detection systems to observe release events with high spatial and temporal resolution.

Monoaminergic neurotransmission is thought to occur largely via volume transmission, meaning that following monoamine release from a presynaptic bouton, the monoamine diffuses in a relatively large distance and is able to act on receptors, and thus regulate the target cells over an area of up to several micrometers from the release site. Diffusing monoamines can also be degraded by specialized enzymes or taken up into neighboring cells which limits the area that is affected by the monoamine.^[9] For example, the half-life of dopamine in the striatum is ~30 ms, meaning that dopamine can potentially diffuse ~7 μm from a release site before degradation or

[a] M. Dinarvand, Dr. S. Kruss
Institute of Physical Chemistry
Göttingen University
Tammannstrasse 2, 37077 Göttingen (Germany)
E-mail: skruss@gwdg.de

[b] S. Elizarova, Dr. J. Daniel
Department of Molecular Neurobiology
Max Planck Institute of Experimental Medicine
37077 Göttingen (Germany)

© 2020 The Authors. Published by Wiley-VCH Verlag GmbH & Co. KGaA.
This is an open access article under the terms of the Creative Commons Attribution License, which permits use, distribution and reproduction in any medium, provided the original work is properly cited. Open access funding enabled and organized by Projekt DEAL.

1 Scientific Background

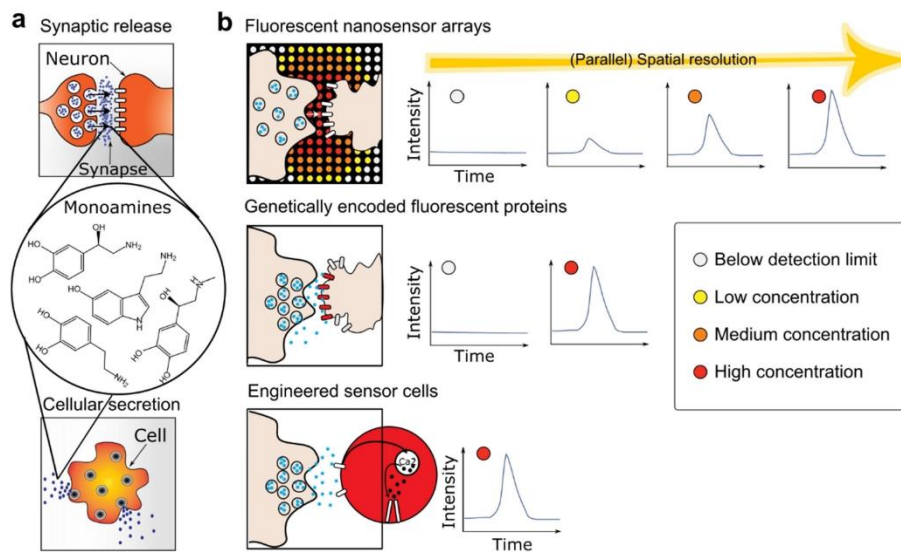


Figure 1. Monoamine detection by fluorescent sensors: **a.** Release of monoamines such as dopamine, epinephrine, norepinephrine or serotonin can occur at synaptic structures (synaptic transmission) of neurons or other release sites of monoaminergic cells. **b.** Optical methods to detect monoamines. Individual nanosensors are capable of reporting the local monoamine concentration through a transient change in their fluorescence. If there are many nanosensors ('array') in close proximity to the cell, they provide a very high spatial resolution (top panel). Genetically encoded sensors are fluorescent proteins that are expressed by cells on their surface and change their fluorescence in response to the analyte, providing information from the cell surface (middle panel). Cell-based sensors are engineered cells that undergo a fluorescence change on the level of the whole cell in response to the analyte. Due to the large size of these cells, this method provides lower spatial resolution (bottom panel). As indicated by schematic traces on the right of the panels, spatial and temporal resolution depends on the size, distribution and density of the sensor/probes and decreases from the top approaches to the bottom.



Meshkat Dinarvand earned her Doctor of Pharmacy degree from Tehran University of Medical Sciences in 2014. She has been working as a research assistant in the field of nanomedicine ever since, including at the nanomedicine and biomaterial lab in Harvard Medical School, Brigham and Women's hospital. She is now working toward her Ph.D. thesis at the Institute of Physical Chemistry, Georg August University of Göttingen. She is interested in designing nanosensors for biological applications with a focus on carbon nanotube-based sensors.



Sofia Elizarova received her B.Sc. degree in biology (University of Hannover) and M.Sc. degree in neurobiology (University of Göttingen) in Germany. Since 2017 she has been undertaking research for her Ph.D. in the Department of Molecular Neurobiology at the Max Planck Institute of Experimental Medicine, Göttingen, Germany, as part of the Göttingen Graduate Center for Neurosciences, Biophysics, and Molecular Biosciences (GGNB). Her current work focuses on the molecular mechanisms that regulate secretion of the neurotransmitter dopamine from presynaptic terminals.



Dr. Daniel completed his Ph.D. in 2008 with Prof. Bryce Vissel at the Garvan Institute of Medical Research (Sydney, Australia), examining presynaptic function in dopaminergic neurons. He then completed postdoctoral training with Prof Phillip Robinson (Children's Medical Research Institute, Sydney, Australia), discovering synaptic vesicle endocytosis inhibitors, and with Prof Nils Brose (Max Planck Institute of Experimental Medicine, Göttingen, Germany), investigating neuronal protein SUMOylation. In 2016, he established his own group within the Department of Molecular Neurobiology, focused on discovering mechanisms that regulate dopamine secretion.



Dr. Sebastian Kruss received his Ph.D. in physical chemistry at Heidelberg University and the Max Planck Institute for Intelligent Systems (Prof. Joachim Spatz). He then moved to the group of Prof. Michael Strano at the Massachusetts Institute of Technology, where he worked on carbon nanomaterials. Since the end of 2014 he heads an independent research group at Göttingen University. His research focuses on novel materials, spectroscopy and microscopy, biosensors and biophysics.

1 Scientific Background

uptake.^[10] Monoamine release sites are also highly heterogeneous.^[11,12] A research investigating neurons that secrete dopamine has shown that presynaptic boutons are formed at various distances from target neurons, meaning that dopamine must diffuse away from the release site to bind to receptors on target neurons.^[12,13] In addition, dopamine can be released not only from boutons but also from the cell body of neurons, which in the brain are located distant from boutons (Figure 1b).^[14] The heterogeneity of release sites is unique to modulatory neurotransmitters and suggests that these neurons use distinct mechanisms for intercellular communication that are not yet understood.

These processes alter the local extracellular concentration of the neurotransmitter, and thus influence signal transmission and integration by other cells. This mode of action is substantially different from fast-acting transmitters such as glutamate and GABA, which are secreted within a nanometer-range from their target receptors in synaptic structures and have a very limited half-life in the extracellular space, limiting their diffusion.^[15,16]

The study of monoamine release requires sensors that detect monoamines. Given the diversity of the structures that release monoamines, as well as the dynamics of monoamine release and diffusion in time and space, an ideal detection method would need both high temporal and spatial resolution.^[17] To achieve high temporal and spatial resolution, optical monoamine detection methods are an elegant solution (Figure 1b). Figure 1 illustrates detection and imaging of monoamines that the three major classes of existing fluorescent sensors/probes can perform. Following a release event, the concentration of the neurotransmitter rapidly changes adjacent to the release site. The spatiotemporal detection limits for the secreted neurotransmitter are thereby determined by the distance between the sensor-probes as well as their kinetics and sensitivity (see section 3.1). Consequently, the spatiotemporal resolution of neurotransmitter detection can be improved by increasing the number of probes in close proximity to the cell, as well as the dynamic range of the probe and optimal kinetics.

This minireview provides a short overview of the classical analytical methods of monoamine neurotransmitter detection (Section 2), with a focus on dopamine and serotonin. We then review advances in fluorescent optical monoamine sensors: a) fluorescent nanosensors that are positioned outside cells, b) engineered fluorescent proteins expressed on the surface of cells, and c) whole cells as fluorescent monoamine sensors. We also provide a short summary of fluorescent probes and label-free methods, although the focus are the mentioned direct methods with high spatial and temporal resolution.

2. Classical methods of monoamine detection

The most extensively used analytical methods to detect monoamine secretion are microdialysis and electrochemistry.^[18] Microdialysis is a procedure in which a sampling probe of approximately 0.15–0.3 mm is surgically implanted in the brain or tissue area of interest, such as the striatum of anesthetized

rodents.^[19] Extra-cellular fluid is then sampled by diffusion through a semi-permeable membrane at the tip of the probe with a constant flow rate of typically 0.5–5 $\mu\text{L}/\text{min}$. This procedure is combined with analytical tools such as liquid chromatography and mass spectrometry to determine the concentration of monoamines in the extracellular fluid. While enabling the investigation of deep areas of the brain with high chemical specificity *in vivo*, the relatively long sampling procedure (in order of minutes) and size of the probe does not allow monitoring of millisecond fluctuations in monoamine concentrations. The method is also relatively invasive and damages brain tissue due to the insertion of the sampling probe. Such a damage can induce an inflammatory response and thus introduce artefacts to the experimental system.^[20]

The temporal and spatial resolution of monoamine detection was greatly improved by the development of the electrochemical methods such as amperometry and fast-scan cyclic voltammetry.^[21–24] In amperometry, a carbon fiber microelectrode held at constant electrical potential is placed either adjacent to cells or in a brain area of interest. Monoamines oxidize at the electrode surface and yield faradaic current as the quantitative indicator of concentration.^[25] Damage to brain tissue is reduced compared to microdialysis due to the relatively small probe radius (3.5 μm or much smaller).^[26] One limitation of amperometry is the lower chemical resolution/selectivity as amperometry cannot distinguish between monoamines of similar redox potential (dopamine, epinephrine, and norepinephrine) and other molecules (e.g. ascorbate). Therefore, it is often used in cultured cells or brain slices in which contamination of the signal from other chemicals can be excluded. Nevertheless, due to the excellent temporal resolution on a submillisecond scale and the high sensitivity, amperometry has become the gold standard of monoamine detection and has been used to record single release events in cultured cells.^[27–29] A subsequent methodological breakthrough was the adaptation of carbon fiber electrochemistry to yield voltammetry-based methods. Fast-scan cyclic voltammetry (FSCV) is widely used for the detection of monoamines *in vivo*, and works by cycling the potential of the electrode between a positive and negative voltage at high rates to rapidly reduce and oxidize the analytes. This results in cyclic voltammograms with characteristic shapes for individual compounds, resulting in greater discrimination of analytes but greatly reduced temporal resolution compared to amperometry.^[29]

While electrochemical methods can provide exquisite temporal resolution, they provide very limited (parallel) spatial resolution. Differentiating sub-cellular release structures or even release from single cells using brain slices or dissociated neuron cultures has proven to be extremely challenging due to the high density of release sites and relatively large size of the carbon electrode.^[27] One strategy to overcome these limitations is using multi-electrode arrays containing 64 microelectrodes with electrode diameters of 3 μm to 12 μm , however this method is limited to use in cell culture.^[30]

1 Scientific Background

3. Fluorescent sensors based on nanomaterials

In general, a fluorescent nanosensor is composed of a nanoscale fluorescent material and equipped with recognition chemistry to bind an analyte. Structures on the 'nanoscale' (in the range of 1–100 nm in at least one dimension^[31]) often acquire novel size and shape dependent optical properties that are not present in the bulk material.^[32] An important property is emission in the near infrared (nIR) tissue transparency window (> 800 nm) that only few fluorophores such as carbon nanotubes, certain silicate nanosheets or quantum dots provide.^[33–35] These size-dependent properties, coupled with tailored surface chemistry make fluorescent nanomaterials sensitive and versatile sensors for biological applications down to the single-molecule level.^[36,37] Furthermore, fluorescent sensors can be detected by non-invasive imaging techniques, which provide high parallel spatial resolution (increased spatial resolution without reducing the field of view). Many nanoscale structures have been studied as detection tools for neurotransmitters, including fluorescent complexes, metallic, polymeric and carbon-based materials. These tailored materials report the presence of the analyte in a biological sample and include quantum dots,^[38] graphene,^[39] and polymeric nanoparticles.^[40] However, they do not all provide spatiotemporal information such as dynamic information of individual release events from cells. In this review, we will focus only on (fluorescent) nanosensors that have successfully visualized release dynamics in a biological system with appropriate temporal and spatial resolution in addition to chemical resolution. In Section 3.1, we will shed light on the kinetic requirements for monoamine imaging. Then, SWCNT-based fluorescent sensors for dopamine and serotonin are discussed (Section 3.2). Finally, polymer nanoparticle approaches will be addressed (Section 3.3).

3.1 Kinetic requirements for fast imaging of neurotransmitter release

In standard analytical techniques, detection of an analyte occurs under equilibrium conditions in which the concentration of the analyte is constant. In this scenario, the binding affinity/limit of detection of the detection system is the most important parameter. In contrast, many biological processes such as neurotransmitter release are characterized by fast concentration changes (ms time scale) and complex spatiotemporal patterns. These patterns are governed by release events, diffusion and uptake. For example, studies have shown that most dopamine receptors (D1 and D2) in the striatum are extra-synaptic.^[41] This means that dopamine spills over from the release site to reach its many target receptors. At short distances from the release site (1–2 μm), only diffusion governs the extent to which the DA signal spread through the extracellular space. However, in the range of 5 to 20 μm from the release site, uptake of dopamine limits dopamine concentration.^[16] For example, a study has shown that if each vesicle contains 3000 molecules, dopamine would diffuse and bind to dopamine receptors in an area of 12 μm however, when dopamine transporters (DAT),

responsible for dopamine uptake from the extracellular space, are missing such as in Parkinson's disease, the diffusion distance of the dopamine precursor L-DOPA may be as high as 32 μm .^[42] These considerations show that secreted monoamine concentration is a complex function of location (x,y,z) and time.

When imaging such highly complex processes with fluorescent sensors, the kinetics of these sensors determine the resolution that can be achieved. To study the relation between kinetics and resolution Meyer *et al.*, developed a theoretical framework to simulate the image of many single fluorescent sensors when exposed to concentration changes of analytes (e.g. neurotransmitters) released from cells.^[43] It is not only valid for nanomaterial-based sensors but for every immobilized/bound fluorescent sensor/probe on or around a cell.

For this purpose, a stochastic kinetic Monte Carlo simulation was implemented and sensors/probes with a certain number of binding sites and rates of binding and unbinding were modelled. As a typical biological scenario, a cell releasing molecules via exocytosis and diffusion through space was used and simulated (Figure 2a). The approach also considered the resolution limit of light microscopy as well as technical aspects such as the imaging speed. This simulation was then used to calculate if a given sensor (array) with certain forward (k_{on}) and backward rate constants (k_{off}) can e.g. distinguish two release events in time or distinguish multiple release sites. Figure 2b shows the concentration profile of a typical single exocytosis event and images of different sensor arrays at different time points. The results show that certain sensors cannot detect the release event while others oversaturate. By simulating many different rate constant combinations it was possible to explore this rate constant design space. Interestingly, sensors with rate constants of $k_{on} = 10^6 \text{ M}^{-1} \text{ s}^{-1}$ and $k_{off} = 10^2 \text{ s}^{-1}$ provide the best spatiotemporal resolution for many scenarios. This means that nanosensors with relatively low binding affinity ($K_d = k_{off}/k_{on} = 100 \text{ }\mu\text{M}$) exhibit the best response profile. At slower binding rates ($k_{on} = 10^3 \text{ M}^{-1} \text{ s}^{-1}$) release events cannot be detected and at faster binding rates ($k_{on} = 10^7 \text{ M}^{-1} \text{ s}^{-1}$) and slow unbinding ($k_{off} = 1 \text{ s}^{-1}$) the response quickly saturates (Figure 2b). These insights are important for the design of monoamine sensors but provide also the tools to analyze data acquired with such sensors and address the inverse problem, i.e. translate an image into a concentration profile.

3.2 Carbon nanotube-based nanosensors

3.2.1 Concept and design of SWCNT-based nIR fluorescent sensors

Carbon based nanomaterials hold a unique position in life science research due to their physicochemical properties (i.e., optical properties, electrical conductivity, mechanical strength, thermal properties).^[44] Nano structures based on carbon have been studied extensively as sensors. Among them, the most promising structures are carbon dots, graphene, and carbon nanotubes.^[36,45]

1 Scientific Background

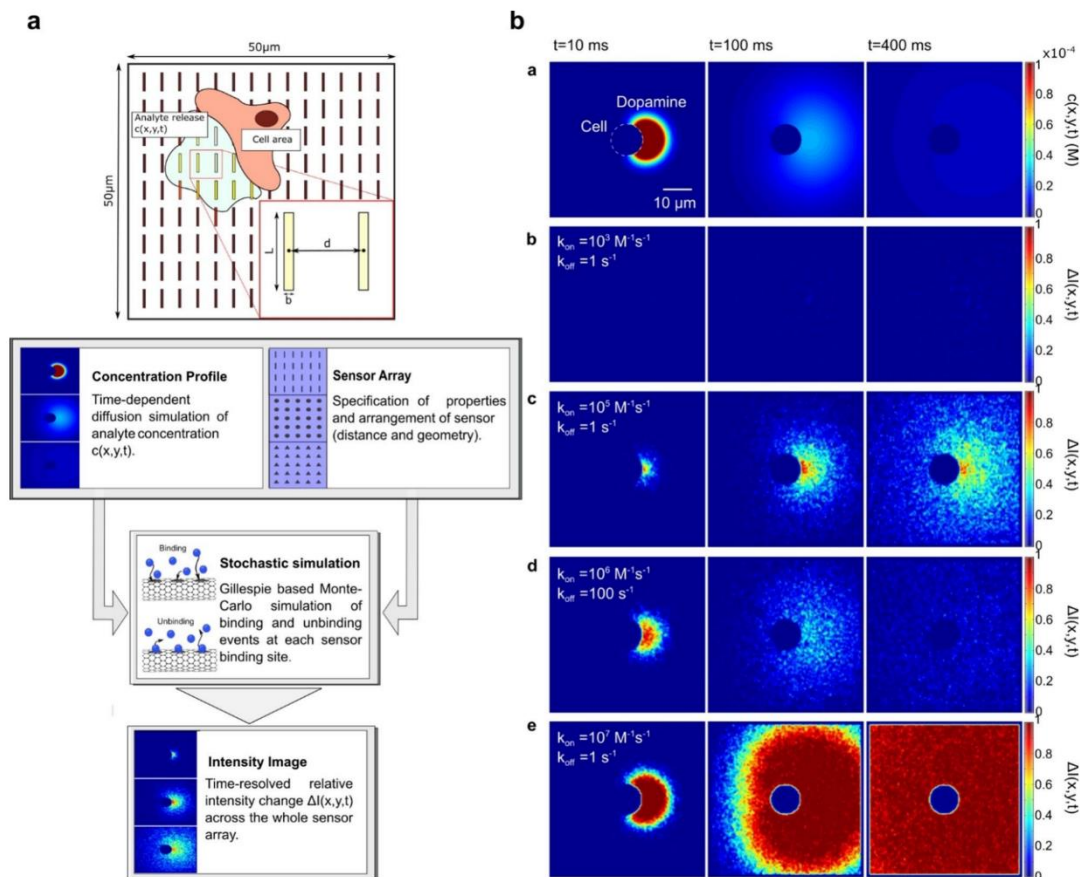


Figure 2. Kinetic requirements for sensors that enable high spatiotemporal resolution imaging. **a**, Model of a surface coated with nanoscale sensors. A cell on top releases a molecule of interest exposing the array to a certain concentration profile $c(x,y,t)$. Bottom: Flow diagram of the simulation: (1) Simulation of neurotransmitter release from a cell and diffusion. (2) Arrangement of the sensors in any arbitrary geometry and size. (3) Stochastic simulation of binding and unbinding events of the analyte to the nanosensor with different rate constants k_{on} and k_{off} . (4) Finally, the image series $\Delta I(x,y,t)$ is calculated by overlaying the fluorescence intensity point spread functions of all sensors and accounting for the resolution limit of light microscopy (Abbe limit), pixel size, and frame rate of the detector. **b**, Fluorescence changes of nanosensors in response to dopamine release from a cell (top row) All other rows: Simulation of fluorescence changes of a nanosensor array after neurotransmitter release from a vesicle at different time points for different k_{on} and k_{off} . The differences show the importance of rate constants for the spatiotemporal resolution and the observed response pattern. Adapted from reference [43] with permission. Copyright 2017 American Chemical Society.

Single walled carbon nanotubes (SWCNTs) can be imagined as rolled up sheets of graphene.^[46] Because of their small diameter (e.g. 0.7 nm) and high length, they can be conceived of as one-dimensional materials. The angle and the direction in which the graphene sheet is 'rolled up' determines distinct lattice structures called chirality and is described by the chiral index (n,m). The special lattice structure causes very unique optical, mechanical and electrical properties. For instance, semiconducting SWCNTs are fluorescent in the near infrared (nIR) region (> 850 nm).^[33] Their electronic band gap structure and nIR emission wavelength depends on the chirality of carbon nanotubes.^[33] For example, (6,5)-SWCNTs emit at around 980 nm while (7,6)-SWCNTs emit at around 1130 nm.

Intrinsic fluorescence in the near infrared region and the ability to manipulate the fluorescence emission patterns, is the basis of optical sensing with SWCNTs.^[33,36] SWCNTs, unlike most organic fluorophores, do not photobleach or blink. Furthermore, SWCNT-based sensors can be designed specifically to resist biofouling which is one limitation of microelectrode-based sensors.^[47] Fluorescent SWCNTs are especially advantageous for biomedical imaging because of the nIR fluorescence in the tissue transparency window, which could potentially facilitate through-cranium imaging.^[48] In the nIR, there is little light absorption by tissue, relatively low light scattering and minimal autofluorescence.^[49] Therefore, this spectral range is desirable for biomedical imaging. The fluorescence of SWCNTs is highly sensitive to its environment, meaning small changes in

1 Scientific Background

the SWCNT's microenvironment can affect their fluorescence emission pattern. However, SWCNTs are extremely hydrophobic and therefore not stable in aqueous solutions. In order to use SWCNTs in biological applications, they must be functionalized to facilitate colloidal stability. Additionally, surface modification can be used to purify chirality enriched SWCNTs.^[50] Non-covalent surface modification with DNA, peptides, proteins and other polymers have been extensively used to tailor the surface chemistry on SWCNTs.^[51–55]

SWCNTs have been used as building blocks for sensors and labels for larger biomolecules such as RNA, DNA and proteins.^[53,56–59] For smaller analytes, it is typically difficult to find good recognition units and therefore designing sensors is more challenging. One approach is indirect sensing of the analyte by detecting the product of the analyte's chemical reaction. An example is SWCNT H₂O₂ sensors equipped with hemin that catalyzes the reaction of H₂O₂ to hydroxyl radicals, which directly quench fluorescence and this indicates the presence of the signalling molecule H₂O₂.^[60] This concept is only feasible for a few reactive/quenching compounds. Interestingly, certain biopolymer wrapped SWCNTs can detect small molecules such as dopamine with high sensitivity and selectivity, even without a known recognition unit (Figure 3a).^[50,61–63] This phenomenon was termed corona phase molecular recognition.^[61] Similar to antibody-antigen recognition, the

molecular recognition relies on the spatial arrangement of the polymer on the SWCNT with a specific 3D structure that binds dopamine. One important class of macromolecules for SWCNT modification is single stranded DNA (Figure 3b). As shown in Figure 3, the baseline fluorescence of certain DNA wrapped SWCNTs increase dramatically when they are exposed to dopamine either in dispersion (Figure 3b) or immobilized on a surface (Figure 3c). Furthermore, the fluorescence increase is concentration dependent (Figure 3d).

Whether a DNA functionalized SWCNT responds to dopamine depends on the DNA sequence.^[61] The first identified and studied sequence was (GT)₁₅ ssDNA on HiPCo SWCNTs. The fluorescence of (GT)₁₅-SWCNTs increased by 80% in solution and up to 400% on the single SWCNT level after addition of dopamine (100 μM). The dynamic range of detection was 10 nM - 10 μM and the limit of detection was 11 nM.^[61] To improve sensitivity and selectivity, the DNA sequence was further explored. Consequently, a study with (6,5) chirality enriched SWCNTs with 10 ssDNA sequences was performed to identify which DNA sequence imparted highest sensitivity and selectivity to dopamine compared to other catecholamines (epinephrine and norepinephrine).^[62] All sequences responded to the catecholamines with an increase in fluorescence signal. However, there was a marked difference in analyte selectivity between different ssDNA sequences (Figure 4). For example,

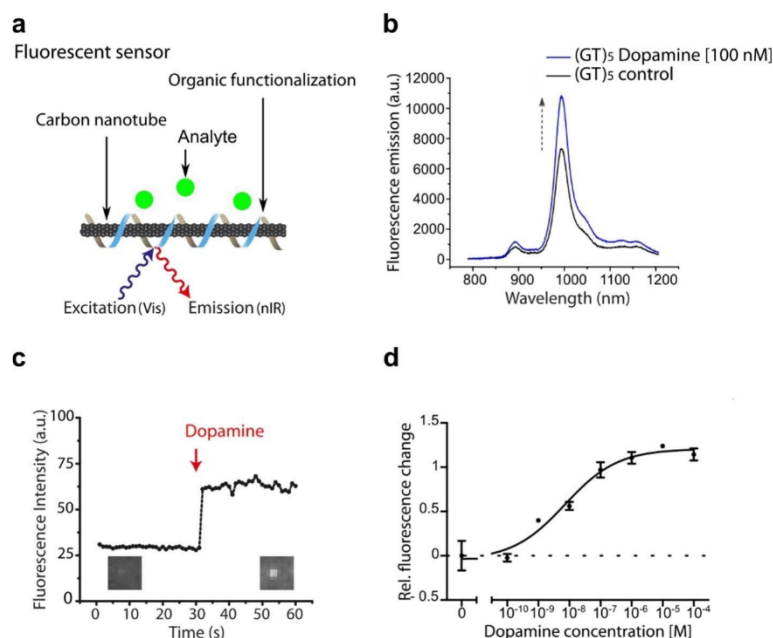


Figure 3. Carbon nanotube-based near infrared fluorescent sensors for dopamine. **a**, Schematic of a functionalized single-walled carbon nanotube (SWCNT) sensor. In presence of the analyte, the nIR fluorescence changes. **b**, Fluorescence emission spectra of (GT)₅ DNA functionalized (6,5) single chirality SWCNTs before (black) and after (blue) addition of dopamine show an increase in fluorescence intensity. **c**, nIR fluorescence intensity of a single SWCNT sensor immobilized on a surface. A sharp increase in fluorescence is observed after addition of dopamine. **d**, Calibration curve of a SWCNT-based dopamine sensor shows nM sensitivity. (a) and (b) adapted from references [61] and [64] with permission. Copyright 2014 and 2019, respectively, American Chemical Society. (c) adapted from reference [65] with permission. Copyright 2017 United States National Academy of Sciences, (d) adapted from reference [62] with permission. Copyright 2017 MDPI.

1 Scientific Background

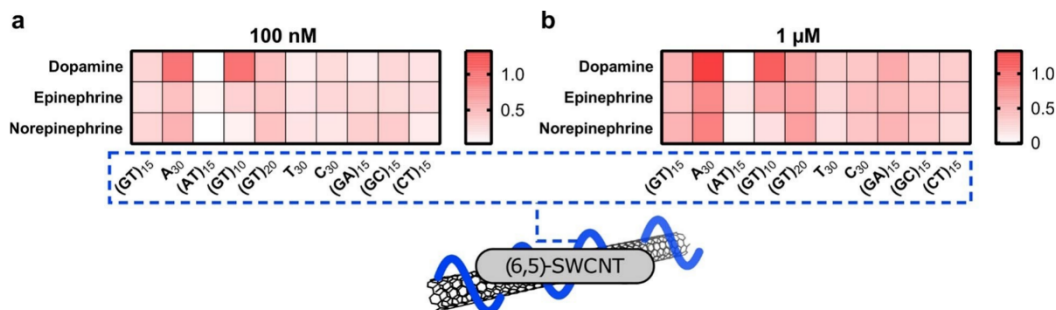


Figure 4. Tuning of SWCNT-based dopamine sensors by exploring the DNA sequence space. Fluorescence intensity changes of various DNA functionalized SWCNTs at **a**, low (100 nM) and **b**, high (1 μ M) catecholamine concentrations. These results indicate e.g. that (GT)₁₀-SWCNTs can discriminate to a certain extent different catecholamines. Reproduced from reference [62] with permission. Copyright 2017 MDPI.

(GT)₁₀-SWCNTs showed the highest selectivity and sensitivity for dopamine (table 1). K_d values of (GT)₁₅ and (GT)₁₀-SWCNT sensors ranged between 395.2 and 9.2 nM respectively. In light of the relevance of kinetics and off-rates for imaging (see previous section) it is crucial that kinetics of a sensor and the required resolution for a specific biological question match. Therefore, a sensor with the highest sensitivity is not necessarily the best fit for a biological experiment. Most dopamine sensors were so far created by using non-purified SWCNTs. Multiplexing approaches have a huge potential and therefore chirality-pure sensors are desired. A recent study used corona phase exchange purification (CPEP) to isolate chirality pure (6,5)-SWCNTs to coat them with e.g. (GT)₅DNA.^[50] The results show that dopamine sensing can be as well performed with purified SWCNTs and well-defined emission features can be obtained (see also figure 3b).

In summary, functionalization of SWCNTs with specific DNA sequences leads to highly sensitive dopamine sensors. The enormous potential sequence space promises many additional discoveries and improvements for the future. One might even speculate that folding of biopolymers such as DNA on a SWCNT could be a generic approach to create recognition motifs.^[66]

3.2.2 Mechanism of fluorescence modulation

The mechanism of SWCNT-based fluorescent sensors is an active area of research and might vary between different

surface chemistry approaches and analytes. However, for DNA-SWCNT-based dopamine sensors there have been insights that are of general importance for the field.

The first insights into the recognition and sensing mechanism were gained by coating SWCNTs with a fluorophore tagged (GT)₁₅ DNA. Initially, adsorption of tagged DNA on SWCNT surface quenched the fluorophore's visible fluorescence. When dopamine was added, this fluorescence increased again.^[61] The best explanation is that the fluorophore moved away from the SWCNT, which recovered its fluorescence that had been quenched by the proximity of the SWCNT. This finding suggests that a conformational change might be responsible for the change of nIR fluorescence.

However, dopamine and other catecholamines are redox-active compounds. Therefore, one could also hypothesize that increase in fluorescence is linked to this property, especially as certain reducing compounds are known to increase nIR fluorescence.^[67] However, the extent of fluorescence change depends on the nature of the polymer wrapping as shown in Figure 5a.^[63] Therefore, the redox potential of the analyte alone cannot be the only reason responsible for the fluorescence response to dopamine. This is further supported by the fact that several compounds of the same redox potential as dopamine do not show this characteristic fluorescence increase. Another possible explanation is electron transfer from dopamine to the DNA phase. Again, a mechanism based solely on electron transfer is unlikely because the dopamine response is reversible. As discussed earlier, selectivity and sensitivity of

Table 1. Dissociation constants (K_d) and limits of detection (LOD) values of various DNA functionalized SWCNTs for catecholamines. Reproduced from reference [62] with permission from MDPI.

	NT	[GT] ₁₅	[GT] ₂₀	[GT] ₁₀	A ₃₀	C ₃₀	T ₃₀	[GA] ₁₅	[GC] ₁₅	[C] ₁₅	[AT] ₁₅
K_d (nmol/L)	D	395.2 ^[a]	42.3	9.2	28.4	499.2 ^[a]	237.2	627.8 ^[a]	0.7 ^[a]	25.8	9438
	E	159.1	112.6	178.2	171.9	177.2	51.1	234.3	49.3	47.1	241.5
	N	70.3	58	71.9	25	193.1	33.6 ^[a]	21.4	2.3	52.8	— ^[1]
LOD ^[b] (nmol/L)	D	6.4 ^[a]	0.6	0.1	3.6	2.7 ^[a]	1.2 ^[a]	507.2	28.5 ^[a]	4.4	3776.6
	E	1.4	2.2	0.7	3.2	1.4	1.0	1.8	0.5	0.8 ^[1]	23.7
	N	3.2	2.4	7.7	1.6	4.8	33.3	3.8	0.5	3.9	— ^[1]

[a] No clear (sigmoidal) fit possible. [b] LOD: Limit of detection definition used = 3x standard error at [c] = 0 nM. D: Dopamine. E: Epinephrine. N: Norepinephrine.

1 Scientific Background

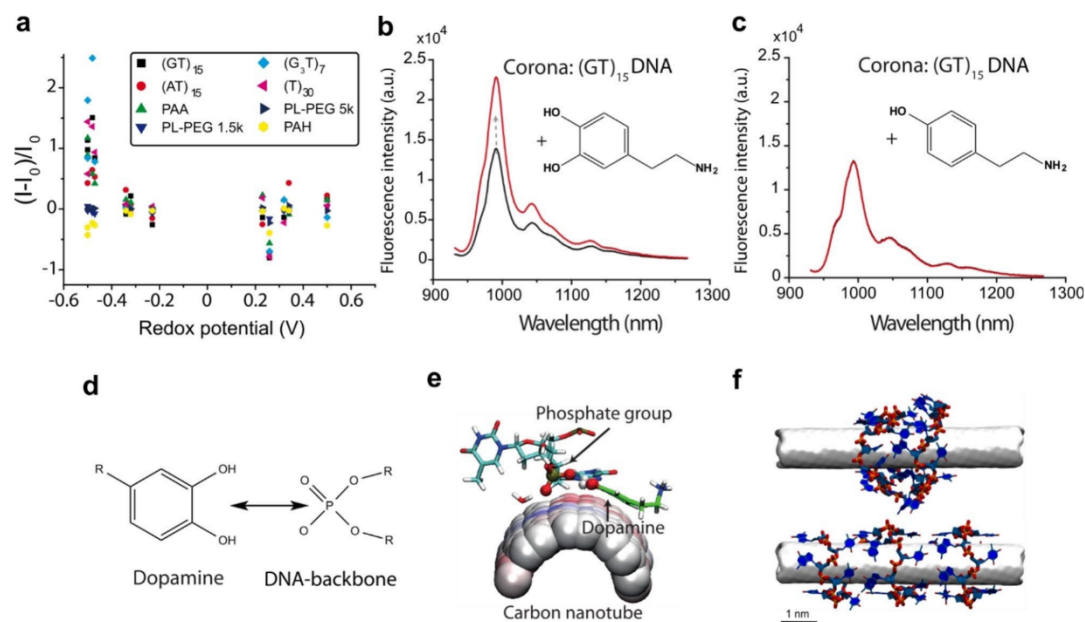


Figure 5. Mechanism of DNA-SWCNT based dopamine sensors. **a**, Fluorescence changes of SWCNT wrapped with various polymers when exposed to redox active molecules show a broad distribution, which cannot be explained by redox potential. **b,c** Fluorescence response of (GT)₁₅-SWCNTs to dopamine (**a**) and tyramine (**b**) before (black) and after (red) addition. The results show that small differences in the analyte structure completely change the response. **d,e**, Dopamine and adsorbed DNA on the SWCNT most likely interact via the phosphate backbone and hydroxy groups. **f**, MD simulations of DNA adsorbed on SWCNTs show that the DNA molecules do not form perfect helices around SWCNTs (top) and stack on each other when experimental numbers of surface coverage are used. In contrast, without any constraints in the simulation helical structures are formed (bottom). (**a**) reproduced from reference [63] with permission. Copyright 2016 American Chemical Society, (**b-e**) reproduced from reference [65] with permission. Copyright 2017 United States National Academy of Sciences, (**f**) reproduced from reference [64] with permission. Copyright 2019 American Chemical Society.

sensors depend on the sequence of DNA strands adsorbed on the surface. This shows that the interaction between the DNA and SWCNT plays an important role in the molecular recognition and formation of the fluorescence response. The surface area of the SWCNT that is covered by DNA molecules and the colloidal stability of the corona are parameters that likely define how the sensors detect dopamine. Therefore, the number of adsorbed ssDNA molecules was determined using an absorption spectroscopy based approach.^[64] When H₂O₂ and riboflavin were used as analytes, the fluorescence response was directly proportional to the number of adsorbed ssDNA molecules. However, no simple correlation was discovered between the fluorescence response for dopamine sensors, indicating that conformational changes of the DNA play a key role.^[64]

Molecular dynamics (MD) simulations can provide insights into interactions between the analyte, the SWCNT and the organic phase. For (GT)₁₅-SWCNT, interactions between the hydroxy groups of dopamine and the phosphate groups of the DNA appear to play an important role (Figures 5d, e).^[64] Due to these interactions, the phosphate groups move closer to the surface of the SWCNT and change the potential landscape through which the exciton diffuses. It is also possible that these conformational changes are associated with changes in ion distribution that are known to affect SWCNT fluorescence.^[65] Experimentally, this interaction is validated because only dopamine homologues with two hydroxy groups show similar responses.^[65] In contrast, tyramine (one hydroxy group) does not

induce any fluorescence change (Figures 5b, c). One should also consider that the structure of DNA on SWCNTs is likely more complex with stacked nucleotides, as recently shown using experimental surface coverage parameters for MD simulations (Figure 5f).^[64]

All mechanistic insights suggest that DNA acts as a flexible quantum yield switch on SWCNTs. For certain DNA sequences, the interaction with an analyte such as dopamine changes the conformation of the DNA, which in turn changes the quantum yield by affecting the exciton fate. Nevertheless, conformational changes due to unspecific changes in microenvironment would cause background signals and decrease selectivity. Therefore, more rigid xeno nucleic acids can be used to stabilize the fluorescence signal in media of different ionic strengths.^[68]

3.2.3 Imaging dopamine release

A nanomaterial that changes its fluorescence in the presence of an analyte such as dopamine is a powerful tool for direct chemical imaging. Even though a single nanosensor responds to dopamine (Figure 3c), imaging many of them at the same time substantially increases the parallel (spatial) resolution.^[65] For *in vitro* cell studies such sensors can be immobilized on a surface (sensor array) and cells cultivated on top (Figure 6a).

1 Scientific Background

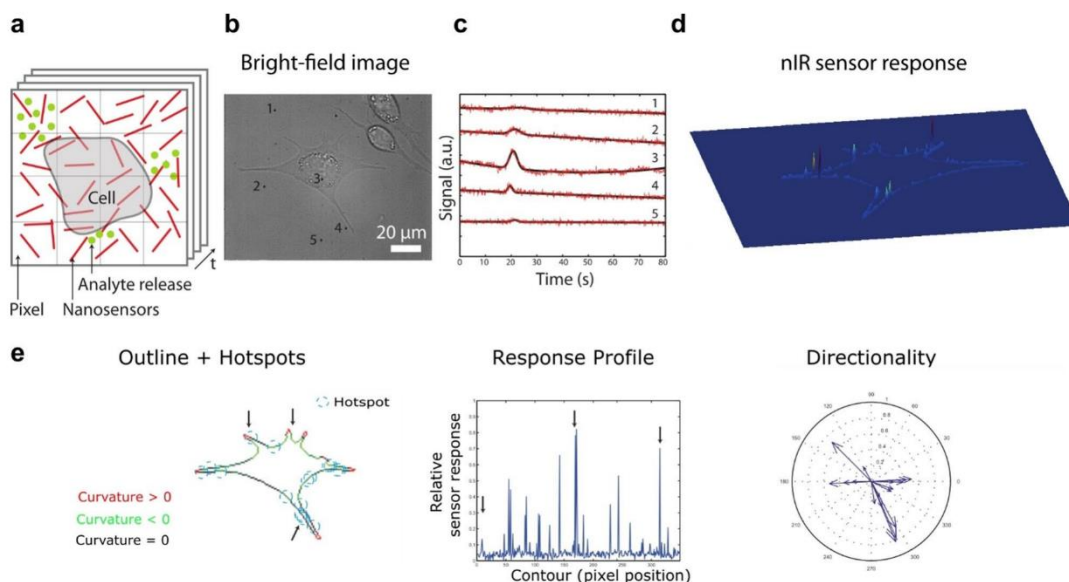


Figure 6. Fast imaging of dopamine release from cells using nanosensors **a**, Schematic of nanosensors immobilized in proximity of cells (like an array). **b**, Brightfield image of a neuroprogenitor PC12 cell incubated on top of a glass surface coated with SWCNT nanosensors. **c**, Fluorescence signal of dopamine nanosensors under and around this cell plotted against time. The differences in the traces show the gain in spatial information by imaging many nanosensors in different locations. **d**, Color-coded maximum responses (at the border) of the same cell showing localized events, denoting hot spots of neurotransmitter exocytosis/release. **e**, Localization of such hotspots around the cell and corresponding cell curvature. Additionally, the same information in directionality plots, which show that hotspots are located along cell protrusions preferentially in regions of negative curvature. Adapted from reference [65] with permission. Copyright 2017 United States National Academy of Sciences.

Above a certain sensor density the resolution limit of light microscopy becomes relevant and therefore the camera does not detect individual sensors anymore but the overlay of many of them. The above mentioned (GT)₁₅-SWCNT sensors and modified versions of it were used in this way to study dynamics of dopamine release from PC12 cells (a model cell line for modulatory neurotransmitter studies) (Figures 6a, b). Figure 6c shows the fluorescence trace of different regions under a cell (figure 6b) during stimulation with potassium, which triggers exocytosis through depolarisation of the cell membrane. The traces show peaks, which indicate increases of the dopamine concentration. The shapes and magnitudes of these traces vary across different regions, which highlights the high spatial resolution of the method (Figure 6c). The heterogenous distribution of maximum responses along the cell membrane is indicative of hotspots of dopamine release. These sensor arrays provide a great deal of temporal and spatial information from single cells, which is a key advantage of this method of dopamine detection. For example, when images are divided to units of 4×4 pixels, a round cell contains approximately 1700 reporter pixels (d = 40 μm) and more than 180 reporter pixels in a 2 μm zone around the cell border. These numbers highlight the gain in spatial resolution compared to electrode-based methods, which generally employ only a single sensor and at most have been able to employ 64 sensors in an electrode array.^[30] In Figure 6, the nanosensors were imaged at 100 ms per frame, which is a lower temporal resolution than amperom-

etry but comparable to FSCV. However, the time resolution was mainly limited by the imaging setup and could be further improved by 1–2 orders of magnitude.

SWCNTs are also useful for biomedical research in tissue samples. For example, single polyethyleneglycole functionalized SWCNTs can be tracked in brain tissue to map the extracellular space.^[69] Along the same lines, a variant of the above mentioned SWCNT-based dopamine sensor has been used to investigate dopamine release in brain slices of mice dorsal striatum,^[70] which contains abundant sites of dopamine release, as it receives extensive axonal projections from dopaminergic neurons residing in the ventral midbrain.

To date, SWCNT-based dopamine nanosensors were either immobilized in arrays under cells or bound/diffused non-specifically in tissue samples. To target SWCNTs directly to specific locations such as a presynaptic structure, tailored sensors with recognition motifs are necessary. One approach is to additionally conjugate nanobodies to the DNA around the SWCNTs.^[58] This approach did not affect dopamine sensing and opens up many opportunities to target such sensors specifically to the most relevant biological locations. Another approach to target dopamine nanosensors to specific locations was to make use of cells to transport them. Recently, it was shown that immune cells can be programmed to take up SWCNT-based dopamine sensors and transport them to desired locations where they are released.^[71] After release, they are still functional

1 Scientific Background

and detect dopamine, which promises interesting *in vivo* applications.

The sensors discussed in this section were identified *de novo* in a screening approach but in general it is faster to synthesize new sensors by relying on known recognition motifs such as antibodies, nanobodies or aptamers. In the next section, a sensor for the neurotransmitter serotonin will be discussed that is based on a DNA aptamer specific for serotonin.^[72]

3.2.4 Imaging of serotonin release

Like dopamine, the local changes of serotonin concentration around neurons are responsible for signal transmission in neural circuits. Therefore, to better understand intracellular signalling by serotonin in the brain and other organs, chemical sensors with high spatial and temporal resolution are required. Again, there are very few (optical) methods that could provide high spatiotemporal resolution and visualize release events *in situ* with minimal invasiveness.

One approach to detect serotonin is the use of organic dyes that change their fluorescence when they react with serotonin, such as coumarin-3-aldehyde. This serotonin binding turn-on fluorophore can be used as a labelling agent to visualize serotonin rich vesicles inside cells and further image the dynamics of vesicular transport of serotonin upon cell secretion.^[73] Even though this dye is relatively selective for

serotonin, the dissociation constant is quite high ($K_d = 2400 \mu\text{M}$). Therefore, this molecule is more suitable for detecting and imaging the presence of serotonin rather than studying dynamic changes in serotonin levels.

The first nIR fluorescent sensor for serotonin is based on SWCNTs (NIRSer).^[72] It consists of (6,5)-SWCNTs that were non-covalently coated with a serotonin-specific DNA aptamer (Figures 7a). In the presence of serotonin, the nIR fluorescence increases (Figure 7b). Consequently, it can be used to image serotonin release from cells. Most of the serotonin in a human body is stored in blood platelets. Therefore, NIRSers were used to image secretion of serotonin from platelets with high spatial and temporal resolution (Figure 7c). By coating surfaces with NIRSers, and seeding adherent platelets on top of the sensors, the release hotspots (localized regions where exocytosis and serotonin release occurs) on the cell membrane were identified (Figures 7d, e, f). NIRSer has a dissociation constant (K_d) of 301 nM and is selective for serotonin compared to potentially interfering substances such as tryptophan. Again, the major advantage is the high spatial resolution. Using this approach, single cells can be studied in detail as well as cell populations.^[72] In this context, the heterogeneity of serotonin release patterns, including onset and magnitude of serotonin release, was described for the first time in human platelets.

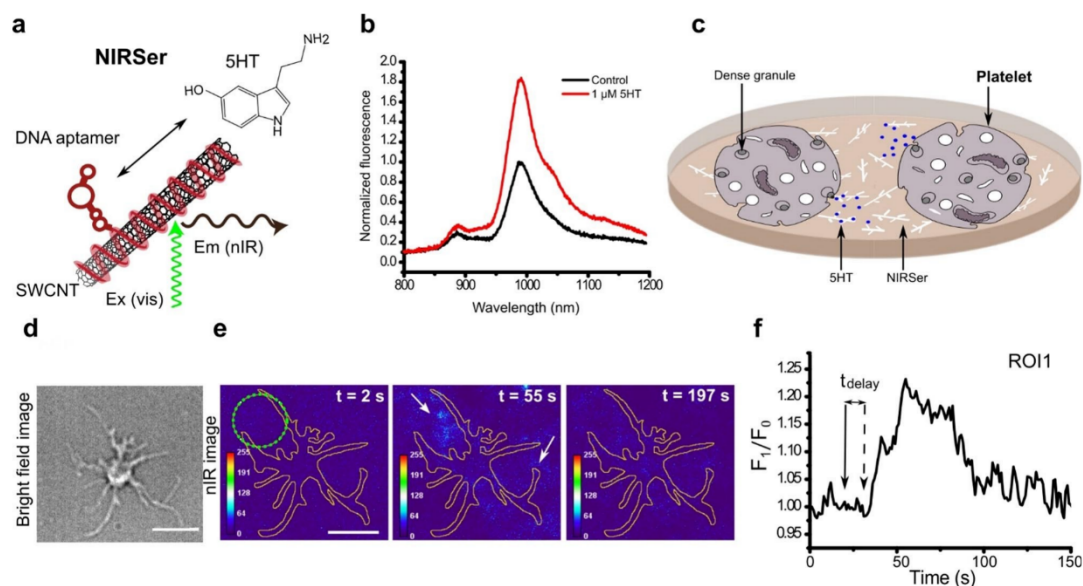


Figure 7. Near infrared fluorescent nanosensors for serotonin (NIRSer). **a**, Binding of serotonin to a serotonin-aptamer functionalized SWCNT leads to a change in aptamer conformation and, consequently, to an increase in the fluorescence of the SWCNT. **b**, Fluorescence spectrum of the nanosensor before and after addition of 1 μM serotonin showing 80% increase in fluorescence intensity. **c**, Schematic of how nanosensors and platelets were interfaced. Following platelet activation, serotonin is released and detected by the sensors. **d**, Bright field image of a single platelet adhered to a nanosensor coated surface. **e**, Color-coded nIR fluorescence images of the platelet in (e) before, during and after serotonin release. **f**, Fluorescence response from a ROI on the cell membrane showing a hotspot of serotonin release on the cell membrane, (green circle in image e). The scale bars are 5 μm. Adapted from reference [72] with permission. Copyright 2019 American Chemical Society.

1 Scientific Background

3.3 Polymer-based nanosensors

Polymer based fluorescent sensors have an intrinsically versatile structure. Most polymers used as sensors in biomedical applications are biocompatible and biodegradable. Furthermore, various recognition units can be covalently or non-covalently attached to the polymer backbone to amplify the fluorescent signal or enable multiplexing.^[74] For instance, several recognition units can be introduced in one nanosensor to increase the signal and sensitivity. One example, is a polymeric nanoparticle that was designed with fluorescent copolymers of fluorene and benzothiadiazole conjugated to phenylboronic acid units as dopamine recognition units. The advantage of this system is that each nanoparticle can have multiple dopamine binding sites. The sensing mechanism is most likely due to dopamine-induced fluorescence quenching. These fluorescent nanoparticles are biocompatible, selective for dopamine and have been successfully used in zebrafish embryos or larvae.^[75] The nanoparticles were taken up by cells, making the system suitable for directly labelling cells that contain dopamine. However, they cannot be applied as an efficient sensor to image dopamine release dynamics at high spatial resolution and to monitor signal transmission through dopamine secretion.^[75]

Polymers and polymer-coatings are widely studied in order to increase biocompatibility of nanoparticles or improve systemic circulation of the particles while avoiding detection by the immune system. For example, spherical nanoparticles with lipophilic core polymers and a biocompatible hydrophilic coating detected histamine *in vivo*.^[76] In this sensor, an amine binding ionophore binds histamine molecules to the core polymer, which changes the local pH and decreases the fluorescence of a pH sensitive fluorophore ($K_d = 1.9$ mM). This nanosensor enabled *in vivo* detection of histamine injections. While the plasma concentration of histamine is around 8 μ M, most cells contain compartments with 100 to 500 mM histamine, leading to high localized histamine concentrations during inflammatory processes. Therefore, such sensors would be useful to detect and image inflammatory processes in tissue.

4. Genetically encoded sensors

An alternative to external sensors is genetically encoded sensors, which are introduced into cells as genetic material. The introduced genetic material causes cells to produce proteins that facilitate a measurable response to dopamine, such as an increase in protein fluorescence. Such sensors are highly suitable for *in vivo* investigations, since the gene encoding a given sensor can be incorporated into the host genome. Sensor expression is therefore non-invasive, and genetic techniques allow for targeted expression in subpopulations of cells, such as neurons. Such approaches can take two forms: cell-based sensor systems and protein-based sensor systems.

A cell-based fluorescent sensor was designed by Muller *et al.*,^[77] named cell-based neurotransmitter fluorescent engineered reporters (CNiFERS). For this purpose, HEK293 Cell lines

were genetically engineered to express D2 dopaminergic receptors coupled to G_q proteins to trigger an intracellular calcium increase upon binding to dopamine. A FRET-based calcium indicator was also genetically encoded in the cells. Thus, when dopamine binds to the D2 receptor, a change in the FRET fluorescence signal indicates the presence of dopamine. These sensor cells (CNiFERS) were implanted in mice frontal cortex and dopamine release during behavioral conditioning was imaged.

One major advantage of this system is incorporating an endogenous sensor of dopamine (the D2 receptor) as the recognition unit. This means that the kinetics of the sensor, including sensitivity, binding affinity and detection range should be similar to that of endogenous dopamine receptors. The CNiFERS were sensitive and specific with $EC_{50} = 2.5 \pm 0.1$ nM, and a 30 times higher sensitivity for dopamine compared to norepinephrine. However, the temporal resolution of the sensor was on the scale of seconds and the spatial resolution was less than 100 μ m due to the size of the implanted HEK cells. Therefore, the spatiotemporal resolution of the sensor was not suitable for resolving release events at a sub-cellular level. Furthermore, the dynamic range was between 1 to 10 nM and the sensor saturated at concentrations close to 100 nM. At individual cells (single sensors), the response to dopamine was detected with 2.9 ± 0.2 s delay after dopamine pulse. The reversibility of the sensor was not instantaneous as the FRET signal would return to baseline in 20 s after a 2.5 s dopamine pulse, which makes detection of fast repetitive or changing dopamine signals more difficult.^[77]

The second approach employs engineered fluorescent proteins that bind to dopamine, which causes a direct increase in protein fluorescence. Thus, the protein is the sensor, rather than the whole cell in the case of CNiFERS. Genetically encoded proteins are much smaller than whole cells and therefore ideally suited to detect analytes on the surface or inside of cells. Therefore, there had been a lot of interest in developing a genetically encoded dopamine sensor. The sensor named dLight1 was designed and successfully used to image dopamine dynamics in deep regions of mice brain during behavioural studies (Figure 8).^[78] It consists of a genetically modified dopamine receptor that includes a circularly permuted GFP module from the genetically encoded calcium indicator GCaMP6 (see structure in Figure 8a). Upon binding of dopamine to its receptor, conformational changes of the receptor are translated to a change in fluorescence intensity of the GFP (Figure 8b). Two variants of the sensor have optimal dissociation constants of $K_d = 330 \pm 30$ nM for dLight1.1 and $K_d = 770 \pm 10$ nM for dLight1.2 (Figure 8c). The sensors are around 70 and 40 times more sensitivity to dopamine than norepinephrine and epinephrine. The maximum concentrations that were detected *in vivo* ranged from 10 μ M to 30 μ M, indicating proximity to the site of release.^[78] This sensor is therefore a useful tool especially for *in vivo* applications. dLight has comparable temporal resolution to cyclic voltammetry. Given the kinetics required for fast detection of dopamine (see Section 3.1) it remains to be seen if this sensor and related ones can detect fast and complex release patterns.

1 Scientific Background

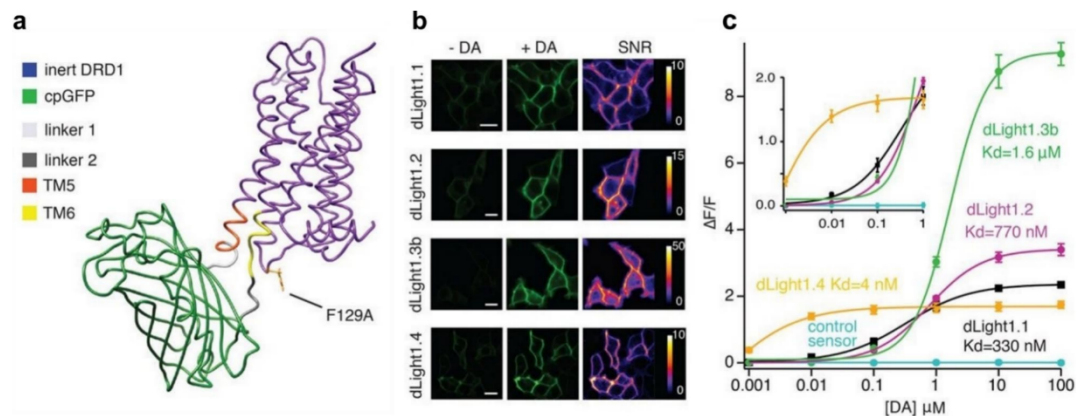


Figure 8. Genetically encoded fluorescent proteins as dopamine sensors. **a**, Structure of the genetically encoded fluorescent probe dLight1 consisting of a DRD1 receptor and cpGFP module. **b**, HEK cells expressing dLight variants. Fluorescence intensity and signal-to-noise ratio (SNR) with and without dopamine are shown. Scale bar = 10 μm . **c**, Calibration curve of various dLight sensors when expressed in HEK cells. Reproduced from reference [78] with permission. Copyright 2018 AAAS, American Association for the Advancement of Science.

Another group also developed a genetically-encoded fluorescent sensor based on the same premise, called GRABDA (G protein-coupled receptor [GPCR]-activation based DA).^[79] Two types of sensors were designed, one with a moderate apparent affinity to dopamine (DA1 m, EC_{50} = 130 nM) and another with a higher apparent affinity (DA1 h, EC_{50} = 10 nM). The EC_{50} of the sensors to norepinephrine was 1.7 μM and 97 nM respectively. The release of dopamine during conditioning behavioural tasks was monitored in mice. A temporal resolution of 100 ms and sub cellular spatial resolution was reported, which is comparable to cyclic voltammetry. When dopamine was applied to cultured cells, the on-rate of the sensor (fluorescence increase) for both DA1 m and DA1 h was fast (60 ± 10 ms for DA1 m and 140 ± 20 ms for DA1 h). However, the off-rate (fluorescence decrease) was slower (2.5 ± 0.3 s for DA1 h and 0.7 ± 0.06 s for DA1 m). In mouse brain slices expressing GRABDA sensors, electrical stimulation of cells produced a fluorescence increase with a rising time constants of 0.1 s for both sensors and decaying time constants of 17 s and 3 s for DA1 h and DA1 m respectively. Although the on-rate of the sensor was very fast, it seems that the slow decaying time of the sensor would preclude detection of fast, individual secretory events.

Genetically encoded sensors require introduction of foreign genetic material encoding the sensor into the host cells (e.g. neurons), usually using viral transduction. Although these genetically encoded sensors offer robust methods with high spatiotemporal resolution for laboratory studies of neural circuits, applying these methods in humans for diagnostic purposes might therefore face challenges because of safety concerns.

5. Fluorescent small molecules

Synthesis of fluorescence false neurotransmitters (FFNs) led to breakthroughs in understanding the kinetics of neurotransmitter uptake, storage and release in monoaminergic cells and neurons. These probes consist of fluorophores with chemical structures similar to neurotransmitters. Gubernator et al.,^[80] first

designed fluorescent molecules that are substrates of VMAT-2 (vesicular monoamine transporter) and mimic the structure of catecholamines. Therefore, they are differentially uptaken by VMAT-2 from the cytoplasm into vesicles and released through exocytosis when the cells are stimulated. Compared to the classical electrochemical-based methods, these molecular probes can visualise clusters of synaptic vesicles present in dopaminergic axons. FFNs also allowed detection of synaptic vesicle fusion with the plasma membrane upon stimulation of the cells, which is the mechanism by which dopamine is secreted. FFN511 was one of the first of such molecules designed. This molecule binds to VMAT2 in synaptic vesicles with an IC_{50} of 1 μM .^[80] However, FFNs are an indirect method because they mimic neurotransmitters rather than directly detecting endogenous monoamines.

6. Direct imaging of monoamines

Monoamines are weakly fluorescent when directly excited in the UV range, which can be used for direct catecholamine imaging. Using this approach in living organisms is challenging because of the phototoxicity of strong UV light. With this approach, living cells could be imaged with 305 nm laser excitation leading to emission at 350 nm and high spatial resolution (0.22 μm) as well as temporal resolution (50 ms). However, the autofluorescence of the cells at this emission range would confound selective and sensitive monoamine detection.^[81] One way to mitigate the UV induced damage to the living cells is to use multi-photon excitation. With two-photon microscopy the UV excitation wavelength is red shifted to longer wavelengths and three-photon microscopy can achieve excitation in the infrared range.^[83] Three-photon excitation (3PE) was employed to excite intrinsic UV fluorescence of dopamine, serotonin and tryptophan in the

1 Scientific Background

Table 2. Advantages and limitations of various monoamine sensors.

Monoamine sensors	Advantages	Limitations	Application	References
Fluorescent SWCNTs	Excellent spatial and parallel resolution, minimal bleaching and blinking, Near Infrared fluorescence in the tissue transparency window	Sensors need to be placed in the biological sample.	<i>In vitro</i> , Primary cells (platelets), brain slices	Kruss <i>et al.</i> , ^[61] Dinarvand <i>et al.</i> , ^[72] Beyenne <i>et al.</i> , ^[70]
Fluorescent polymer-based particles	Multivalent binding that increases selectivity.	Limited spatial and temporal resolution.	<i>In vitro</i> , cell culture, <i>In vivo</i>	Cash <i>et al.</i> , ^[76]
Fluorescent small molecules	High resolution at subcellular levels.	Indirect imaging, rapid bleaching.	Cell culture, Tissue sections	Gubernator <i>et al.</i> , ^[80]
Genetically encoded fluorescent receptors	Suitable temporal resolution, employment of biological monoamines receptors in the detection process.	Less spatial resolution than SWCNT sensors, the need for genetic manipulation.	<i>In vivo</i> , Live and freely moving animal models	Patriarchi <i>et al.</i> , ^[78] Sun <i>et al.</i> , ^[79]
UV imaging	Label free	Phototoxicity	<i>In vitro</i> , Cell culture	Tan <i>et al.</i> , ^[81]
PET and SPECT	Clinical application	Low spatial resolution, Expensive (needs a cyclotron on-site)	Clinical diagnosis and patient care	Beliveau <i>et al.</i> , ^[82]

infrared range. Monoamines (serotonin and dopamine) were visualized at granular level (concentrations above 50 mM) the theoretical spatial resolution was <200 nm in the radial directions and ~500 nm in the axial direction at 700 nm excitation wavelength.^[84] Overall, while UV imaging of monoamines does not require exogenous sensors it will be difficult to translate it to *in vivo* or *in vitro* studies in cells because of the extensive photo-damage by UV light, the weak fluorescence of monoamines and autofluorescence of cellular components in the same emission range.

7. Other non-fluorescent molecular imaging techniques

Radiotracers for PET (positron emission tomography) and SPECT (single photon emission computed tomography) can be used for catecholamine imaging.^[85] PET and SPECT are established *in vivo* imaging methods of monoaminergic pathways to understand the pathophysiology of many neurological and psychiatric disorders with broad clinical application, they are non-invasive and highly sensitive. In the case of PET and SPECT a radioactive tracer is injected and gamma rays are detected with 2D cross-sectional scans. A 3D image is then constructed from the 2D scans. However, PET and SPECT have extremely limited spatial resolution.^[86] For instance, a high resolution PET imaging system was investigated for constructing a human serotonin brain atlas, which increased the resolution of conventional PET scans from 4.4 mm to an approximate in-plane resolution of 2 mm.^[82]

8. Conclusion

Reliable, specific and fast detection of (monoamine) neurotransmitters in biological scenarios has been a major challenge in neuroscience and cell biology to date. The development of such cutting-edge analytical tools for neurotransmitter detection has therefore been a major research focus and the basis for breakthrough discoveries in our understanding of monoamine biology. While electrochemical detection methods have been leading the research on monoamines since the late 1970s, they have been unable to overcome certain limitations with respect to chemical selectivity and spatial resolution. Table 2 outlines the main advantages and disadvantages of the methods discussed in this paper. Recently developed fluorescence-based sensors, both those based on genetically encoded proteins and non-genetically encoded nanomaterials, provide powerful alternatives to older established methods. For example, carbon nanotube-based sensors for dopamine achieved desirable spatial resolution which is required for investigation of monoamine release on the level of individual cellular release sites. Due to their unique properties such as access to the nIR tissue transparency window, such nanosensors are highly promising materials for future studies in neuroscience. Even though translation of these methods into clinical scenarios to facilitate diagnosis and patient care is still a relatively long-term goal the emerging methods summarized in this review article will help to answer long-standing questions in cell biology and neuroscience.

1 Scientific Background

Acknowledgements

We thank the DFG for funding (Kr 4242/4-1). We thank Nils Brose for fruitful discussions and support. Open access funding enabled and organized by Projekt DEAL.

Conflict of Interest

The authors declare no conflict of interest.

Keywords: carbon nanotubes · catecholamines · fluorescence imaging · neuroscience · sensors

- [1] E. R. Travis, R. M. Wightman, *Annu. Rev. Biophys. Biomol. Struct.* **1998**, *27*, 77–103.
- [2] R. Jahn, D. Fasshauer, *Nature* **2012**, *490*, 201–207.
- [3] J. DeFelipe, L. Alonso-Nanclares, J. I. Arellano, *J. Neurocytol.* **2002**, *31*, 299–316.
- [4] J. R. Wickens, G. W. Arbuthnott, in *Handb. Chem. Neuroanat.*, Elsevier, **2005**, pp. 199–236.
- [5] R. Y. Moore, F. E. Bloom, *Annu. Rev. Neurosci.* **1979**, *2*, 113–168.
- [6] K. Racké, A. Reimann, H. Schwörer, H. Kilbinger, *Behav. Brain Res.* **1995**, *73*, 83–87.
- [7] I. Papa, D. Saliba, M. Ponzoni, S. Bustamante, P. F. Canete, P. Gonzalez-Figueroa, H. A. McNamara, S. Valvo, M. Grimbaldston, R. A. Sweet, H. Vohra, I. A. Cockburn, M. Meyer-Hermann, M. L. Dustin, C. Doglioni, C. G. Vinuesa, *Nature* **2017**, *547*, 318–323.
- [8] J. Bergquist, A. Tarkowski, R. Ekman, A. Ewing, *Proc. Mont. Acad. Sci.* **1994**, *91*, 12912–12916.
- [9] S. J. Cragg, C. Nicholson, J. Kume-Kick, L. Tao, M. E. Rice, *J. Neurophysiol.* **2001**, *85*, 1761–1771.
- [10] D. Sulzer, S. J. Cragg, M. E. Rice, *Basal Ganglia* **2016**, *6*, 123–148.
- [11] C. Liu, L. Kershberg, J. Wang, S. Schneeberger, P. S. Kaeser, *Cell* **2018**, *172*, 706–718.
- [12] J. A. Daniel, S. Galbraith, L. Iacovitti, A. Abdipranoto, B. Vissel, *J. Neurosci.* **2009**, *29*, 14670–14680.
- [13] L. Descarries, K. C. Watkins, S. Garcia, O. Bosler, G. Doucet, *J. Comp. Neurol.* **1996**, *375*, 167–186.
- [14] M. E. Rice, J. C. Patel, *Philos. Trans. R. Soc. London Ser. B* **2015**, *370*, 20140185.
- [15] J. D. Clements, R. A. Lester, G. Tong, C. E. Jahr, G. L. Westbrook, *Science* **1992**, *258*, 1498–1501.
- [16] S. J. Cragg, M. E. Rice, *Trends Neurosci.* **2004**, *27*, 270–277.
- [17] R. M. Wightman, L. J. May, A. C. Michael, *Anal. Chem.* **1988**, *60*, 769A–793A.
- [18] E. S. Bucher, R. M. Wightman, *Annu. Rev. Anal. Chem.* **2015**, *8*, 239–261.
- [19] N. Plock, C. Kloft, *Eur. J. Pharm. Sci.* **2005**, *25*, 1–24.
- [20] L. M. Borland, G. Shi, H. Yang, A. C. Michael, *J. Neurosci. Methods* **2005**, *146*, 149–158.
- [21] F. Gonon, R. Cespuglio, J. L. Ponchon, M. Buda, M. Jovet, R. N. Adams, J. F. Pujol, *C. R. Acad. Sci. Hebd. Seances Acad. Sci. D.* **1978**, *286*, 1203–1206.
- [22] R. M. Wightman, E. Strobe, P. M. Plotsky, R. N. Adams, *Nature* **1976**, *262*, 145.
- [23] P. T. Kissinger, J. B. Hart, R. N. Adams, *Brain Res.* **1973**, *55*, 209–213.
- [24] X. Li, J. Dunevall, A. G. Ewing, *Acc. Chem. Res.* **2016**, *49*, 2347–2354.
- [25] M. L. A. V. Heien, M. A. Johnson, R. M. Wightman, *Anal. Chem.* **2004**, *76*, 5697–5704.
- [26] J. L. Peters, L. H. Miner, A. C. Michael, S. R. Sesack, *J. Neurosci. Methods* **2004**, *137*, 9–23.
- [27] R. G. W. Staal, S. Rayport, D. Sulzer, in *Electrochem. Methods Neurosci.*, CRC Press/Taylor & Francis, **2007**.
- [28] I. Hafez, K. Kislér, K. Berberian, G. Dernick, V. Valero, M. G. Yong, H. G. Craighead, M. Lindau, *Proc. Natl. Acad. Sci. USA* **2005**, *102*, 13879–13884.
- [29] B. Zhang, M. L. A. V. Heien, M. F. Santillo, L. Mellander, A. G. Ewing, *Anal. Chem.* **2011**, *83*, 571–577.
- [30] A. Yakushenko, E. Kätelhön, B. Wolfrum, *Anal. Chem.* **2013**, *85*, 5483–5490.
- [31] O. C. Farokhzad, R. Langer, *ACS Nano* **2009**, *3*, 16–20.
- [32] D. Brabazon, *Chapter 04103 - Nanostructured Materials*, Elsevier, **2016**.
- [33] M. J. O'Connell, S. H. Bachilo, C. B. Huffman, V. C. Moore, M. S. Strano, E. H. Haroz, K. L. Rialon, P. J. Boul, W. H. Noon, C. Kittrell, J. Ma, R. H. Hauge, R. B. Weisman, R. E. Smalley, *Science* **2002**, *297*, 593–596.
- [34] G. Selvaggio, A. Chizhik, R. Nißler, L. Kuhlemann, D. Meyer, L. Vuong, H. Preiß, N. Herrmann, F. A. Mann, Z. Lv, T. A. Oswald, A. Spreinat, L. Erpenbeck, J. Großhans, K. Volker, A. Janshoff, J. Pablo Giraldo, S. Kruss, *Nat. Commun.* **2020**, *11*, 1495.
- [35] O. T. Bruns, T. S. Bischof, D. K. Harris, D. Franke, Y. Shi, L. Riedemann, A. Bartelt, F. B. Jaworski, J. A. Carr, C. J. Rowlands, M. W. B. Wilson, O. Chen, H. Wei, G. W. Hwang, D. M. Montana, I. Coropceanu, O. B. Achorn, J. Kloepper, J. Heeren, P. T. C. So, D. Fukumura, K. F. Jensen, R. K. Jain, M. G. Bawendi, *Nat. Biomed. Eng.* **2017**, *1*, 1–11.
- [36] S. Kruss, A. J. Hilmer, J. Zhang, N. F. Reuel, B. Mu, M. S. Strano, *Adv. Drug Delivery Rev.* **2013**, *65*, 1933–1950.
- [37] E. Polo, S. Kruss, *Anal. Bioanal. Chem.* **2016**, *408*, 2727–2741.
- [38] Q. Mu, H. Xu, Y. Li, S. Ma, X. Zhong, *Analyst* **2014**, *139*, 93–98.
- [39] J. Zhao, L. Zhao, C. Lan, S. Zhao, *Sensors Actuators B Chem.* **2016**, *223*, 246–251.
- [40] X. Zhang, X. Chen, S. Kai, H.-Y. Wang, J. Yang, F.-G. Wu, Z. Chen, *Anal. Chem.* **2015**, *87*, 3360–3365.
- [41] K. Fuxe, D. O. Borroto-Escuela, W. Romero-Fernandez, Z. Diaz-Cabiale, A. Rivera, L. Ferraro, S. Tanganelli, A. O. Tarakanov, P. Garriga, J. A. Narváez, F. Ciruela, M. Guescini, L. F. Agnati, *Front. Physiol.* **2012**, *3*, 136.
- [42] E. V. Mosharov, A. Borgkvist, D. Sulzer, *Mov. Disord.* **2015**, *30*, 45–53.
- [43] D. Meyer, A. Hagemann, S. Kruss, *ACS Nano* **2017**, *11*, 4017–4027.
- [44] C. Cha, S. R. Shin, N. Annabi, M. R. Dokmeci, A. Khademhosseini, *ACS Nano* **2013**, *7*, 2891–2897.
- [45] G. Hong, S. Diao, A. L. Antaris, H. Dai, *Chem. Rev.* **2015**, *115*, 10816–10906.
- [46] M. S. Dresselhaus, G. Dresselhaus, P. C. Eklund, A. M. Rao, in (Ed.: W. Andreoni), Springer Netherlands, Dordrecht, **2000**, pp. 331–379.
- [47] V. K. K. Upadhyayula, V. Gadhamshetty, *Biotechnol. Adv.* **2010**, *28*, 802–816.
- [48] G. Hong, S. Diao, J. Chang, A. L. Antaris, C. Chen, B. Zhang, S. Zhao, D. N. Atochin, P. L. Huang, K. I. Andreasson, *Nat. Photonics* **2014**, *8*, 723–730.
- [49] A. Spreinat, G. Selvaggio, L. Erpenbeck, S. Kruss, *J. Biophotonics* **2020**, *13*, 1–8.
- [50] R. Nißler, F. A. Mann, H. Preiß, G. Selvaggio, N. Herrmann, S. Kruss, *Nanoscale* **2019**, *11*, 11159–11166.
- [51] M. Zheng, A. Jagota, E. D. Semke, B. A. Diner, R. S. McLean, S. R. Lustig, R. E. Richardson, N. G. Tassi, *Nat. Mater.* **2003**, *2*, 338–342.
- [52] F. A. Mann, J. Horlebein, N. F. Meyer, D. Meyer, F. Thomas, S. Kruss, *Chem. Eur. J.* **2018**, *24*, 12241–12245.
- [53] G. Bisker, J. Dong, H. D. Park, N. M. Iverson, J. Ahn, J. T. Nelson, M. P. Landry, S. Kruss, M. S. Strano, *Nat. Commun.* **2016**, *7*, 1–14.
- [54] E. Polo, T. T. Nitka, E. Neubert, L. Erpenbeck, L. Vuković, S. Kruss, *ACS Appl. Mater. Interfaces* **2018**, *10*, 17693–17703.
- [55] J. Budhathoki-Uprety, J. D. Harvey, E. Isaac, R. M. Williams, T. V. Galassi, R. E. Langenbacher, D. A. Heller, *J. Mater. Chem. B* **2017**, *5*, 6637–6644.
- [56] J. D. Harvey, H. A. Baker, M. V. Ortiz, A. Kentsis, D. A. Heller, *ACS Sens.* **2019**, *4*, 1236–1244.
- [57] A. Hendler-Neumark, G. Bisker, *Sensors* **2019**, *19*, 5403.
- [58] F. A. Mann, Z. Lv, J. Grosshans, F. Opazo, S. Kruss, *Angew. Chem. Int. Ed.* **2019**, *58*, 11469–11473.
- [59] J. P. Giraldo, H. Wu, G. M. Newkirk, S. Kruss, *Nat. Nanotechnol.* **2019**, *14*, 541–553.
- [60] H. Wu, R. Nißler, V. Morris, N. Herrmann, P. Hu, S. J. Jeon, S. Kruss, J. P. Giraldo, *Nano Lett.* **2020**, *20*, 2432–2442.
- [61] S. Kruss, M. P. Landry, E. Vander Ende, B. M. A. Lima, N. F. Reuel, J. Zhang, J. Nelson, B. Mu, A. Hilmer, M. Strano, *J. Am. Chem. Soc.* **2014**, *136*, 713–724.
- [62] F. A. Mann, N. Herrmann, D. Meyer, S. Kruss, *Sensors* **2017**, *17*, 1521.
- [63] E. Polo, S. Kruss, *J. Phys. Chem. C* **2016**, *120*, 3061–3070.
- [64] R. Nißler, F. A. Mann, P. Chaturvedi, J. Horlebein, D. Meyer, L. Vuković, S. Kruss, *J. Phys. Chem. C* **2019**, *123*, 4837–4847.
- [65] S. Kruss, D. P. Salem, L. Vuković, B. Lima, E. Vander Ende, E. S. Boyden, M. S. Strano, *Proc. Mont. Acad. Sci.* **2017**, *114*, 1789–1794.
- [66] G. Bisker, J. Ahn, S. Kruss, Z. W. Ulissi, D. P. Salem, M. S. Strano, *J. Phys. Chem. C* **2015**, *119*, 13876–13886.
- [67] A. J. Lee, X. Wang, L. J. Carlson, J. A. Smydyer, B. Loesch, X. Tu, M. Zheng, T. D. Krauss, A. J. Lee, X. Tu, M. Zheng, T. D. Krauss, *Nano Lett.* **2011**, *11*, 1636–1640.

1 Scientific Background

- [68] A. J. Gillen, J. Kupis-Rozmysł Owicz, C. Gigli, N. Schuergers, A. A. Boghossian, *J. Phys. Chem. Lett.* **2018**, *9*, 4336–4343.
- [69] A. G. Godin, J. A. Varela, Z. Gao, N. Danné, J. P. Dupuis, B. Lounis, L. Groc, L. Cognet, *Nat. Nanotechnol.* **2017**, *12*, 238–243.
- [70] A. G. Beyene, K. Delevich, J. T. Del Bonis-O'Donnell, D. J. Piekarski, W. C. Lin, A. Wren Thomas, S. J. Yang, P. Kosillo, D. Yang, G. S. Prounis, L. Wilbrecht, M. P. Landry, *Sci. Adv.* **2019**, *5*, eaaw3108.
- [71] D. Meyer, S. Telele, A. Zelená, A. J. Gillen, A. Antonucci, E. Neubert, R. Nißler, F. A. Mann, L. Erpenbeck, A. A. Boghossian, S. Köster, S. Kruss, *Nanoscale* **2020**, *12*, 9104–9115.
- [72] M. Dinarvand, E. Neubert, D. Meyer, G. Selvaggio, F. A. Mann, L. Erpenbeck, S. Kruss, *Nano Lett.* **2019**, *19*, 6604–6611.
- [73] K. S. Hettie, T. E. Glass, *ACS Chem. Neurosci.* **2016**, *7*, 21–25.
- [74] H. N. Kim, Z. Guo, W. Zhu, J. Yoon, H. Tian, *Chem. Soc. Rev.* **2011**, *40*, 79–93.
- [75] C.-G. Qian, S. Zhu, P.-J. Feng, Y.-L. Chen, J.-C. Yu, X. Tang, Y. Liu, Q.-D. Shen, *ACS Appl. Mater. Interfaces* **2015**, *7*, 18581–18589.
- [76] K. J. Cash, H. A. Clark, *Sensors* **2012**, *12*, 11922–11932.
- [77] A. Muller, V. Joseph, P. A. Slesinger, D. Kleinfeld, *Nat. Methods* **2014**, *11*, 1245.
- [78] T. Patriarchi, J. R. Cho, K. Merten, M. W. Howe, A. Marley, W.-H. Xiong, R. W. Folk, G. J. Broussard, R. Liang, M. J. Jang, H. Zhong, D. Dombek, M. von Zastrow, A. Nimmerjahn, V. Gradinaru, J. T. Williams, L. Tian, *Science* **2018**, *360*, eaat4422.
- [79] F. Sun, J. Zeng, M. Jing, J. Zhou, J. Feng, S. F. Owen, Y. Luo, F. Li, H. Wang, T. Yamaguchi, Z. Yong, Y. Gao, W. Peng, L. Wang, S. Zhang, J. Du, D. Lin, M. Xu, A. C. Kreitzer, G. Cui, Y. Li, *Cell* **2018**, *174*, 481–496.e19.
- [80] N. G. Gubernator, H. Zhang, R. G. W. Staal, E. V. Mosharov, D. B. Pereira, M. Yue, V. Balsanek, P. A. Vadola, B. Mukherjee, R. H. Edwards, D. Sulzer, D. Sames, *Science* **2009**, *324*, 1441–1444.
- [81] W. Tan, V. Parpura, P. G. Haydon, E. S. Yeung, *Anal. Chem.* **1995**, *67*, 2575–2579.
- [82] V. Beliveau, M. Ganz, L. Feng, B. Ozenne, L. Højgaard, P. M. Fisher, C. Svarer, D. N. Greve, G. M. Knudsen, *J. Neurosci.* **2017**, *37*, 120–128.
- [83] B. K. Maity, S. Maiti, *Neuronal Signal.* **2018**, *2*, DOI 10.1042/ns20180132.
- [84] S. Maiti, J. B. Shear, R. M. Williams, W. R. Zipfel, W. W. Webb, *Science* **1997**, *275*, 530–532.
- [85] J. C. Soares, R. B. Innis, *Biol. Psychiatry* **1999**, *46*, 600–615.
- [86] V. Kaasinen, J. O. Rinne, *Neurosci. Biobehav. Rev.* **2002**, *26*, 785–793.

Manuscript received: March 27, 2020
Revised manuscript received: June 5, 2020
Accepted manuscript online: June 11, 2020

2 Results

2.1 Detection of Serotonin Exocytosis from Platelets

2.1.1 Manuscript

Near-Infrared Imaging of Serotonin Release from Cells with Fluorescent Nanosensors

Meshkat Dinarvand¹, Elsa Neubert^{1,2}, Daniel Meyer¹, Gabriele Selvaggio¹, Florian A. Mann¹, Luise Erpenbeck², and Sebastian Kruss^{1*}

¹Institute of Physical Chemistry, Göttingen University, Göttingen 37077, Germany

²Department of Dermatology, Venereology, and Allergology, University Medical Center, Göttingen 37075, Germany

Publication Date: August 16, 2019

<https://doi.org/10.1021/acs.nanolett.9b02865>

This manuscript was published in Nano Letter by American Chemical Society

Reprinted with permission from {Nano Lett. 2019, 19, 9, 6604–6611}. Copyright {2019} American Chemical Society."

Near-Infrared Imaging of Serotonin Release from Cells with Fluorescent Nanosensors

Meshkat Dinarvand,[†] Elsa Neubert,^{†,‡} Daniel Meyer,[†] Gabriele Selvaggio,[†] Florian A. Mann,[†] Luise Erpenbeck,[‡] and Sebastian Kruss^{*,†,‡}

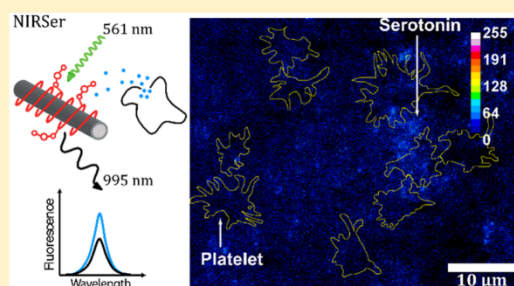
[†]Institute of Physical Chemistry, Göttingen University, Göttingen 37077, Germany

[‡]Department of Dermatology, Venereology, and Allergology, University Medical Center, Göttingen 37075, Germany

Supporting Information

ABSTRACT: Serotonin is an important neurotransmitter involved in various functions of the nervous, blood, and immune system. In general, detection of small biomolecules such as serotonin in real time with high spatial and temporal resolution remains challenging with conventional sensors and methods. In this work, we designed a near-infrared (nIR) fluorescent nanosensor (NIRSer) based on fluorescent single-walled carbon nanotubes (SWCNTs) to image the release of serotonin from human blood platelets in real time. The nanosensor consists of a nonbleaching SWCNT backbone, which is fluorescent in the beneficial nIR tissue transparency window (800–1700 nm) and a serotonin binding DNA aptamer. The fluorescence of the NIRSer sensor (995 nm emission wavelength for (6,5)-SWCNTs) increases in response to serotonin by a factor up to 1.8. It detects serotonin reversibly with a dissociation constant of $301 \text{ nM} \pm 138 \text{ nM}$ and a dynamic linear range in the physiologically relevant region from 100 nM to $1 \mu\text{M}$. As a proof of principle, we detected serotonin release patterns from activated platelets on the single-cell level. Imaging of the nanosensors around and under the platelets enabled us to locate hot spots of serotonin release and quantify the time delay ($\approx 21\text{--}30 \text{ s}$) between stimulation and release in a population of platelets, highlighting the spatiotemporal resolution of this nanosensor approach. In summary, we report a nIR fluorescent nanosensor for the neurotransmitter serotonin and show its potential for imaging of chemical communication between cells.

KEYWORDS: Carbon nanotubes, aptamer, biosensors, serotonin, near-infrared fluorescence, biophotonics



Detection of signaling molecules with high spatial and temporal resolution is essential to understand biochemical signaling between cells.^{1,2} Due to their size and novel optoelectronic properties, nanomaterials can provide solutions to engineer nanoscale sensors that perform this task.^{3–8} A very important class of signaling molecules are neurotransmitters such as serotonin. Most serotonin sensors are electrochemical sensors and use carbon electrodes, polypyrrole-modified electrodes, or carbon nanomaterial-coated electrodes to enhance sensitivity.^{9–11} The disadvantage of an electrode-based approach is the limited (parallel) spatial resolution, biofouling, and cross-reactivity to molecules of similar redox potential.^{12,13} In contrast, optical methods could fulfill several figures of merit such as having high temporal and spatial resolution, being less-invasive and potentially more biocompatible. One example of a fluorescence-based approach is a coumarin-3-aldehyde scaffold, which binds serotonin and changes its fluorescence.¹⁴ It was used to label catecholamine containing vesicles, but, as with all organic dyes, it suffers from bleaching. Nanoscale fluorescent sensors could overcome the challenges in serotonin detection and promise a high spatiotemporal resolution.

Single-walled carbon nanotubes (SWCNTs) have many unique properties that are beneficial for biosensing, imaging, and delivery applications.^{15,16} Semiconducting SWCNTs fluoresce in the near-infrared (nIR) tissue transparency window of the spectrum (800–1700 nm) and do not bleach.¹⁷ Additionally, their high surface area allows various surface functionalization schemes either through direct functionalization or coating with DNA, peptides, or polymers.^{18–23} Such approaches allow the study of conformational changes of single molecules on SWCNTs.²⁴ Previously, functionalized SWCNTs have been used as biosensors for various important biomolecules such as reactive oxygen species, proteins, sugars, and small signaling molecules.^{3,25–28} For example, certain DNA wrapped SWCNTs change their fluorescence in response to the neurotransmitter dopamine and reveal its release from neurons.^{29,30} The selectivity and sensitivity of these dopamine sensors depend on the exact DNA sequence, and short (GT)

Received: July 14, 2019

Revised: August 14, 2019

Published: August 16, 2019

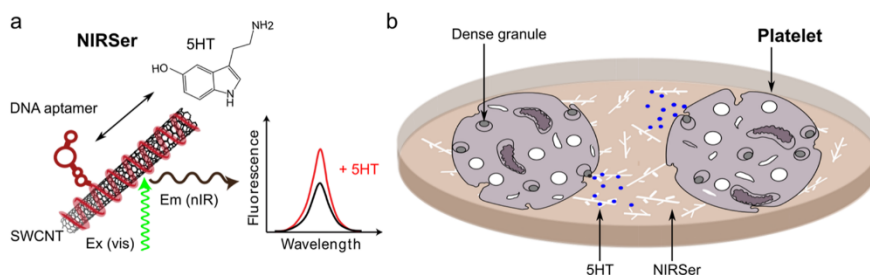


Figure 1. Design principle of the NIR fluorescent serotonin nanosensor NIRSer. (a) Serotonin (5HT) binds to the NIRSer, leading to a change in aptamer conformation and consequently an increase in the fluorescence of the SWCNT. (b) Schematic of adhering platelets on top of a NIRSer-coated surface. When activated, platelets release serotonin from dense granules, and the image of the sensors reveals the spatiotemporal concentration change.

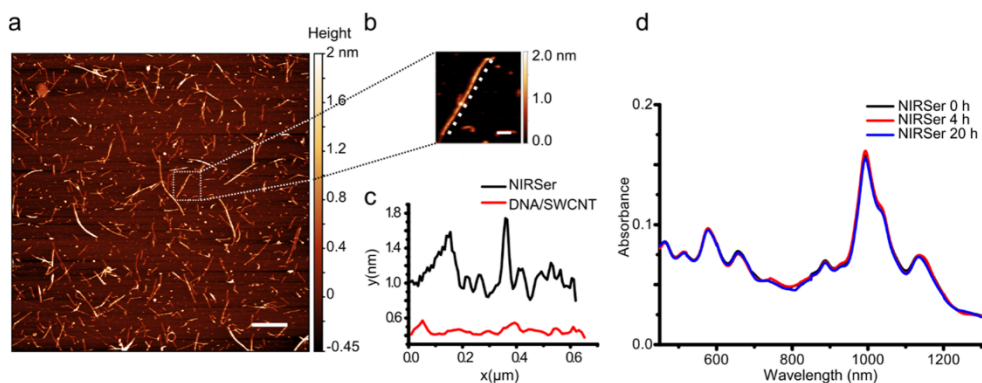


Figure 2. NIRSer characterization and stability. (a) AFM of NIRSers shows homogeneous functionalized carbon nanotubes. Scale bar is $1 \mu\text{m}$. (b) AFM image of a single SerApt functionalized SWCNT. The dotted line represents the AFM height trace of the NIRSer (axis offset of 4 pixels for clarity). Scale bar is 100 nm . (c) Height profile along the length of the NIRSer shown in (b) compared to a $(\text{GT})_{15}$ ssDNA wrapped SWCNT. (d) Absorbance spectra of NIRSer (in PBS) at 0, 4, and 20 h after preparation, showing the long-term stability.

repeats, for example $(\text{GT})_{10}$, appear to have the lowest dissociation constant.^{31,32} The mechanism of this sensor was attributed to conformational changes of the phosphate groups upon dopamine binding.^{29,31,33} In order to further expand sensing to other targets, conjugation of high-affinity recognition units was employed, such as small peptides to target cell surface receptors or the conjugation of nanobodies.^{34,35} Protein-based recognition units such as antibodies and nanobodies are highly specific for their target, but there are also potential drawbacks such as cost of production, stability, and size. Another class of recognition units are aptamers that are identified through processes such as systematic evolution of ligands by exponential enrichment (SELEX).³⁶ Aptamers provide beneficial properties, for example, simple synthesis, high stability, and small size compared to other recognition units.³⁷ Aptamer functionalized SWCNT nanosensors have been previously explored to detect macromolecules, peptides like insulin, and certain proteins.^{38,39} For example, an electrical biosensor was designed based on aptamer functionalized carbon nanotubes to simultaneously detect three different analytes in real time.⁴⁰ Recently, a serotonin-specific aptamer was developed and attached to a field-effect transistors (FET) for efficient detection of serotonin.⁴¹ We employed the same sequence to our design to produce a NIR fluorescent nanosensor for detection and imaging of serotonin.

Serotonin is a neurotransmitter responsible for modulating the brain activity, but it is also involved in many other important biological functions in the immune system,⁴² blood homeostasis, and the gastrointestinal function.⁴³ Despite the huge role that serotonin plays in the central nervous system (CNS), more than 90% of serotonin is produced outside of the nervous system by enterochromaffin cells (ECs) and stored in platelets.⁴⁴ Platelets are the second most abundant cells in the blood and participate in a wide range of activities. Blood platelets take up serotonin released by ECs in the gastrointestinal tract and store them in dense granules. It has been shown that apart from maintaining the vascular integrity, platelets contribute to many important functions. Platelet-derived serotonin is involved in blood pressure homeostasis,⁴⁵ blood pH homeostasis, fibrosis,⁴⁶ vasculature permeability and reactivity,⁴⁷ organ development and regeneration, and many immune responses.^{48,49} The role of serotonin signaling in the blood system is not well understood, and one reason is the lack of appropriate techniques to reveal it with high spatial and temporal resolution.

In this work, we have designed a serotonin-selective nanosensor (NIRSer) based on SWCNTs functionalized with a serotonin binding DNA aptamer.⁵⁰ The serotonin aptamer is wrapped around the SWCNT, producing a corona phase which disperses the highly hydrophobic SWCNT in aqueous solution and mediates the interaction with serotonin and a change in

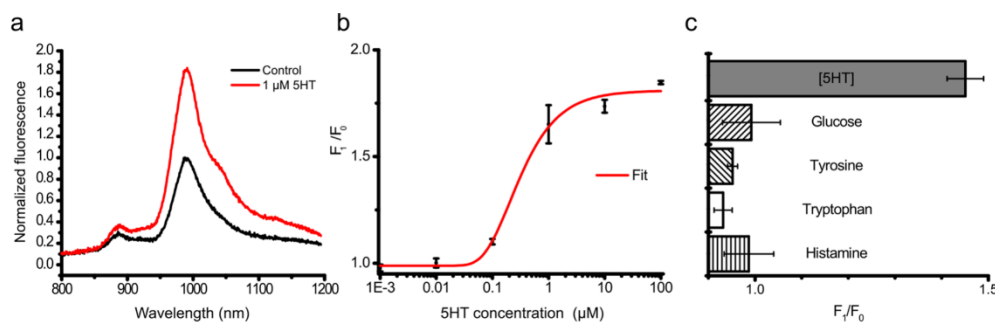


Figure 3. Sensitivity and selectivity of NIRSer. (a) Fluorescence spectrum of NIRSers in PBS before and after addition of 1 μM serotonin (SHT) indicating $\approx 80\%$ increase in fluorescence intensity. (b) Calibration curve as measured by the fluorescence intensity ratios at the 995 nm emission peak before (F_0) and after addition of serotonin (F_1). The red line corresponds to a five-parameter logistic curve fit. K_d value was $0.307 \mu\text{M} \pm 0.138 \mu\text{M}$. (c) Response to potentially interfering molecules (100 nM). All data are mean values \pm SEM of at least $N = 3$.

fluorescence intensity (Figure 1a). These nanosensors are then placed around and under serotonin releasing cells, and the collective image of many of them provides novel insights into serotonin release patterns with unprecedented spatial resolution (Figure 1b).

The NIRSers were prepared by a noncovalent functionalization approach of (6,5)-chirality enriched SWCNTs (emission maximum around 995 nm) with the mentioned serotonin aptamer (SerApt).⁵⁰ This aptamer contains a linear tail that does not contribute to the three-dimensional (3D) structure, and we hypothesized that this part would wrap around and disperse the SWCNTs. The functional part of the aptamer could still bind the target molecule leading to conformational changes of the DNA corona and consequently a fluorescence change. We previously showed that for DNA/SWCNT-based dopamine sensors, the conformational change of the DNA affects exciton decay routes most likely through changes in exposure to water and ions.^{29,33} Therefore, we expect a similar mechanism for the approach presented here.

Atomic force microscopy (AFM) images confirmed the fabrication of homogeneous non-aggregated single NIRSers (Figure 2a). The height profile of NIRSer compared to normal ssDNA wrapped SWCNT indicated additional features, which we attributed to the secondary structure of the serotonin aptamer (Figure 2b,c). Absorption spectra in phosphate buffered saline (PBS) showed stable dispersions with a (6,5) chirality S_{11} absorption maximum at ≈ 995 nm, which indicates that the extended structure of the aptamer does not decrease colloidal stability (Figure 2d and Figure S1). There is no sign of aggregation 4 h and >20 h after preparation of the NIRSer. A ζ -potential of -28.6 ± 2.8 mV further supported colloidal stability (Figure S2). All these data indicate that SerApt adsorbs onto SWCNTs and forms stable and monodisperse conjugates.

Next, we investigated the SerApt functionalized SWCNTs response to serotonin and other molecules. Addition of 1 μM serotonin in PBS increased the fluorescence intensity by $\approx 80\%$ (Figure 3a). Therefore, we named these SerApt functionalized SWCNTs NIRSer sensors. The corresponding calibration curve in the range from 1 nM to 100 μM is shown in Figure 3b. Here, the normalized increase in fluorescence intensity at the maximum emission peak (995 nm) was recorded in PBS (Figure 3b). The dissociation constant was determined to be $307 \text{ nM} \pm 138 \text{ nM}$ by fitting a five-parameter logistic function (red line, Figure 3b). The (linear) dynamic range of this sensor

is 100 nM and 1 μM , which is a desirable range to detect release events from serotonin secreting cells⁵¹ and serotonergic neurons (Figure S3c).⁵² Additional information about the sensor's dynamic range can be found in Figure S3. Furthermore, the 2D excitation–emission spectra of the NIRSer before and after addition of 1 μM serotonin were obtained (Figure S4). The results showed that other SWCNT chiralities besides (6,5)-SWCNTs also responded to serotonin.⁵³

We also determined the selectivity of the nanosensor by studying the fluorescence response of the nanosensors to other molecules that have a similar structure to serotonin such as tryptophan (the precursor of serotonin biosynthesis), histamine (secretory product of platelets), tyrosine, and glucose as an abundant molecule in the plasma that could potentially interfere with the response to serotonin. As shown in Figure 3c, NIRSers are highly selective to serotonin, and there is no significant change in the fluorescence emission pattern after addition of the other molecules. We further analyzed the selectivity of NIRSers to observe whether the serotonin response is due to unspecific displacement of DNA aptamer in response to changes in the environment or specific interactions. Therefore, we compared the serotonin response of the NIRSers to a SWCNT functionalized with a scrambled DNA sequence of the same nucleotide composition. These DNA functionalized SWCNTs did not respond to serotonin at all (Figure S5).

NIRSers also respond to a smaller extent to the neurotransmitter dopamine (11% increase at 100 nM) compared to 45% increase of serotonin (Figure S5). This result is expected because it is known that hydroxy groups of the catecholamines interact with most ssDNA sequences on SWCNTs and lead to a change in fluorescence intensity.^{32,33} This phenomenon is similar to biological receptors that bind to an array of ligands and discriminate between molecules partly due to the local concentration of the ligand. For instance, in one study, the binding of serotonin and dopamine to serotonin type 3 (5-HT₃) receptors was investigated, and the EC_{50} of $2.7 \pm 0.2 \mu\text{M}$ and $195 \pm 16 \mu\text{M}$ was calculated for serotonin and dopamine, respectively.⁵⁴ Thus, NIRSer provides an affinity/selectivity for serotonin similar to a biological receptor. Furthermore, we expect that this cross-reactivity would not pose a significant problem especially in blood cells, as cells that secrete both serotonin and other biogenic amines are not known. Along the same lines serotonergic and dopaminergic

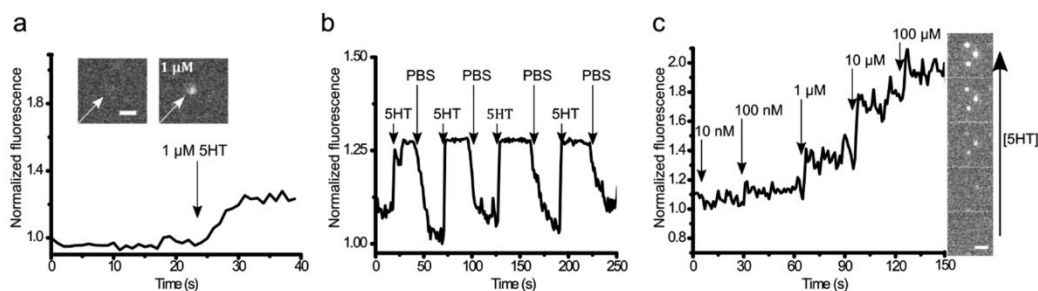


Figure 4. Reversibility and single nanosensor imaging. (a) Fluorescence trace of a single NIRSer during addition of $1 \mu\text{M}$ serotonin (SHT). The inset shows the image of this single NIRSer (white arrow) before and after addition of SHT. (b) Reversibility shown by alternating between $1 \mu\text{M}$ serotonin solution and PBS solution in a flow chamber. The trace is the average of a small NIRSer coated area ($0.55 \mu\text{m}^2$, 145 pixels). (c) Step by step increase in fluorescence intensity of single NIRSers in response to increasing concentrations of serotonin (10 nM to $100 \mu\text{M}$) in PBS. All scale bars are $1 \mu\text{m}$.

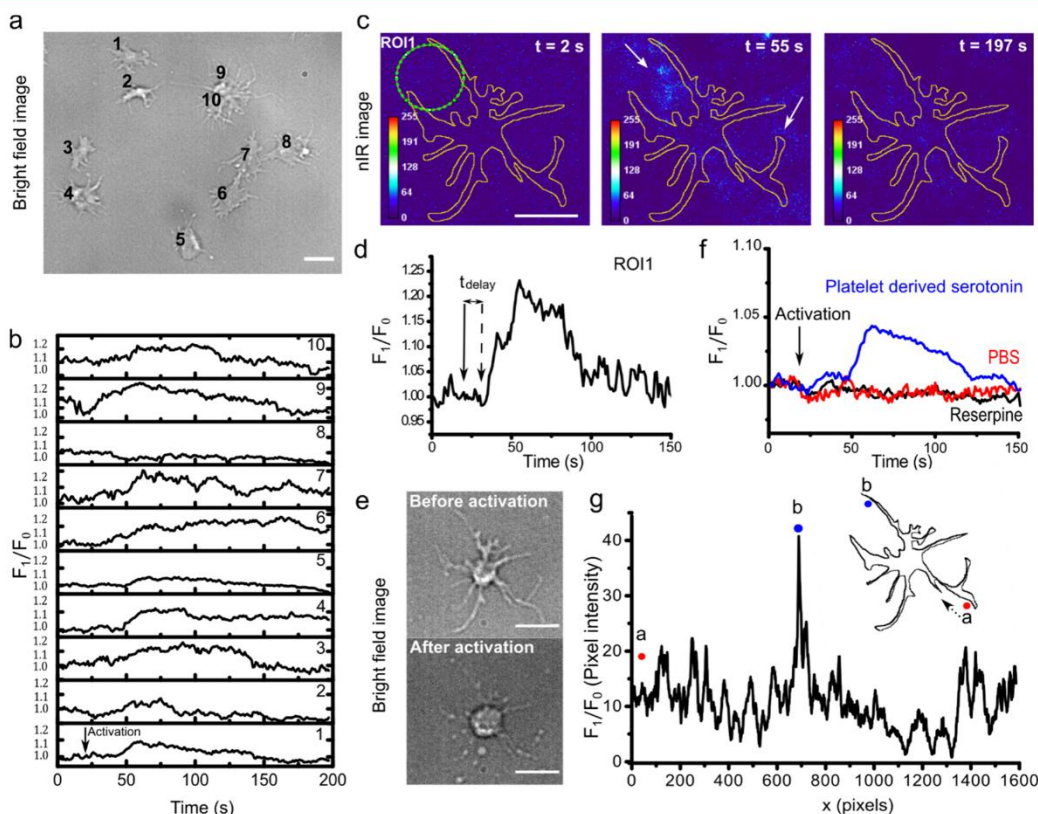


Figure 5. Spatiotemporal imaging of serotonin release from platelets. (a,b) Bright-field image of platelets and fluorescence responses (from the area under the cell). Fluorescence responses are normalized to the starting intensity F_0 . Scale bar corresponds to $10 \mu\text{m}$. (c) Color-coded nIR response images of a single adherent platelet on a NIRSer-coated surface at three time points (before, during and after serotonin release). (d) Fluorescence response from a ROI (green circle in c). The straight arrow denotes the activation time point ($t \approx 20 \text{ s}$) and the dashed arrow onset of release, defining the delay time T_{delay} (see Figure S9 for statistics). (e) Bright-field images of the platelet analyzed in (c) before and after activation. (f) Serotonin response (complete field of view, multiple cells) after addition of ionomycin (positive control, blue), after addition of PBS (negative control, red), and after addition of ionomycin to cells pretreated with reserpine (negative control, black). (g) Serotonin response ($t = 55 \text{ s}$) along the border (10 pixel wide ribbon) of the platelet shown in (c) starting at position a (clockwise). Peaks indicate hot spots of serotonin release. All scale bars represent $5 \mu\text{m}$ unless otherwise stated.

neurons occupy distinct regions in the brain, and the basal concentration of these amines in the circulation is minimal.

We aimed to design a nanoscale sensing system for biomedical applications. Therefore, it should be reversible to

record multiple events. Additionally, it is necessary that even single sensors respond and not just the ensemble in solution. Therefore, the sensors were immobilized on a glass surface in such a way that single sensors could be resolved (Figure S7c). In Figure 4a, the fluorescence response of a single NIRSer to 1 μM serotonin is shown.

To investigate the reversibility of the sensor, the nIR fluorescence response in flow chambers with alternating serotonin (1 μM) and buffer (PBS) exposure was analyzed. There was a distinct fluorescence increase of $\approx 25\%$ when serotonin (1 μM) was flowing through the chamber coated with sensors. Interestingly, when serotonin solution was exchanged to buffer, the fluorescence intensity decreased to the initial value (Figure 4b). This exchange between serotonin and PBS was repeated multiple times. The small differences in the baseline were attributed to focus changes and potential drift in the optical setup. These results show that NIRSer is a reversible sensor and not based on an irreversible displacement of the aptamer from the SWCNT surface. On the single sensor level, one can furthermore observe the stepwise increase in fluorescence with serotonin concentration (Figure 4c) expected from the calibration curve in solution (Figure 3b). These findings demonstrate that single NIRSers report reversibly about the local concentration of serotonin even with a certain serotonin background.

Activated platelets interact and communicate with various blood cells. These interactions result in platelet degranulation and secretion. Platelet granules store more than 300 distinct molecules, including small molecules and, proteins⁵⁵ that could prompt progression or suppression of critical events such as metastasis, inflammation, and immune response.

We verified the presence of serotonin-containing vesicles by staining with FFN511, a fluorescent false neurotransmitter that is transported similar to serotonin by vesicular monoamine transporter 2 (VMAT2) (Figure S6).⁵⁶ Many of the molecules released from platelets have contradictory functions. This highlights the importance of studying how the release events happen and their distinct pattern in space and time. With our newly designed serotonin sensor, we aimed to visualize release events with high spatial resolution at a single-cell level and pinpoint release spots around the cell membrane. Platelets isolated from human blood (see Supporting Information) were incubated on a NIRSer-coated glass surface additionally coated with fibrinogen (human type 1) to facilitate integrin-mediated platelet adhesion (Figure 5a, see Figure S7 for sensor density). Non-adherent platelets were washed away. To activate platelets, ionomycin, an ionophore that increases the cytosolic $[\text{Ca}^{2+}]$ and activates cells, was added to the medium, and image sequences were captured in a custom-built nIR fluorescence microscope at 1 frame per second or faster (see Supporting Information). Figure 5b shows the fluorescence response traces of the sensors under the cells (+2 μm margin outside each cell) for the 10 cells shown in the bright-field image in Figure 5a.

These traces contain information about the release pattern such as onset of release and differences between cells. Out of the 10 cells in Figure 5a, 9 cells showed significant fluorescence increases. The onset of release (T_{delay} , defined as the time lag between activation of platelets and the first significant peak) in cells that were stimulated at the same time varied significantly (see traces Figure 5b and quantification in Figure S9). Around 50% of the cells released serotonin within 21–30 s after stimulation. However, there was a broad distribution (3–34 s),

which could only be detected because with optical nano-sensors, multiple cells can be imaged at the same time. This cellular behavior is different from neurons that respond much faster to stimuli.

The spatial resolution of our fluorescent nanosensors allowed to further study the release patterns from single cells (Figures 5c, Figure S7). For example, a region of interest (ROI) close to the surface of the platelet was selected to analyze serotonin secretion (ROI1 in Figure 5c). At $t = 20$ s, ionomycin (1 μM) was added, and at around $t = 35$ s, the sensor's fluorescence intensity in this area started to increase (Figure 5d). This spike in fluorescence indicates a local increase in serotonin concentration near the surface of the cell due to degranulation of platelets and secretion of serotonin. The fluorescence remained at the same level until around $t = 85$ s before it decreased again. This observation suggests that serotonin stored in the dense granules requires a certain time to be released, probably because the vesicles are transported to the cell membrane. The sensor response decreases on the seconds time scale because of the slow sensor off rates (Figure 4 b) and because serotonin needs to diffuse away.² The fluorescence intensity did not decrease to its original value because of the remaining serotonin levels in the medium. Further analysis of a single platelet is presented in Figure S7f. Negligible fluorescent signals are observed before activation with ionomycin probably due to background serotonin leakage. However, starting from $t = 26$ –30 s, a significant increase in fluorescence is visible in localized regions around the border of the cell highlighting hotspots of serotonin secretion. In Figure 5c and Figure S7b, there are isolated regions with increased fluorescence response that appear to be further away from a platelet. However, those regions were actually adjacent to platelets that were outside the field of view. The full images with the cropped regions can be seen in Figure S8.

As negative control, we studied the fluorescence response of platelets pretreated with reserpine (incubation for 60 min), an irreversible VMAT2 inhibitor which depletes granules from serotonin.⁵⁷ We also studied the fluorescent signals from a control sample that received PBS instead of ionomycin. The sensors indicated no serotonin release on platelet-coated surfaces that were exposed to PBS or reserpine treated platelets exposed to ionomycin. In contrast, the fluorescence intensity of ionomycin activated cells increased by around 4.5% (Figure 5f). Note that the spike in fluorescence intensity would be significantly higher at release hotspots, but even the average intensity of an entire image shows an increase during serotonin secretion.

There is additional information provided by NIRSer sensors. The spatial resolution allows to analyze the fluorescence response around the cell border, which is the most important part for communication with other cells. Figure 5g shows the fluorescence response at the cell border (10 pixel ribbon corresponding to around 600 nm) of the platelet shown in Figure 5c at $t = 55$ s. This trace around the cell was not homogeneous. For instance, at point b (blue dot), a maximum indicated a hot spot of serotonin secretion, which can also be seen in the color-coded image in Figure 5c. Therefore, NIRSer sensors clearly identify localized release spots around the platelet with high spatial resolution (restricted by the pixel size to 60 nm and by the Abbe limit to around 500 nm).

Activation and degranulation of platelets go furthermore hand in hand with changes in adhesion and morphology (Figure 5e, Figure S7d). In order to check whether platelets

were indeed functional on our nanosensor surface, we investigated the adhesion area of platelets by reflection interference contrast microscopy (RICM) imaging. Platelets quickly adhered to the nanosensor-coated surface and underwent a typical morphological change from discoid shape to pseudopodia, essential for their function (Figure S10).

These experiments show the potential of fluorescent nanosensors to reveal new insights in serotonin signaling by human platelets and beyond. The great advantage compared to electrochemical electrode-based approaches is the additional spatial information (on single cell level) and the amount of data (multiple cells at the same time) that can be collected. In the experiments shown above, there were approximately 1000 pixels under one platelet (length of one pixel \approx 63 nm). Every pixel can be seen as a local sensor corresponding to one or more NIRSer sensors even though the optical resolution limit convolutes the signal. Consequently, it is possible to analyze serotonin release patterns with subcellular nanoscale resolution simultaneously in multiple cells. In the future, these SWCNT-based serotonin sensors could be further improved by fine-tuning the ssDNA sequence, as it had been shown for SWCNT-based dopamine sensors.³² Additionally, the use of monochiral SWCNTs could further increase signal/noise ratios.⁵³ This work highlights how the properties of a nanomaterial enables a powerful tool for biomedical research. As such, SWCNTs have been used, for example, in neuroscience to image dopamine release from single cells/brain slices or to study mechanical properties of cells or tissue.^{29,58–60} Serotonin is an important signaling molecule, and the serotonin sensor presented in this work will allow researchers to study its physiological role in much greater detail, for example, the cross-talk between platelets and immune cells during inflammation or coagulation.

In conclusion, we created a near-infrared fluorescent nanosensor (NIRSer) to visualize release of the neurotransmitter serotonin. We used its high sensitivity and new level of spatiotemporal resolution to gain novel insights into serotonin release by human blood platelets. This nanosensor has the potential to reveal in great detail how cells shape chemical signals in space and time to exchange information.

■ ASSOCIATED CONTENT

📄 Supporting Information

The Supporting Information is available free of charge on the ACS Publications website at DOI: [10.1021/acs.nanolett.9b02865](https://doi.org/10.1021/acs.nanolett.9b02865).

Experimental details, characterization figures, additional sensor response data (PDF)

■ AUTHOR INFORMATION

Corresponding Author

*E-mail: skruss@uni-goettingen.de.

ORCID

Sebastian Kruss: [0000-0003-0638-9822](https://orcid.org/0000-0003-0638-9822)

Notes

The authors declare no competing financial interest.

■ ACKNOWLEDGMENTS

This project was supported by the state of Lower Saxony (life@nano). Part of this work was supported by the Cluster of Excellence and DFG Research Center Nanoscale Microscopy

and Molecular Physiology of the Brain (CNMPB) and a DFG grant (Kr 4242/4-1). The authors thank Anna Zelená and Sarah Köster for help with platelets.

■ REFERENCES

- (1) Thurley, K.; Gerecht, D.; Friedmann, E.; Höfer, T. Three-Dimensional Gradients of Cytokine Signaling between T Cells. *PLoS Comput. Biol.* **2015**, *11* (4), No. e1004206.
- (2) Meyer, D.; Hagemann, A.; Kruss, S. Kinetic Requirements for Spatiotemporal Chemical Imaging with Fluorescent Nanosensors. *ACS Nano* **2017**, *11* (4), 4017–4027.
- (3) Kruss, S.; Hilmer, A. J.; Zhang, J.; Reuel, N. F.; Mu, B.; Strano, M. S. Carbon Nanotubes as Optical Biomedical Sensors. *Adv. Drug Delivery Rev.* **2013**, *65* (15), 1933–1950.
- (4) Polo, E.; Kruss, S. Nanosensors for Neurotransmitters. *Anal. Bioanal. Chem.* **2016**, *408* (11), 2727–2741.
- (5) Kim, E. H.; Chin, G.; Rong, G.; Poskanzer, K. E.; Clark, H. A. Optical Probes for Neurobiological Sensing and Imaging. *Acc. Chem. Res.* **2018**, *51* (5), 1023–1032.
- (6) Rong, G.; Corrie, S. R.; Clark, H. A. In Vivo Biosensing: Progress and Perspectives. *ACS Sensors* **2017**, *2* (3), 327–338.
- (7) Jeon, S.-J.; Kwak, S.-Y.; Yim, D.; Ju, J.-M.; Kim, J.-H. Chemically-Modulated Photoluminescence of Graphene Oxide for Selective Detection of Neurotransmitter by “Turn-On” Response. *J. Am. Chem. Soc.* **2014**, *136* (31), 10842–10845.
- (8) Robinson, J. T.; Wu, J. Z.; Zhang, B.; Hong, G.; Dai, H.; Wang, H. Three-Dimensional Imaging of Single Nanotube Molecule Endocytosis on Plasmonic Substrates. *Nat. Commun.* **2012**, *3* (1), 700–709.
- (9) Shiigi, H.; Okamura, K.; Kijima, D.; Deore, B.; Sree, U.; Nagaoka, T. An Overoxidized Polypyrrole/Dodecylsulfonate Micelle Composite Film for Amperometric Serotonin Sensing. *J. Electrochem. Soc.* **2003**, *150* (5), H119–H123.
- (10) Goyal, R. N.; Oyama, M.; Gupta, V. K.; Singh, S. P.; Sharma, R. A. Sensors for 5-Hydroxytryptamine and 5-Hydroxyindole Acetic Acid Based on Nanomaterial Modified Electrodes. *Sens. Actuators, B* **2008**, *134* (2), 816–821.
- (11) Han, H. S.; You, J.-M.; Jeong, H.; Jeon, S. Synthesis of Graphene Oxide Grafted Poly(Lactic Acid) with Palladium Nanoparticles and Its Application to Serotonin Sensing. *Appl. Surf. Sci.* **2013**, *284*, 438–445.
- (12) Manica, D. P.; Mitsumori, Y.; Ewing, A. G. Characterization of Electrode Fouling and Surface Regeneration for a Platinum Electrode on an Electrophoresis Microchip. *Anal. Chem.* **2003**, *75* (17), 4572–4577.
- (13) Yang, C.; Denno, M. E.; Pyakurel, P.; Venton, B. J. Recent Trends in Carbon Nanomaterial-Based Electrochemical Sensors for Biomolecules: A Review. *Anal. Chim. Acta* **2015**, *887*, 17–37.
- (14) Hettie, K. S.; Glass, T. E. Turn-On Near-Infrared Fluorescent Sensor for Selectively Imaging Serotonin. *ACS Chem. Neurosci.* **2016**, *7* (1), 21–25.
- (15) Hong, G.; Diao, S.; Antaris, A. L.; Dai, H. Carbon Nanomaterials for Biological Imaging and Nanomedicinal Therapy. *Chem. Rev.* **2015**, *115* (19), 10816–10906.
- (16) Giraldo, J. P.; Wu, H.; Newkirk, G. M.; Kruss, S. Nanobiotechnology Approaches for Engineering Smart Plant Sensors. *Nat. Nanotechnol.* **2019**, *14* (6), 541–553.
- (17) O’Connell, M. J.; Bachilo, S. M.; Huffman, C. B.; Moore, V. C.; Strano, M. S.; Haroz, E. H.; Rialon, K. L.; Boul, P. J.; Noon, W. H.; Kittrell, C.; et al. Band Gap Fluorescence from Individual Single-Walled Carbon Nanotubes. *Science* **2002**, *297* (5581), 593–596.
- (18) Ménard-Moyon, C.; Kostarelos, K.; Prato, M.; Bianco, A. Functionalized Carbon Nanotubes for Probing and Modulating Molecular Functions. *Chem. Biol.* **2010**, *17* (2), 107–115.
- (19) Prato, M.; Kostarelos, K.; Bianco, A. Functionalized Carbon Nanotubes in Drug Design and Discovery. *Acc. Chem. Res.* **2008**, *41* (1), 60–68.

- (20) Amoroso, G.; Ye, Q.; Cervantes-Salguero, K.; Fernandez, G.; Ceconello, A.; Palma, M. DNA-Powered Stimuli-Responsive Single-Walled Carbon Nanotube Junctions. *Chem. Mater.* **2019**, *31* (5), 1537–1542.
- (21) Giacalone, F.; Campisciano, V.; Calabrese, C.; La Parola, V.; Syrgiannis, Z.; Prato, M.; Gruttadauria, M. Single-Walled Carbon Nanotube–Polyamidoamine Dendrimer Hybrids for Heterogeneous Catalysis. *ACS Nano* **2016**, *10* (4), 4627–4636.
- (22) Tu, X.; Manohar, S.; Jagota, A.; Zheng, M. DNA Sequence Motifs for Structure-Specific Recognition and Separation of Carbon Nanotubes. *Nature* **2009**, *460* (7252), 250–253.
- (23) Mann, F. A.; Horlebein, J.; Meyer, N. F.; Meyer, D.; Thomas, F.; Kruss, S. Carbon Nanotubes Encapsulated in Coiled-Coil Peptide Barrels. *Chem. - Eur. J.* **2018**, *24* (47), 12241–12245.
- (24) Bouilly, D.; Hon, J.; Daly, N. S.; Trocchia, S.; Vernick, S.; Yu, J.; Warren, S.; Wu, Y.; Gonzalez, R. L.; Shepard, K. L.; et al. Single-Molecule Reaction Chemistry in Patterned Nanowells. *Nano Lett.* **2016**, *16* (7), 4679–4685.
- (25) Harvey, J. D.; Jena, P. V.; Baker, H. A.; Zerze, G. H.; Williams, R. M.; Galassi, T. V.; Roxbury, D.; Mittal, J.; Heller, D. A. A Carbon Nanotube Reporter of MicroRNA Hybridization Events in Vivo. *Nat. Biomed. Eng.* **2017**, *1* (4), 0041.
- (26) Bisker, G.; Dong, J.; Park, H. D. H. D.; Iverson, N. M. N. M.; Ahn, J.; Nelson, J. T. J. T.; Landry, M. P. M. P.; Kruss, S.; Strano, M. S. M. S. Protein-Targeted Corona Phase Molecular Recognition. *Nat. Commun.* **2016**, *7*, 10241.
- (27) Reuel, N. F.; Grassbaugh, B.; Kruss, S.; Mundy, J. Z.; Opel, C.; Ogunniyi, A. O.; Egodage, K.; Wahl, R.; Helk, B.; Zhang, J.; et al. Emergent Properties of Nanosensor Arrays: Applications for Monitoring IgG Affinity Distributions, Weakly Affined Hypermannosylation, and Colony Selection for Biomanufacturing. *ACS Nano* **2013**, *7* (9), 7472–7482.
- (28) Antonucci, A.; Kupis-Rozmyslowicz, J.; Boghossian, A. A. Noncovalent Protein and Peptide Functionalization of Single-Walled Carbon Nanotubes for Biodelivery and Optical Sensing Applications. *ACS Appl. Mater. Interfaces* **2017**, *9* (13), 11321–11331.
- (29) Kruss, S.; Salem, D. P.; Vuković, L.; Lima, B.; Vander Ende, E.; Boyden, E. S.; Strano, M. S. High-Resolution Imaging of Cellular Dopamine Efflux Using a Fluorescent Nanosensor Array. *Proc. Natl. Acad. Sci. U. S. A.* **2017**, *114* (8), 1789–1794.
- (30) Kruss, S.; Landry, M. P.; Vander Ende, E.; Lima, B. M. A.; Reuel, N. F.; Zhang, J.; Nelson, J.; Mu, B.; Hilmer, A.; Strano, M. Neurotransmitter Detection Using Corona Phase Molecular Recognition on Fluorescent Single-Walled Carbon Nanotube Sensors. *J. Am. Chem. Soc.* **2014**, *136* (2), 713–724.
- (31) Nißler, R.; Mann, F. A.; Chaturvedi, P.; Horlebein, J.; Meyer, D.; Vuković, L.; Kruss, S. Quantification of the Number of Adsorbed DNA Molecules on Single-Walled Carbon Nanotubes. *J. Phys. Chem. C* **2019**, *123* (8), 4837–4847.
- (32) Mann, F. A. F. A.; Herrmann, N.; Meyer, D.; Kruss, S. Tuning Selectivity of Fluorescent Carbon Nanotube-Based Neurotransmitter Sensors. *Sensors* **2017**, *17* (7), 1521.
- (33) Polo, E.; Kruss, S. Impact of Redox-Active Molecules on the Fluorescence of Polymer-Wrapped Carbon Nanotubes. *J. Phys. Chem. C* **2016**, *120* (5), 3061.
- (34) Polo, E.; Nitka, T. T.; Neubert, E.; Erpenbeck, L.; Vuković, L.; Kruss, S. Control of Integrin Affinity by Confining RGD Peptides on Fluorescent Carbon Nanotubes. *ACS Appl. Mater. Interfaces* **2018**, *10* (21), 17693–17703.
- (35) Mann, F. A.; Lv, Z.; Grosshans, J.; Opazo, F.; Kruss, S. Nanobody Conjugated Nanotubes for Targeted Near-Infrared in Vivo Imaging and Sensing. *Angew. Chem.* **2019**, *131*, 11591–11596.
- (36) Stoltenburg, R.; Reinemann, C.; Strehlitz, B. SELEX—A (r)Evolutionary Method to Generate High-Affinity Nucleic Acid Ligands. *Biomol. Eng.* **2007**, *24* (4), 381–403.
- (37) Song, S.; Wang, L.; Li, J.; Fan, C.; Zhao, J. Aptamer-Based Biosensors. *TrAC, Trends Anal. Chem.* **2008**, *27* (2), 108–117.
- (38) Cha, T.-G.; Baker, B. A.; Sauffer, M. D.; Salgado, J.; Jaroch, D.; Rickus, J. L.; Porterfield, D. M.; Choi, J. H. Optical Nanosensor Architecture for Cell-Signaling Molecules Using DNA Aptamer-Coated Carbon Nanotubes. *ACS Nano* **2011**, *5* (5), 4236–4244.
- (39) Landry, M. P.; Ando, H.; Chen, A. Y.; Cao, J.; Kottadiel, V. I.; Chio, L.; Yang, D.; Dong, J.; Lu, T. K.; Strano, M. S. Single-Molecule Detection of Protein Efflux from Microorganisms Using Fluorescent Single-Walled Carbon Nanotube Sensor Arrays. *Nat. Nanotechnol.* **2017**, *12* (4), 368.
- (40) Xu, X.; Clément, P.; Eklöf-Österberg, J.; Kelley-Loughnane, N.; Moth-Poulsen, K.; Chávez, J. L.; Palma, M. Reconfigurable Carbon Nanotube Multiplexed Sensing Devices. *Nano Lett.* **2018**, *18* (7), 4130–4135.
- (41) Nakatsuka, N.; Yang, K.; Abendroth, J. M.; Cheung, K.; Xu, X.; Yang, H.; Zhao, C.; Zhu, B.; Rim, Y. S.; Yang, Y.; et al. Aptamer – Field-Effect Transistors Overcome Debye Length Limitations for Small-Molecule Sensing. *Science* **2018**, *362* (6412), 319–324.
- (42) Ahern, G. P. 5-HT and the Immune System. *Curr. Opin. Pharmacol.* **2011**, *11* (1), 29–33.
- (43) Gershon, M. D.; Tack, J. The Serotonin Signaling System: From Basic Understanding To Drug Development for Functional GI Disorders. *Gastroenterology* **2007**, *132* (1), 397–414.
- (44) Berger, M.; Gray, J. A.; Roth, B. L. The Expanded Biology of Serotonin. *Annu. Rev. Med.* **2009**, *60* (1), 355–366.
- (45) Watts, S. W.; Morrison, S. F.; Davis, R. P.; Barman, S. M. Serotonin and Blood Pressure Regulation. *Pharmacol. Rev.* **2012**, *64* (2), 359–388.
- (46) Dees, C.; Akhmetshina, A.; Zerr, P.; Reich, N.; Palumbo, K.; Horn, A.; Jüngel, A.; Beyer, C.; Krönke, G.; Zwerina, J.; et al. Platelet-Derived Serotonin Links Vascular Disease and Tissue Fibrosis. *J. Exp. Med.* **2011**, *208* (5), 961–972.
- (47) Cloutier, N.; Paré, A.; Farndale, R. W.; Schumacher, H. R.; Nigrovic, P. A.; Lacroix, S.; Boilard, E. Platelets Can Enhance Vascular Permeability. *Blood* **2012**, *120*, 1334.
- (48) Lesurtel, M.; Graf, R.; Aleil, B.; Walther, D. J.; Tian, Y.; Jochum, W.; Gachet, C.; Bader, M.; Clavien, P.-A. Platelet-Derived Serotonin Mediates Liver Regeneration. *Science (Washington, DC, U. S.)* **2006**, *312* (5770), 104–107.
- (49) Mammadova-Bach, E.; Mauler, M.; Braun, A.; Duerschmied, D. Autocrine and Paracrine Regulatory Functions of Platelet Serotonin. *Platelets* **2018**, *29*, 541–548.
- (50) Nakatsuka, N.; Yang, K. A.; Abendroth, J. M.; Cheung, K. M.; Xu, X.; Yang, H.; Zhao, C.; Zhu, B.; Rim, Y. S.; Yang, Y.; et al. Aptamer-Field-Effect Transistors Overcome Debye Length Limitations for Small-Molecule Sensing. *Science* **2018**, *362* (6412), 319–324.
- (51) Ge, S.; Woo, E.; Haynes, C. L. Quantal Regulation and Exocytosis of Platelet Dense-Body Granules. *Biophys. J.* **2011**, *101* (10), 2351–2359.
- (52) John, C. E.; Jones, S. R. Fast Scan Cyclic Voltammetry of Dopamine and Serotonin in Mouse Brain Slices. In *Electrochemical methods for neuroscience*; CRC Press/Taylor & Francis: Boca Raton, FL, 2007.
- (53) Nißler, R.; Mann, F. A.; Preiß, H.; Selvaggio, G.; Herrmann, N.; Kruss, S. Chirality Enriched Carbon Nanotubes with Tunable Wrapping via Corona Phase Exchange Purification (CPEP). *Nanoscale* **2019**, *11* (23), 11159–11166.
- (54) Solt, K.; Ruesch, D.; Forman, S. A.; Davies, P. A.; Raines, D. E. Differential Effects of Serotonin and Dopamine on Human 5-HT_{3A} Receptor Kinetics: Interpretation within an Allosteric Kinetic Model. *J. Neurosci.* **2007**, *27* (48), 13151–13160.
- (55) Rendu, F.; Brohard-Bohn, B. The Platelet Release Reaction: Granules' Constituents, Secretion and Functions. *Platelets* **2001**, *12* (5), 261–273.
- (56) Zhang, H.; Mosharov, E. V.; Sames, D.; Edwards, R. H.; Mukherjee, B.; Balsanek, V.; Gubernator, N. G.; Vadola, P. A.; Staal, R. G. W.; Pereira, D. B.; et al. Fluorescent False Neurotransmitters Visualize Dopamine Release from Individual Presynaptic Terminals. *Science* **2009**, *324* (5933), 1441–1444.
- (57) Lovrić, J.; Dunevall, J.; Larsson, A.; Ren, L.; Andersson, S.; Meibom, A.; Malmberg, P.; Kurczy, M. E.; Ewing, A. G. Nano

2 Results

Secondary Ion Mass Spectrometry Imaging of Dopamine Distribution Across Nanometer Vesicles. *ACS Nano* **2017**, *11* (4), 3446–3455.

(58) Beyene, A. G.; Delevich, K.; Del Bonis-O'Donnell, J. T.; Piekarski, D. J.; Lin, W. C.; Thomas, A. W.; Yang, S. J.; Kosillo, P.; Yang, D.; Prounis, G. S.; et al. Imaging Striatal Dopamine Release Using a Nongenetically Encoded near Infrared Fluorescent Catecholamine Nanosensor. *Sci. Adv.* **2019**, *5* (7), eaaw3108.

(59) Godin, A. G.; Varela, J. A.; Gao, Z.; Danné, N.; Dupuis, J. P.; Lounis, B.; Groc, L.; Cognet, L. Single-Nanotube Tracking Reveals the Nanoscale Organization of the Extracellular Space in the Live Brain. *Nat. Nanotechnol.* **2017**, *12* (3), 238–243.

(60) Fakhri, N.; Wessel, A. D.; Willms, C.; Pasquali, M.; Klopfenstein, D. R.; MacKintosh, F. C.; Schmidt, C. F. High-Resolution Mapping of Intracellular Fluctuations Using Carbon Nanotubes. *Science* **2014**, *344* (6187), 1031–1035.

2 Results

2.1.2 Supplementary Material

The Supporting Information is available free of charge on the ACS Publications website at DOI: [10.1021/acs.nanolett.9b02865](https://doi.org/10.1021/acs.nanolett.9b02865).

This section includes experimental details, characterization figures, and additional sensor response data

Supplementary Information

Near Infrared imaging of serotonin release from cells with fluorescent nanosensors

*Meshkat Dinarvand¹, Elsa Neubert^{1,2}, Daniel Meyer¹, Gabriele Selvaggio¹, Florian A. Mann¹,
Luise Erpenbeck², Sebastian Kruss^{1*}*

¹ Institute of Physical Chemistry, Göttingen University, Germany

² Department of Dermatology, Venereology and Allergology, University Medical Center,
Göttingen, Germany

* Corresponding author: Sebastian Kruss (skruss@uni-goettingen.de)

2 Results

Materials and Methods

Synthesis of aptamer functionalized SWCNTs (NIRSers)

(6,5) enriched SWCNTs (41% (6,5) chirality, carbon $\leq 95\%$, $\geq 93\%$ carbon as SWCNT, Signis[®] SG65i, 0.7–0.9 nm diameter (Sigma-Aldrich, Germany) and the serotonin aptamer (a 57–mer sequence of 5'-CTCTCGGGACGACTGGTAGGCAGATAGGGGAAGCTGATTCGATGCGTGGGTCGTCCC-3' ¹ synthesized by Sigma-Aldrich, Germany) were mixed in MilliQ water to reach the final concentration of 0.5 mg/mL and 50 μ M respectively. The dispersion was tip sonicated (Fisher Scientific Model 120 Sonic Dismembrator) at 30 % amplitude for 20 minutes. Then, the dispersion was centrifuged (Eppendorf centrifuge 5415 D) at 16000 x g for 30 minutes twice and the supernatant was collected for further investigation.

NIRSer Characterization

Absorption spectra were collected with a UV–vis–NIR spectrometer (JASCO V-670, Spectra Manager Software). The prepared NIRSers were diluted in PBS. The concentrations of NIRSer in the samples were calculated by integrating the area under the peak belonging to (6,5) SWCNTs and using the extinction coefficient together with an estimated length of 600 nm to calculate the concentration. ² The concentration of NIRSer was adjusted accordingly for each experiment.

For atomic force microscopy (AFM) 10 μ L of NIRSer was deposited on muscovite mica by spin coating (G3 Spin Coater, Specialty Coating Systems, Inc.) at 500 RPM (7 RCF) for 2 min (ramp time = 5 s, dwell time = 30 s). The mica substrate was then thoroughly washed with MilliQ water directly before the measurement. AFM images were acquired in AC mode using an Asylum Research MFP-3D Infinity device (Oxford Instruments, software version 15.01.103) equipped with

2 Results

Olympus AC-160-TS rectangular cantilevers (resonance frequency = 300 kHz, spring constant = 26 N/m). Gwyddion (version 2.51) was used for data analysis.

The number of bound aptamers per SWCNT was calculated by measuring the concentration of bound aptamer from subtracting the concentration of free aptamer from the total aptamer used. To measure the concentration of free aptamer, the prepared NIRsers were precipitated by a spin filter (300 kDa cut off) after 20 minutes of centrifugation at 15000 x g. The supernatant was collected and the absorbance was measured at 260 nm. A calibration curve was plotted using known concentrations of serotonin aptamer. The concentration of free aptamer was calculated from the calibration curve. We determined the ratio (w/w) of aptamer to SWCNT to be 6.419 ± 0.003 .

Fluorescence Spectroscopy

The concentration of NIRser nanosensors were adjusted to 2 nM. The nanosensors were excited with a monochromator at 561 nm coupled with an Olympus IX73 microscope. The emission spectra from 800 nm to 1300 nm were obtained from an Andor iDus InGaAs 491 array NIR detector attached to a Shamrock 193i spectrograph (Andor Technology Ltd., Belfast, Northern Ireland) and typically a 5 s exposure time.

To obtain a calibration curve, the NIRsers were excited at 561 nm using a monochromator. First the emission spectra of NIRser dispersions were collected. Then, 2 μ L of serotonin (Alfa AesarTM, Germany) solution was added to the dispersions and the emission spectra were collected again. Six known concentrations of serotonin (0.001, 0.01, 0.1, 1, 10, 100 μ M final concentration of serotonin in NIRser dispersion) were used in triplicates. The fluorescence intensity changes at the maximum emission intensity peak (around 995 nm) was quantified and OriginPro 8.5 was used to fit a 5 parameter logistic function.

2 Results

To investigate NIRSer selectivity, the NIRSers were excited with a 561 nm laser. First the emission spectra of NIRSer dispersions were collected. Then, a solution containing serotonin or an interfering molecule was added to the dispersions to reach the final concentration of 100 nM and the emission spectra were collected again. Measurements were carried out in triplicates. The fluorescence intensity change at the emission intensity peak was calculated for each molecule.

Fluorescence Microscopy

NIRSers were immobilized on glass surfaces by incubating the surfaces with 4 nM NIRSer dispersion overnight. Before measurements, the surfaces were washed with MilliQ water thoroughly and PBS was added. For the imaging, an Olympus BX53 microscope with a 100x objective lens (UPLSAPO100XS, Olympus, Tokyo, Japan) was used. The nanosensors were excited at 561 nm with a 500 mW laser (Cobolt Jive™ laser, Cobolt AB, Solna, Sweden). The images were obtained with an Andor Zyla 5.5 sCMOS camera, (Andor Technology Ltd., Belfast, UK) at 1 s exposure time. Then, serotonin solution was added to the PBS to reach final concentrations of 0.001, 0.01, 0.1, 1, 10 and 100 μ M. The changes in fluorescence intensity of the images were analysed using ImageJ 1.52n.

To investigate the stepwise increase in fluorescence of the nanosensor, glass coverslips were coated with NIRSers and a sticky slide VI 0.4 (ibidi, Germany) was used as a flow chamber. Image sequences were taken with an Andor Zyla 5.5 sCMOS camera while increasing concentrations of serotonin, ranging from 10 nM to 100 μ M were flushed through the chamber. To investigate reversibility, the same procedure was performed with 1 μ M serotonin while after each serotonin flush, PBS was flushed through the chamber to wash away the bound serotonin and observe the reversibility of the response to serotonin.

2 Results

Isolation of human platelets

We either collected fresh blood from donors and purified the platelets or Platelet rich plasma (PRP) was provided by Luise Erpenbeck/Michael Schön (Göttingen University Medical Center). In both cases all the procedures were approved by the ethic committee of the University Medical Center Goettingen. Blood donors were fully informed and the declaration of consent confirmed. Fresh blood was centrifuged at 200 ×g for 20 min with the break off, and the upper layer containing the platelets were collected. Then, either plasma containing platelets or the PRP was mixed with 1 μM PGE1 (Sigma-Aldrich, Germany) and centrifuged at 2000 ×g for 10 minutes with breaks off. The pelleted platelets were suspended in Tyrode's buffer (pH 6.5, 1 μM PGE1) and centrifuged again at 2000 x g. This step was repeated 2 times to obtain a purified platelet pellet. Finally, for all platelet experiments the pellet was resuspended in Tyrode's buffer (pH 7.4 containing 2.5 mM CaCl₂ without PGE1). In order to activate platelets, 1 μM Ionomycin (ionomycin calcium salt from Streptomyces, Sigma-Aldrich, Germany) was added to the cell suspension and incubated for 1 minute.

RICM imaging

Glass bottom well plates were incubated in 10 μg/mL Fibrinogen (fibrinogen, human type I from human Sigma-Aldrich, Germany) 6 hours in 4°C. Then, NIRSer dispersion (4 nM) was immobilized on top and incubated overnight in 4°C. The surface was washed with PBS thoroughly and a dispersion of washed platelets in Tyrode's buffer was added to the wells. Immediately after addition of the platelets the RICM images were acquired every 60 s. After complete attachment of platelets to the surface, 1 μM ionomycin was added to the media and the changes in platelet morphology were observed. A 63x magnified objective lens was used (EC Plan-Neofluar Ph3

2 Results

objective/420481-9911-000, 1.6x Optovar, Zeiss). And samples were illuminated with XCite Series 120Q, and observed with a Zyla sCMOS camera (AndorZyla 5.5).

Platelet adhesion study

Fibrinogen (10 $\mu\text{g}/\text{mL}$) was coated on glass surface and incubated for 6 hours in 4°C. NIRSer dispersion (4 nM) was immobilized on top and incubated overnight in 4°C. Before the experiments, the functionalized surfaces were washed thoroughly with Tyrode's buffer. Unstimulated washed platelets (1×10^7 cells/mL) in Tyrode's buffer pH 7.4, supplemented with 2.5 mM CaCl_2 were added and incubated at RT for 35 minutes to let the platelets adhere to the surface. Using an inverted microscope, image sequences were taken of live platelets before and after activation with 1 μM ionomycin. The degranulation of platelets and release of serotonin were visualized by bright-field microscopy with a sCMOS camera.

Supplementary Figures

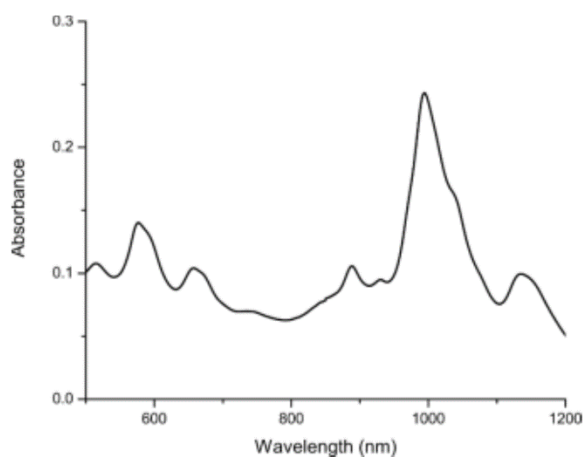


Figure S1, Vis/nIR absorbance spectrum of NIRSer in buffer. The NIRSers were diluted in a PBS buffer (1:100). The absorption spectra were collected with a UV-vis-nIR spectrometer (JASCO V-670, Spectra Manager Software) from 450 nm to 1300 nm. The peak absorbance at approximately 995 nm was attributed to (6,5) chirality SWCNTs. We used the extinction coefficient of (6,5) chirality SWCNTs to calculate the concentration of the NIRSer in the dispersion.

2 Results

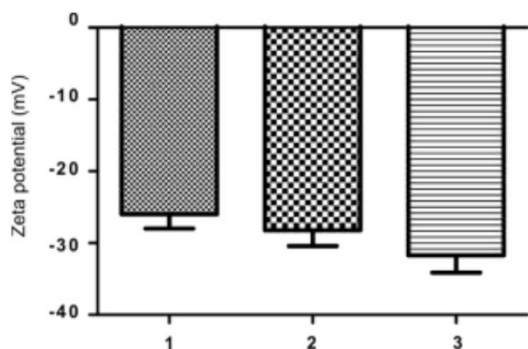


Figure S2 Zeta potential of NIRSers. Zeta potential of 2 nM NIRSer dispersed in PBS. The mean zeta potential is -28.6 ± 2.8 from the three shown independent samples. Mean \pm SD of technical replicates.

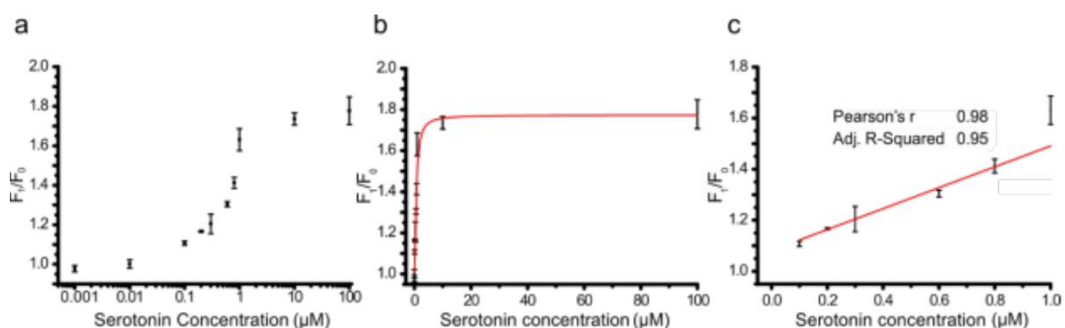


Figure S3 NIRSer response to serotonin in solution. *a*, Fluorescence response to serotonin in semi logarithmic scale, showing the sensitivity of the nanosensor in a broad range of concentrations. *b*, Fluorescence response to serotonin concentration plot in linear x scale, showing the linear dynamic range. *c*, The linear dynamic range from 100 nM to 1 μM with strong linearity. All data are mean values \pm SEM of $N = 3$.

2 Results

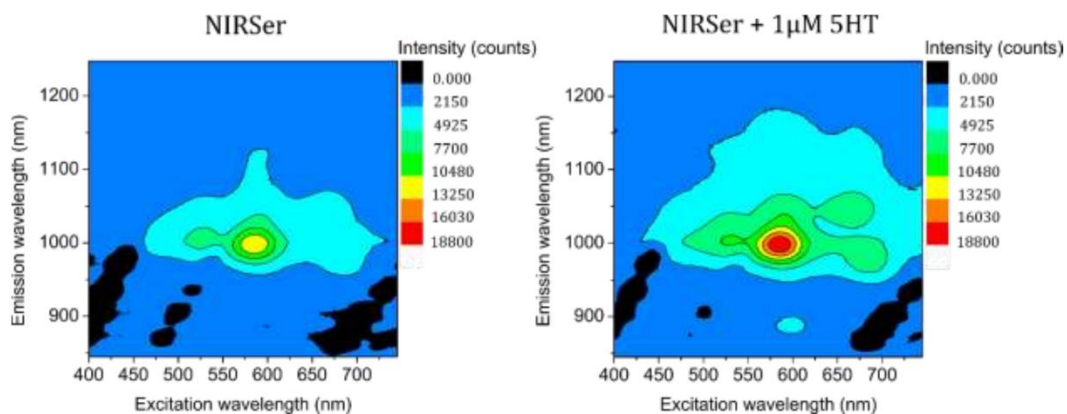


Figure S4 2D excitation/emission map of NIRSer before and after addition of serotonin. The nIR spectra were collected before and after addition of serotonin (1 μ M) at an excitation range from 400 nm to 745 nm at 5 nm intervals. With 5 s exposure time. Other SWCNT chiralities than (6,5) also significantly respond to serotonin.

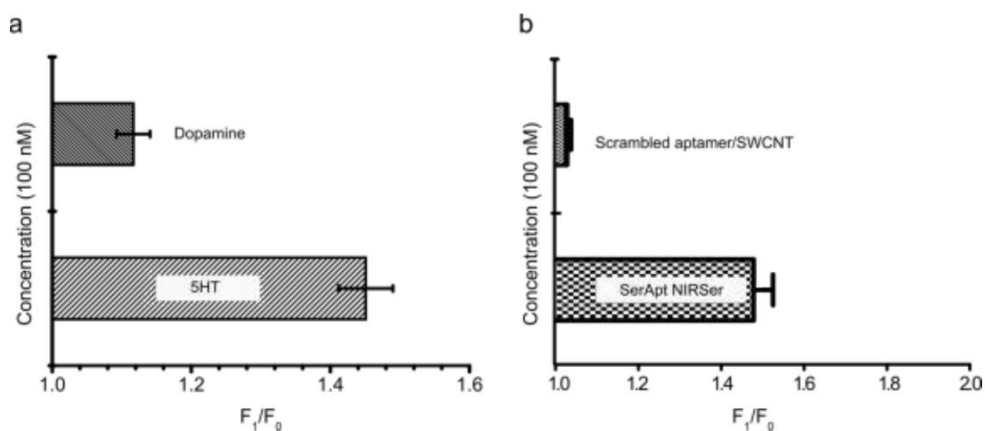


Figure S5 Selectivity of NIRSer sensors. **a**, NIRSers were exposed to 100 nM dopamine and serotonin (5HT) and the change in the intensity of maximum emission was calculated. **b**, Fluorescence response of SWCNTs functionalized with scrambled aptamer compared to the response of NIRSer sensors functionalized with serotonin specific aptamer. The SWCNTs and NIRSer were excited with a 561 nm laser and the exposure time was 5 s. $N = 3$ and the values are mean \pm SEM.

2 Results

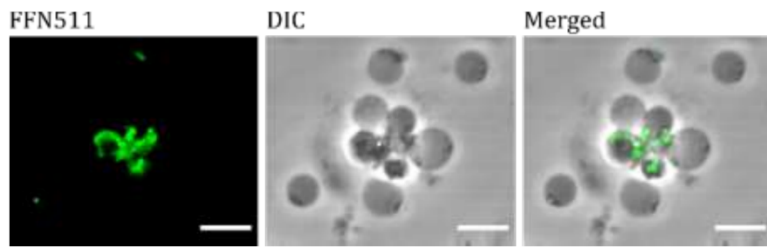


Figure S6 False fluorescent neurotransmitter (FFN) uptake through VMAT2 visualizes serotonin containing vesicles. The uptake of the FFN (FFN511), by platelets is visualized. The scale bars represent 5 μ m.

2 Results

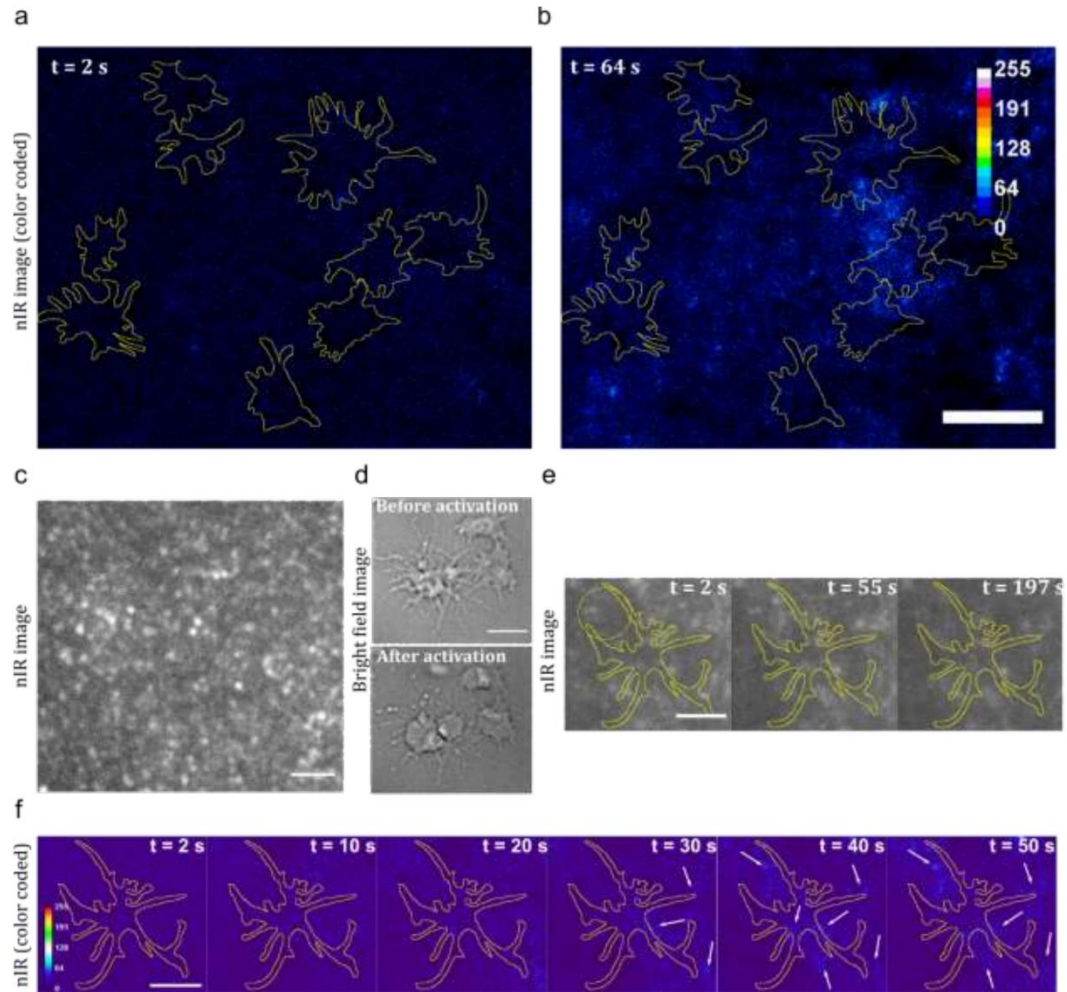


Figure S7 Cell studies on NIRSer surface. *a, b*, Color-coded nIR images of cell coated on NIRSer surfaces before and during serotonin release (each frame subtracted from the first frame). Image sequences were taken at 1 fps. Ionomycin was added at $t=20$ s, a visible increase corresponding to the release of serotonin is visible in frame 64 s. The scale bars represent $10\ \mu\text{m}$. *c*, nIR image of the NIRSer coated surface, indicating a homogenous single nanosensor coating. *d*, Degranulation of platelets and release of dense granules before and after ionomycin treatment on a NIRSer coated surface (bright field image). *e*, Raw nIR image of a single cell before, during and after serotonin release, the yellow circle denotes the ROI that is analyzed in figure 5d in main manuscript and

2 Results

showed a localized increase in fluorescence which is attributed to serotonin release. The yellow line indicates the outline of the cell not seen in the nIR fluorescence image. **f**, Color-coded nIR image of the same cell at the initial stages of serotonin release. At time points $t = 10$ s and $t = 20$ s there is a small background signal probably due to serotonin leakage from cells before activation. The white arrows show localized serotonin release spots. All scale bars represent $5 \mu\text{m}$ unless otherwise stated.

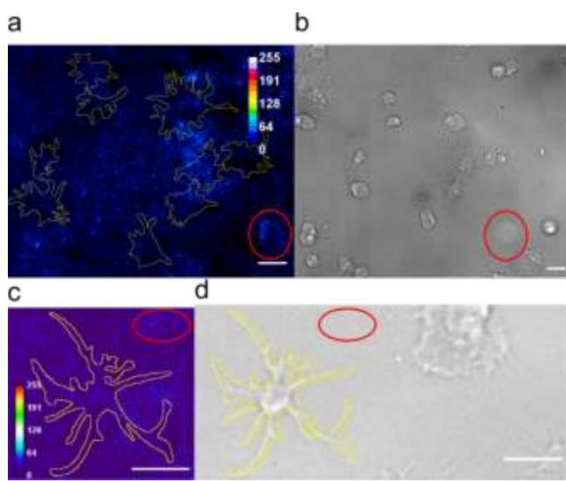


Figure S8 nIR color-coded and bright-field images of platelets. a,b, The increased fluorescence (marked area) in image a, is close to the border of a platelet shown in image b. In this case the bright field image furthermore indicates that there could be a non-adherent platelet above. **c,d**, The increased fluorescence (marked area) in image c, is close to the border of a platelet shown in image d. All scale bars are $5 \mu\text{m}$.

2 Results

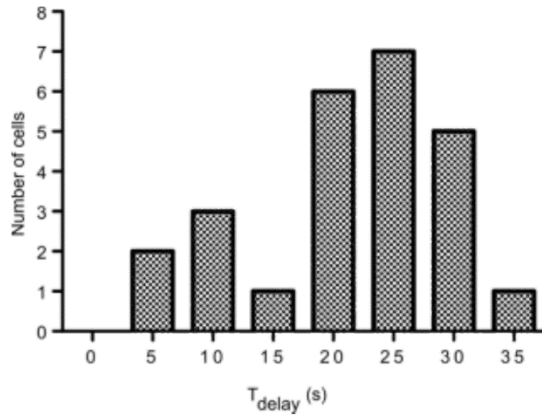


Figure S9 Delay time between stimulation of platelets and release of serotonin. T_{delay} marks the time from addition of ionomycin to the release of serotonin (measured by the first increase in NIRSer fluorescence). The frequency distribution histogram shows that there is a marked variation between the onset of release in platelets. However, in more than 50% of the cells, the release onset was in the range of 21-30 s after the addition of ionomycin which corroborates existing studies.³

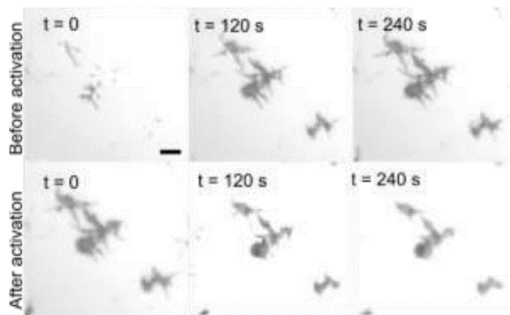


Figure S10 Adhesion of platelets to NIRSer coated surfaces. RICM images of platelet adhesion to the NIRSer surface. Ionomycin was added 240 s after starting imaging, at time point 0 after activation images were taken at certain time points. the scale bar is 5 μm .

2 Results

References

1. Nakatsuka N, Yang K-A, Abendroth JM, et al. Aptamer–field-effect transistors overcome Debye length limitations for small-molecule sensing. *Science* (80-). 2018;362(6412):319 LP - 324. doi:10.1126/science.aao6750
2. Nißler R, Mann FA, Chaturvedi P, et al. Quantification of the Number of Adsorbed DNA Molecules on Single-Walled Carbon Nanotubes. *J Phys Chem C*. 2019;123(8):4837-4847. doi:10.1021/acs.jpcc.8b11058
3. Ge S, Woo E, Haynes CL. Quantal regulation and exocytosis of platelet dense-body granules. *Biophys J*. 2011;101(10):2351-2359.

2.2 Detection of Dopamine Exocytosis from Neutrophils

2.2.1 Manuscript

Serotonin Triggers Dopamine Exocytosis by Neutrophils in a Functional Negative Feedback Loop

Meshkat Dinarvand¹, Anne Schmitz², Elsa Neubert², Thea Mara Husar², Antonia Luise Gruhn², Benedetta Fazari³, Magdalena Shumanska⁴, Ivan Bogeski⁴, Joseph P. Huston³, Luise Erpenbeck^{2*}, and Sebastian Kruss^{1,5*}

¹Institute of Physical Chemistry, Göttingen University, Göttingen 37077, Germany

²Department of Dermatology, Venereology, and Allergology, University Medical Center, Göttingen 37075, Germany

³Center for Behavioral Neuroscience, Institute of Experimental Psychology, University of Düsseldorf, Düsseldorf, Germany

⁴Molecular Physiology, Institute of Cardiovascular Physiology, University Medical Center, Göttingen, Germany

⁵Physical Chemistry II, Bochum University, Germany

This manuscript is part of an unpublished work/project, which includes contributions from multiple collaborators. Human neutrophils were isolated and characterized by M.D. E.N., A.S., T.H., A.G. and L.E. Receptor staining were performed by E.N., T.H. M.D. and L.E. FACS analysis was performed by A.S. and L.E. FFN experiments were performed by M.D. Dopamine imaging experiments, nanosensor preparation and Ca imaging experiments were performed by M.D. Platelet were isolated by M.D. NETosis assays were performed by E.N., A.G. and L.E. HPLC analysis was performed by B.F. and M.D. Data analysis was performed by all authors. Image analysis was performed by M.D. and S.K. The research idea was designed by L.E. and S.K.

Serotonin triggers dopamine exocytosis by neutrophils in a functional negative feedback loop

Meshkat Dinarvand¹, Anne Schmitz², Elsa Neubert², Thea Mara Husar², Antonia Luise Gruhn², Benedetta Fazari³, Magdalena Shumanska⁴, Ivan Bogeski⁴, Joseph P. Huston³, Luise Erpenbeck^{2*}, and Sebastian Kruss^{1,5*}

*Corresponding author.

Abstract

The dopaminergic system controls important functions in the nervous system. Non-neuronal dopamine signaling has been discovered in immune cells as well. For instance, peripheral immune cells express dopaminergic components; but the extent to which dopamine regulates the immune response has remained elusive. Conventional analytical tools for investigating dopaminergic signaling largely disregard the inherent heterogeneity and complexity of immune cells. Immune cells are highly sensitive to their microenvironment; hence their response should be investigated within their spatial context. In this manuscript, we investigate the dopaminergic machinery in human neutrophils by a novel fluorescent nanosensor based on single-walled carbon nanotubes with high spatiotemporal resolution. Protein components of the dopaminergic system were studied in neutrophils and we established that neutrophils produce, store and release dopamine. We discovered that serotonin induced receptor-mediated exocytosis of dopamine containing vesicles via Ca^{2+} mobilization. Exocytosis of dopamine from neutrophils was imaged by our nanosensor tool. The acquired images revealed the temporal orchestration of dopamine exocytosis from neutrophils induced by platelet-derived serotonin. We further discovered that dopamine as a paracrine immune modulator reduced the rate of NETosis in neutrophils. These findings enabled studying paracrine dopamine signaling within the cells complex spatiotemporal context.

2 Results

Introduction

Dopamine is a signaling molecule that mediates cellular communication in the nervous (known as neurotransmitter) and the endocrine system (known as hormone). The physiological reach of dopamine extends to the immune system as well. There is growing evidence that dopamine is synthesized and/or recognized by various immune cells which suggests that it acts as an autocrine/paracrine regulator of the immune response. Several early studies discovered components from the dopaminergic system (including dopamine itself and proteins involved in biosynthesis, storage, and metabolism) in various immune cells.¹⁻⁴ The expression of dopamine receptors were also studied in various immune cell types.⁵ Until recently, little was known about the extent of the immunomodulatory effects of dopamine. Resident immune cells in the central nervous system (CNS) are exposed to dopamine during spillover from synapses, where dopamine is abundantly available. Changes in the function of the immune cells of the CNS, as a result of altered dopamine concentrations (in pathological conditions such as drug abuse, Parkinson's disease), has been discovered.^{3,6-9}

Even less is known about the regulatory role of dopamine in the peripheral immune system because circulating immune cells are not readily exposed to dopamine. In this study, we focus on the dopaminergic system in neutrophils as the secretory components of neutrophils are important drivers of the immune response.¹⁰ Although on a single cell basis, neutrophils synthesize less secretory molecules than single lymphocytes or macrophages, they are more abundant than any other immune cell.¹¹

There is evidence that neutrophils synthesize monoamines such as dopamine, and release them upon activation.^{1,12,13} The complex behavior of immune cells is tightly controlled by the spatial context of their microenvironment. This includes a myriad of inflammatory mediators, white blood cells and secretory components that at times, induce cellular functions that seem to be contradictory to each other when studied outside their spatial context. Hence, it is important to study the dynamics of dopamine release from neutrophils with high spatiotemporal resolution.

First, we studied the components of the dopaminergic system in neutrophils by conventional methods. Then we studied exocytosis of dopamine from neutrophils in real

2 Results

time with a novel fluorescent nanosensor based on functionalized single-walled carbon nanotubes (SWCNT). Previously, fluorescent SWCNT nanosensors were employed for visualization of single dopamine release events from PC12 cells.¹⁴ We also designed a serotonin SWCNT nanosensor based on the same premise that could successfully visualize exocytosis of serotonin from activated platelets with high spatial resolution in the nanoscale region (only limited by the abbe limit).¹⁵ Here, we used the same platform to study the release of dopamine from stimulated neutrophils.

Secondly, the dynamics of dopamine exocytosis and the signaling pathway was studied. The role of serotonin in mediating dopamine release from neutrophils was investigated. Platelet-derived serotonin has been reported to modulate several neutrophil activities such as recruitment and degranulation.¹⁶⁻¹⁸ More than ninety percent of the serotonin content of the human body is produced and released by enterochromaffin cells in the gastric lumen¹⁹ and stored in circulating platelets. Platelets maintain hemostasis and participate in immunity by interacting with immune cells, mainly neutrophils. Here, with our novel sensing tool, we investigated this complex process. conventional analytical methods such as mass spectroscopy, chromatography and immune assays although highly specific and selective, lack spatial and temporal resolution. Electrochemical methods such as amperometry and voltammetry are gold standards to study neurotransmitter release events in neurons but they also lack spatial resolution as the resolution is limited by the number and diameter of the electrode used. For this reason, functionalized SWCNTs that fluoresce in the near infrared region have gained interest in recent years. Our lab has established a home-built microscopic system to detect live monoamine release.

We visualized the release of dopamine from neutrophils upon activation with platelet-derived serotonin for the first time. And finally, we study the implications of dopamine as an autocrine/paracrine immune regulator on one of the key neutrophil immune responses, which is the formation of neutrophil extracellular traps (NETosis).

Results:

Nanosensor Synthesis

2 Results

The nanosensors (NIRDA) comprise a (6,5)-enriched chirality single-walled carbon nanotube (SWCNT) backbone that is functionalized with (GT)₁₀ oligonucleotides. (GT)₁₀-SWCNTs are fluorescent in the near infrared (nIR) region. NIRDA suspension absorbed light at ~1000 nm (Fig. S2A.). The basis of the detection was an increase in the fluorescence emission intensity upon interaction with dopamine when the nanosensors were excited with a 561 nm laser (Fig. 1A.). FigS2B shows an almost 50% increase at the maximum emission wavelength after addition of 100 μ M dopamine. for *in vitro* cellular detection purposes, the nanosensors were immobilized on glass surface. Simple incubation of NIRDA suspension on glass bottom chamber slides in room temperature created a homogenous coverage of the glass surface. As shown in Fig. S2D, the NIRDA surface was imaged with a nIR camera at 561 nm excitation. Dim nanotubes brightened upon exposure to dopamine molecules (Fig. 1A.). As shown in Fig. 1B, freshly isolated human neutrophils from healthy donors were seeded on NIRDA surface and upon stimulation of neutrophils, hot-spots of dopamine release could be visualized as fluorescently bright regions since the nanotubes became brighter when they were exposed to dopamine molecules.

2 Results

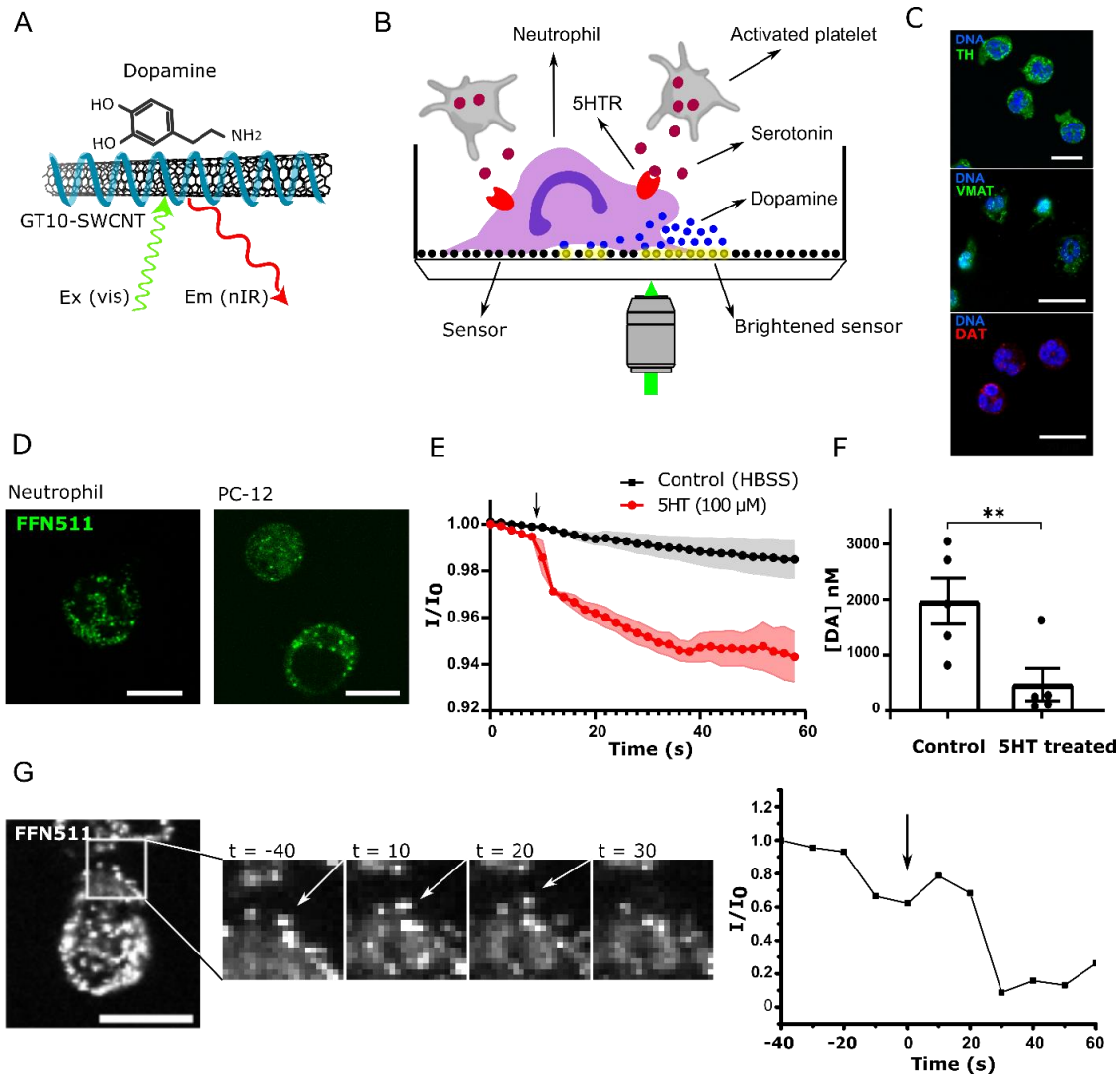


Fig. 1. The dopamine detection strategy and dopaminergic machinery in neutrophils. (A), The nanosensor schematic showing a carbon nanotube backbone functionalized with (GT)10-SWCNT. Interaction of the dopamine molecule with phosphate groups in DNA molecule leads to a change in the fluorescence emission pattern of the nanosensors. (B), Schematic shows the sensing of dopamine exocytosis from neutrophils stimulated by platelet-derived serotonin. Neutrophils are adhered on a surface functionalized with nanosensors. When serotonin interacts with its receptors on neutrophils, it triggers exocytosis of dopamine. Nanosensors brighten when they come in to contact with dopamine, creating a map showing pattern of release as shiny dots. (C), Dual antibody staining of DAPI and tyrosine hydroxylase (top), VMAT-2 (middle) and dopamine transporter (bottom). The scale bar is 10 μm for top image, and 20 μm for middle and bottom images. (D), Fluorescence imaging of FFN511 filled vesicles in live neutrophils and PC-12 cells (positive control cell-line). Scale bar is 10 μm . (E), Exocytosis of FFN511 from neutrophils stimulated with 100 μM serotonin analyzed by measuring the fluorescence intensity changes over time. Data is mean \pm SEM of triplicates. (F),

2 Results

Intracellular dopamine content of neutrophils in resting state and after stimulation with 100 μ M serotonin. $N=5$, mean \pm SEM, $P \leq 0.01$. (G), Tracking of a single FFN511 vesicle in a neutrophil before, during and after stimulation with 100 μ M serotonin, over time. Vesicle trafficking toward cell membrane, fusion with membrane and extracellular release of FFN511 is observed and analyzed by plotting the fluorescence intensity of the vesicle over time. Scale bar is 10 μ m.

Neutrophils Synthesize, Store, and Release Dopamine upon Serotonin Stimulation

Before employing NIRDA for detection, we first established the presence of a dopaminergic signaling pathway in the neutrophils. Tyrosine hydroxylase (TH), dopamine transporter (DAT) and vesicular monoamine-2 (VMAT-2) antibody staining of resting neutrophils are presented in Fig. 1C. Selective antibody staining for TH, DAT and VMAT are compared to their isotype controls in Fig. S1.

Next, fluorescent false neurotransmitters (FFN) were employed to visualize dopamine-filled vesicles and image exocytosis of dopamine from neutrophils. FFNs are fluorescent dopamine analogs that mimic the kinetics of catecholamines.²⁰ Here, we incubated neutrophils with FFN511, which has high affinity for DAT and VMAT-2; therefore, simulates the behavior of dopamine.²¹ When FFN511 is supplied to neutrophils, they are predominantly uptaken by DAT and stored in VMAT vesicles, and are further released to the extracellular media through an active process of vesicles trafficking to the cellular membrane, merging with the membrane and releasing their content into the extracellular media. To investigate whether neutrophils indeed are capable of uptaking, storage and release of dopamine in response to stimulation, we incubated the neutrophils with FFN511 and imaged the neutrophils. As shown in Fig. 1D, FFN511 molecules were stored in granular structures inside neutrophils comparable to PC-12 cells which are shown here as positive controls. Image sequences of FFN511 treated neutrophils were taken and neutrophils were stimulated with serotonin. We observed that treating neutrophils with serotonin (100 μ M) compared to buffer, led to significant exocytosis of FFN511 molecules which was shown by a rapid reduction in the fluorescent of the FFN-filled vesicles in Fig. 1E. A reduction in fluorescence intensity is in line with release of FFNs from vesicles and diffusion in the media. We also employed another FFN molecule, FFN102. FFN102 is a

2 Results

pH sensitive molecule with high affinity for DAT and VMAT-2.²² When it is stored inside vesicles, because of the slightly acidic pH (~5.5) of the vesicles, the fluorescence is very dim. However, upon release from vesicles, and diffusion in neutral pH (~7) of the extracellular media, the FFNs become significantly brighter. In Fig. S2C, it is shown that after stimulation with serotonin, the fluorescence intensity of the extracellular media around the neutrophils increased significantly (between 5-10 %) compared to when buffer is added to the neutrophils.

Since serotonin is also uptaken by VMATs, it is important to show that FFN511 release from neutrophils following serotonin treatment wasn't merely a result of substitution of FFN511 with serotonin. Therefore, we analyzed the dopamine content of resting neutrophils when treated with serotonin and compared it to control neutrophils by HPLC coupled to an EC detector.

The concentration of dopamine in resting neutrophils was almost ~2000 nM/cell or 2×10^{-18} mol/cell. After neutrophils were treated with serotonin, the intracellular concentration of dopamine reduced to less than 500 nM which marks a decrease to a fourth (Fig. 1F). By FFN511 imaging, we were able to track a single vesicle during serotonin induced exocytosis events and image vesicle migration toward the cytoplasmic membrane. Diffusion of the vesicle with the cytoplasmic membrane and releasing its content marked by a stark decrease in the fluorescent intensity of the vesicle as shown in Fig. 1G.

Serotonin Induces Calcium Mobilization Followed by VMAT-vesicle Exocytosis in Neutrophils

We studied the effect of serotonin stimulation on calcium (Ca^{2+}) mobilization in neutrophils. Ca^{2+} is one of the main drivers of intracellular signaling, as such it controls cellular function.²³ To observe whether serotonin-induced dopamine exocytosis is a Ca^{2+} sensitive process, we analyzed generation of Ca^{2+} waves in neutrophils by Fluo4-am, a Ca^{2+} indicator. Indeed, serotonin induced a significant spike in the intracellular concentration of Ca^{2+} (>50 % increase) compared to buffer and dopamine itself (Fig. 2C). While dopamine also induced a small [Ca^{2+}] increase, it was not significant compared to buffer (Fig. 2A-C).

2 Results

We employed our novel sensing strategy to visualize exocytosis of dopamine from neutrophils simultaneously with generation of Ca^{2+} signals after stimulation with serotonin (Fig. 2D, E). Neutrophils were seeded on NIRDA surface, in the fluorescence visible channel (GFP), the fluo-4am fluorescence was imaged and in the nIR channel the fluorescence of NIRDA was recorded. Images were taken with 5 fps speed and upon addition of serotonin, an immediate increase in the Ca^{2+} was observed. After a time-delay of ~ 20 s, the fluorescence of NIRDA in localized regions corresponding to the cell surface and around it became brighter indicating dopamine release. Because of the high spatial resolution of our sensor we could record release events of many cells in parallel and investigate specific regions of the cells that released dopamine as the resolution limit of NIRDA is only limited by the abbe limit. Fig. 2E shows the fluorescence intensity of both Fluo-4am and the nanosensors corresponding to intracellular Ca^{2+} release and dopamine exocytosis respectively for 3 cells marked in Fig. 2D.

2 Results

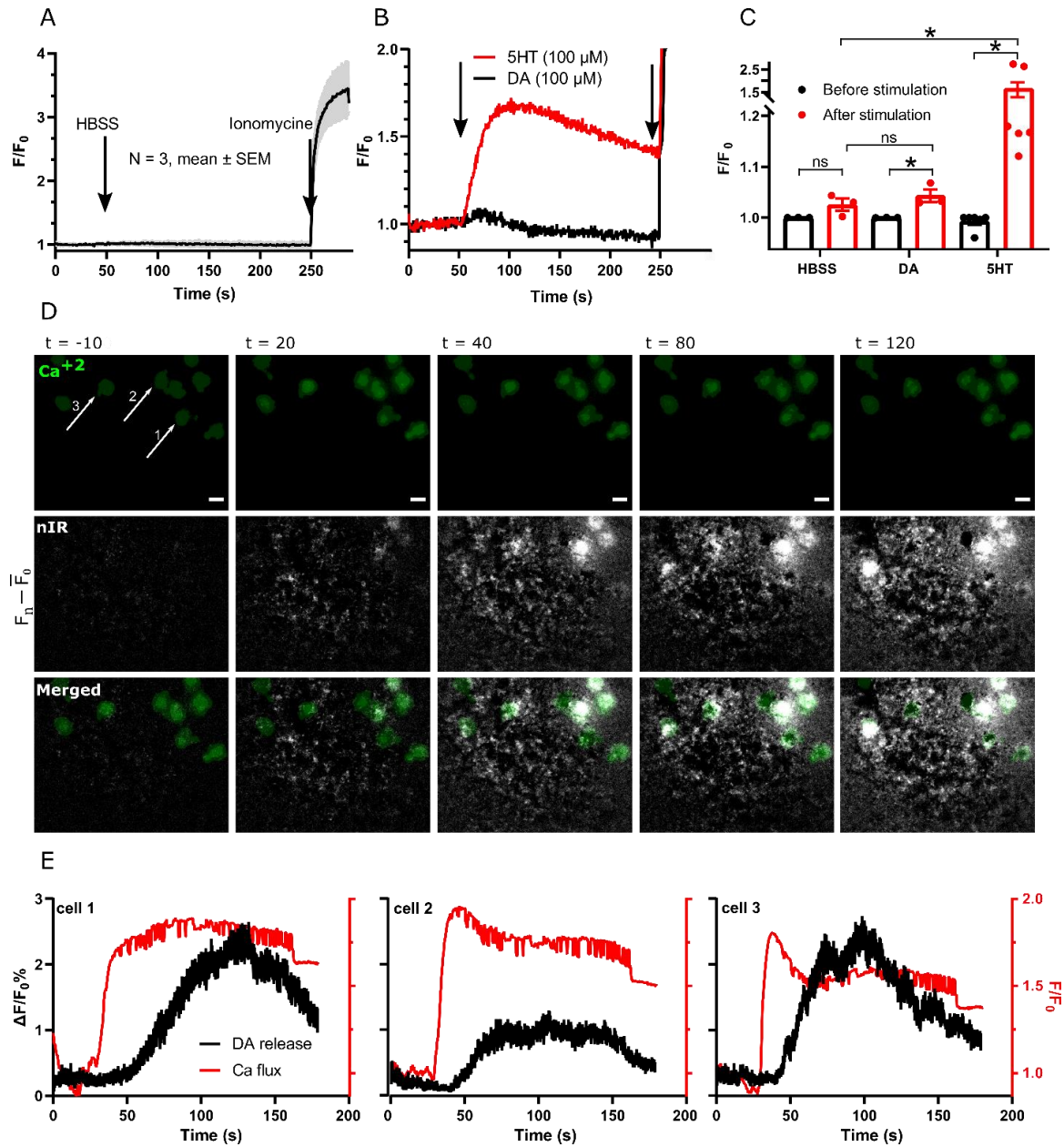


Fig. 2. Serotonin induces Ca^{2+} mobilization led by dopamine exocytosis in neutrophils. (A), Fluorescence signal of neutrophils incubated with Fluo-4, AM, Ca^{2+} indicator, over time when HBSS (buffer, negative control) was added at $t = 50$ s and Ionomycin (Ca^{2+} ionophore, positive control, 5 μ M) was added at $t = 250$ s. Data is shown as mean \pm SEM of triplicates (B), Fluorescence signal of neutrophils incubated with Fluo-4, AM over time when serotonin or dopamine (100 μ M) was added at $t = 50$ s and Ionomycin (5 μ M) at $t = 250$ s. (C), Maximum fluorescence increase after stimulation with buffer, dopamine and serotonin indicating statistically significant difference between dopamine and serotonin groups compared to their baseline and control group. Data is shown as mean \pm SEM of at least triplicates. Each point represents a single experiment. (D), Neutrophils are adhered on nanosensor surfaces. Image sequences recorded intracellular calcium mobilization

2 Results

(top) and fluorescence intensity changes in the nIR channel, indicative of dopamine release, (middle) and merged channels (bottom) before and after stimulation with serotonin (100 μ M). All scale bars are 10 μ m. (E) The fluorescence intensity changes of NIRDA in the nIR channel (indicative of dopamine release) and Fluo-4, AM (indicative of Ca^{2+} mobilization) are plotted against time for 3 neutrophils shown with an arrow in section (D).

Imaging Dopamine exocytosis by NIRDA nanosensors

The release of dopamine from neutrophils was visualized. We were also able to detect directionality in the exocytosis and heterogeneity amongst cells of the same origin as shown in Fig. 3A. As expected, we observed variation in dopamine exocytosis amongst donors (Fig. 3B) as well. The response of NIRDA to various molecules was examined (Fig. 3C). 100 μ M dopamine (positive control) induced a \sim 30% percent increase in the fluorescence intensity of NIRDA. Serotonin and Ionomycin (a membrane permeable Ca^{2+} ionophore used as a positive control to induce intracellular Ca mobilization) did not affect the fluorescence intensity of the nanosensors at all. Addition of buffer (negative control) to neutrophils adhered on NIRDA surface also did not affect the fluorescence intensity of the nanosensors. The fluorescence response of NIRDA to exocytosis of dopamine in a single cell is presented in Fig. 3D, showing an almost 6% increase in fluorescence.

Neutrophils release various molecules upon activation. This includes reactive oxygen species (ROS), enzymes, peptides and inflammatory mediators. To exclude the fact that the localized fluorescence spikes belonged to exocytosis of other molecules from neutrophils, we depleted the neutrophils from dopamine by incubating them with FFN102 molecules. At high concentrations, FFN102 depletes VMAT vesicles from dopamine and inhibits dopamine reuptake.²² FFN102 treated neutrophils were stimulated with serotonin and exocytosis was imaged in the GFP channel (to observe FFN102 release) while dopamine exocytosis was imaged in the nIR channel simultaneously as shown in Fig. 3E. The neutrophils were only depleted from dopamine but contained all of their other vesicular and granular components. If the NIRDA was not selective to dopamine, we would expect that upon activation with serotonin and degranulation of the non-catecholamine granules, a fluorescence response would be produced in the nIR channel. However, we observed no fluorescence increase in the nIR channel but a fluorescence increase in the GFP channel

2 Results

was observed which confirmed exocytosis of FFN102 molecules from neutrophils upon activation. Indicating that indeed exocytosis of VMAT vesicles occurred but the vesicles didn't contain dopamine. We also measured the fluorescence change after serotonin stimulation in both channels which is presented in Fig. 3F. There is a statistically significant difference between fluorescence changes in the nIR channel (~0%) and GFP channel (75%). The response of nanosensors to H_2O_2 was also recorded since reactive oxygen species (ROS) could be extracellularly released from neutrophils upon activation. We observed no changes in the fluorescence signal of NIRDA (Fig. S2E).

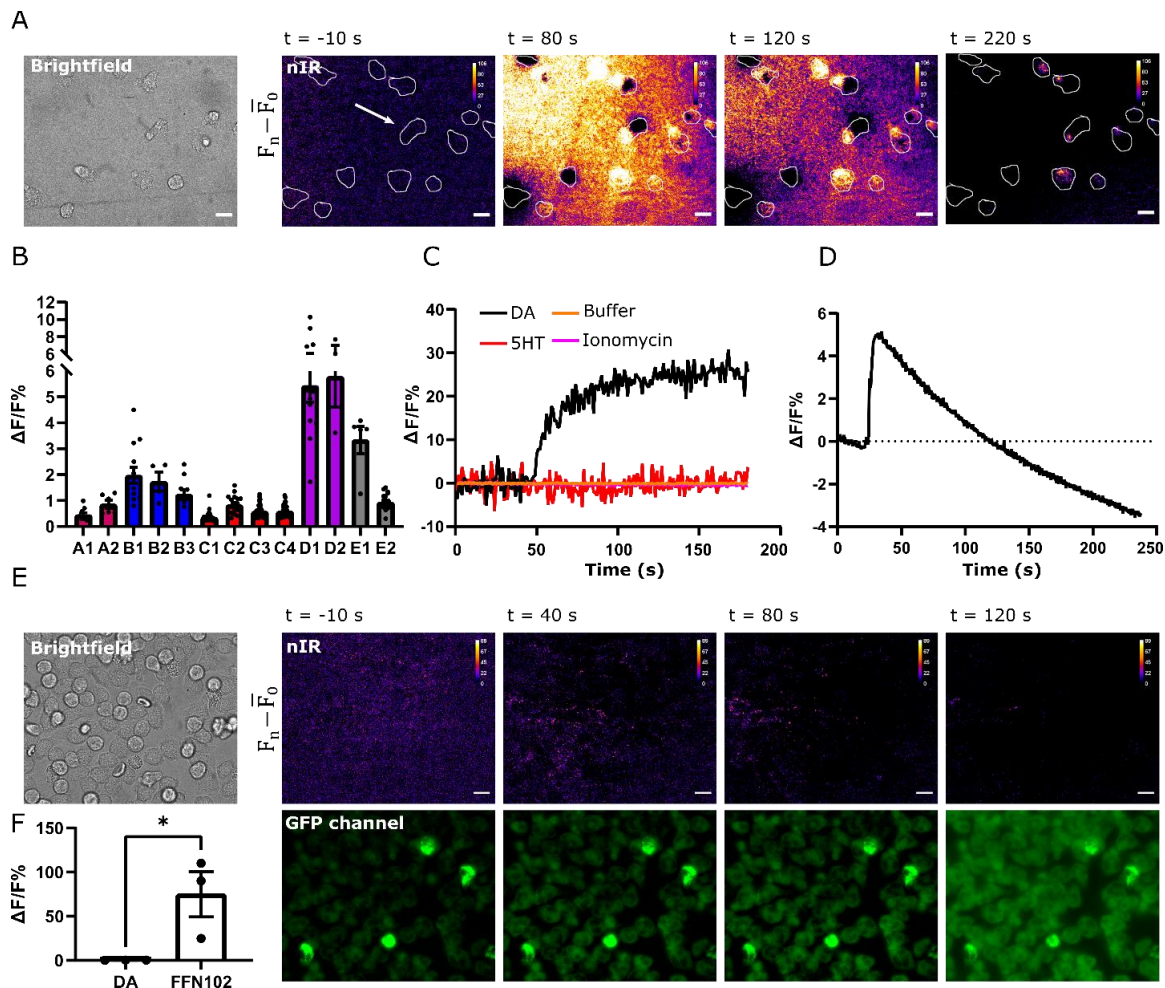


Fig. 3. Live imaging of dopamine exocytosis from neutrophils. (A), Brightfield image (left) and nIR Image sequence (right) of neutrophils adhered on nanosensor surface. Addition of serotonin ($100 \mu M$) at $t = 0$ induced an increase in the fluorescence of NIRDA in localized regions corresponding to cell regions indicating exocytosis of dopamine. Scale bar is $10 \mu m$. (B), The maximum fluorescence response of NIRDA after release of dopamine from neutrophils stimulated by serotonin. Each bar represents an independent

2 Results

experiment and each dot is a single neutrophil. (C), The fluorescence response of NIRDA to dopamine, serotonin, Ionomycin (blank nanosensors) and to buffer (neutrophil adhered nanosensors) over time. (D), The fluorescence response of nanosensors to dopamine exocytosis from a single neutrophil after stimulation with serotonin (shown with an arrow in section (A)). (E), Brightfield images (cells, top-left), nIR image sequence (nanosensors, top right) and GFP channel (FFN102, bottom) of neutrophils incubated with FFN102 before and after addition of serotonin (100 μ M). There is no fluorescence change in the nIR, indicating no dopamine release. The GFP channel shows an increase in fluorescence indicating FFN102 release. Scale bar is 10 μ m. (F), Maximum fluorescence change of the nanosensors (dopamine release) and FFN102 upon stimulation with serotonin. Data represents \pm SEM of triplicates. P value is 0.02 and each dot represents an independent experiment.

Dopamine Exocytosis Is Mediated by Serotonin Receptors

To investigate whether dopamine exocytosis induced by serotonin is serotonin receptor (5HTR) mediated as opposed to serotonin activating neutrophils in an unspecific manner, we treated the neutrophils with a 5HTR antagonist. For this purpose, Ketanserin was employed. Ketanserin is a 5HTR-2 selective antagonist²⁴ that in high concentrations can inhibit the activity of other 5HTRs as well. Ketanserin also binds to VMATs.²⁵ For this experiment, after neutrophils were adhered on NIRDA, ketanserin (100 μ M) was added to the media for 2-5 minutes. Then, imaging was started and serotonin was added to neutrophils. Ketanserin-treated neutrophils did not release dopamine when stimulated with serotonin as shown in Fig. 4A. We wanted to investigate whether Ca^{2+} mobilization which is induced after serotonin stimulation is sufficient for dopamine release or if 5HTR engagement is necessary. After stimulating Ketanserin-treated neutrophils with serotonin (shown in Fig. 4A top panel), we stimulated them with Ionomycin (shown in Fig. 4A bottom panel) to induce an intracellular Ca^{2+} increase. In the experiment shown in Fig 5A, after Ionomycin stimulation, there is a slight increase in the fluorescent signal at localized regions around cells corresponding to dopamine release which is significantly higher than that of ketanserin (Fig. 4B). However, when the average fluorescence intensity changes of multiple independent experiments were taken together, the difference between the two groups was not statistically significant (Fig. 4D). We conclude that 5HTR engagement is necessary for dopamine exocytosis in neutrophils. We also investigated dopamine

2 Results

exocytosis from neutrophils when they were stimulated by a 5HTR agonist. For this purpose, CP809 was used. CP809 induced exocytosis of dopamine in neutrophils as visualized by a spike in the fluorescence of the nanosensors in localized regions around the cell membrane (Fig. 4E-G).

2 Results

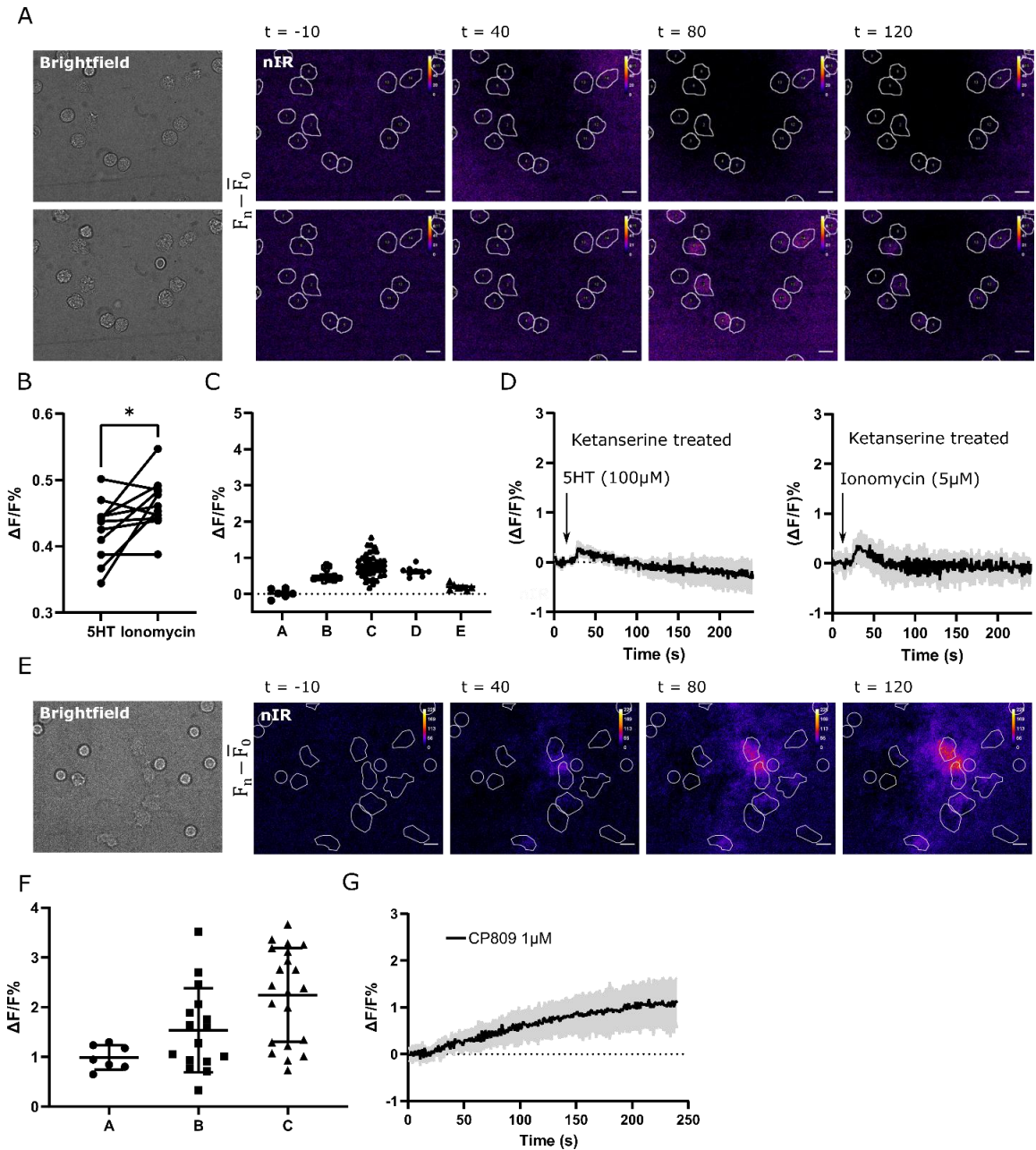


Fig. 4. Imaging dopamine exocytosis in neutrophils incubated with 5HTR agonists/antagonists. (A), Brightfield image (left) and nIR Image sequences (right) of neutrophils adhered on NIRDA surface. Neutrophils are first incubated with Ketanserin (100 μ M), and stimulated with serotonin (100 μ M) at $t = 0$ (top). The same cells were then stimulated with 5 μ M ionomycin (bottom). (B), Maximum fluorescence signal after stimulation of cells in section (A). P value is 0.0150. (C), Maximum fluorescence increases of nanosensors after stimulation with serotonin in Ketanserin-treated neutrophils. Each column is an independent experiment and each dot represents a single neutrophil. (D), Fluorescence signal of neutrophils treated with Ketanserin and stimulated with serotonin (first plot) and Ionomycin (second plot) over time. Data is presented as mean \pm SEM of

2 Results

triplicates. (E), Brightfield image (left) and nIR Image sequence (right) of neutrophils adhered on NIRDA surface before and after stimulation with CP809. (F), Maximum fluorescence increases of nanosensors after stimulation with CP809 ($1 \mu\text{M}$). Each column is an independent experiment and each dot represents a single neutrophil. (G), Fluorescence signal over time of neutrophils stimulated with CP809 ($1 \mu\text{M}$). Data is presented as mean \pm SEM of triplicates. All scale bars are $10 \mu\text{m}$.

Platelet-Neutrophil Interactions

After establishing that serotonin induced receptor mediated exocytosis of dopamine, we studied platelet-neutrophil interaction by seeding platelets and neutrophils together on NIRDA surface. Then, platelets were stimulated with thrombin to release serotonin. We studied the exocytosis of dopamine from neutrophils stimulated by platelet-derived serotonin (Fig. 5A). Thrombin did not induce a fluorescence change when applied to blank NIRDA. We also recorded the fluorescence of NIRDA in response to platelets stimulated with thrombin. Serotonin or any other component that is released from platelets during stimulation did not produce a false fluorescence signal (Fig. 5B). Dopamine exocytosis from neutrophils was visualized in single cells. The fluorescence signal over time shows the pattern of release and the maximum fluorescence intensity changes show the maximal release from single cells (Fig. 5C, D).

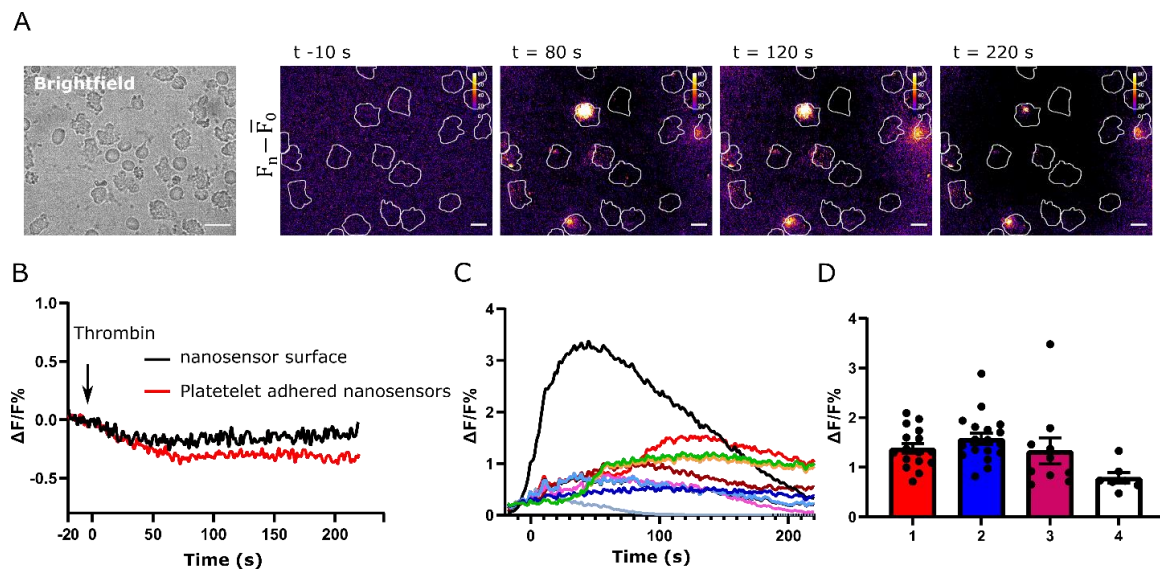


Fig. 5. Imaging dopamine exocytosis from neutrophils stimulated by activated platelets. (A), Brightfield image (left) and nIR Image sequence (right) of neutrophils and platelets

2 Results

adhered on NIRDA surface. nIR images are recorded before and after stimulation of platelets with thrombin (1 Unit/mL). (B), The fluorescence response of blank nanosensors to thrombin (blank) and platelet adhered NIRDA to thrombin (red). (C), Fluorescence signal over time of neutrophils stimulated by activated platelets. Each trace belongs to a region of interest in the neutrophils of section (A). (D), Maximum fluorescence intensity changes. Each column presents an independent experiment and each dot represents a single neutrophil. Data is presented as mean \pm SEM.

Paracrine Modulatory Role of Dopamine on Formation of Neutrophil Extracellular Traps

The expression of dopamine receptors (DR) in neutrophils were studied by antibody staining (Fig. 6A, B, for isotype controls see Fig. S3). We were able to establish expression of D2-like receptors (D2, D3). There was minimal expression of D5 receptor and D1 receptors was not present. Finally, we examine the effect of dopamine on the rate of NETosis after stimulation with Phorbol-12-myristate-13-acetate (PMA). NETosis is an immune response specific to neutrophils where neutrophils release their DNA content with a mixture of proteases into the extracellular matrix in response to pathogens to trap them and reduce their spread. We investigated the effect of dopamine (10, 100, 1000 μ M), epinephrine (E, 100 μ M) and norepinephrine (NE, 100 μ M) on NETosis in the presence and absence of PMA (a neutrophil stimulator). We observed that, dopamine at all concentrations significantly reduces NET formation compared to the control group in a concentration dependent manner (Fig. 6C, D., Fig. S4.). We also observed that serotonin reduced the rates of NETosis in a concentration-dependent manner. This could be due to the effect of serotonin in inducing dopamine release from neutrophils or the effect of serotonin on NETs rate independent of dopamine. By comparing the rate of NET formation in dopamine treated groups with NE and E treated groups, we excluded that the effect of dopamine on NET was due to the reducing effect of dopamine since catecholamines with similar redox activity (E and NE) did not reduce NET formation. (Fig. 6D.).

2 Results

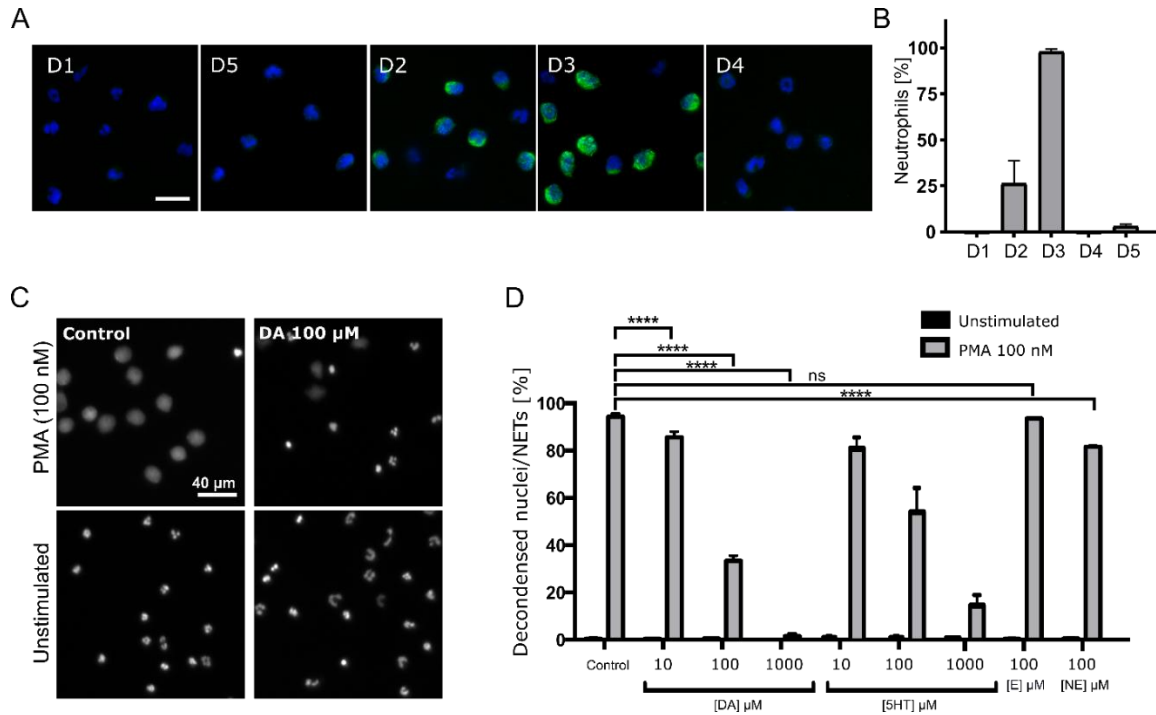


Fig. 6. Dopamine is a neutrophil immune-modulator through paracrine signaling. *A*, Double antibody staining of Hoechst (nucleus) and DRs in neutrophils (see Fig. S3. for isotype controls). the scale bar is 20 μ m. *B*, The expression of DRs in neutrophils by FACS. *C*, The effect of dopamine on the rate of NETosis in neutrophils stimulated with or without PMA. *D*, The effect of dopamine, serotonin and other catecholamines on the rate of NETosis in neutrophils stimulated with or without PMA.

Discussion

The role of dopamine in regulating complex immunological responses isn't completely understood. Studying the immunomodulating effects of dopamine in peripheral immune cells is even more challenging because circulating immune cells are not readily exposed to dopamine concentrations the same way immune cells in the neuroimmune system are. There are growing evidence that changes in the baseline level of dopamine occurring in pathological conditions affects the function of circulating immune cells.^{26–28} Immune cells also synthesize and release dopamine when they form immune synapses.²⁹ Dopamine was found to be synthesized in neutrophil^{1,12,13} as well as all immune cells.³⁰ The complex mechanism in which immune cells synthesize, store, release and respond to dopamine

2 Results

remains elusive to this day. Most studies either investigate the expression of proteins involved in the dopaminergic system or the effect of dopamine on the function of immune cells without recognizing the heterogeneity of the cells that release dopamine and changes in dopamine concentration in the microenvironment of the immune cell which shape the complex immunomodulatory role of dopamine. The dopaminergic system in immune cells is highly dynamic. The immunoregulatory role of dopamine is controlled by several factors; such as the immune cell subtype, the activation state of the immune cell, the pattern and abundance of DRs and dopamine concentration.³⁰ For this purpose, we aimed to study the dopaminergic system in neutrophils with a novel approach by SWCNT nanosensors to take the spatial context of neutrophils into account. This nanosensor platform is especially beneficial to investigate dopamine exocytosis in immune synapses on subcellular levels as for instance, dopamine synthesis and exocytosis from T cells was reported to be highly heterogeneous and dependent on T cell-B cell receptor engagement and synapse formation.³¹ These findings highlight the need for novel tools to analyze dopamine exocytosis in immune cells with high spatial resolution.

First, we confirmed the findings of a previous study¹² that TH is expressed in neutrophils (Fig. 1.) but contrary to another study³², we found that VMAT-2 is expressed in neutrophils (Fig. 1.). We also observed DAT expression. After establishing the expression of proteins involved in dopaminergic machinery in neutrophils, we focused on the mechanisms of dopamine exocytosis. We observed a direct link between platelet-derived serotonin and exocytosis of dopamine in neutrophils as shown by HPLC data (Fig. 1.), FFN exocytosis data (Fig. 1.) and dopamine exocytosis imaging by nanosensors (Fig. 2., 3. and 4.).

FFNs are powerful tools to investigate kinetics of catecholamine release in neuronal studies.^{21,22} FFN511 has high affinity for DAT and VMAT-2. We took advantage of this tool to visualize uptake of dopamine in VMAT vesicles and study their release upon cell activation. We observed that after incubating neutrophils with FFN511, granular structures were filled with FFN511, indicating that the FFN molecules were uptaken in VMAT vesicles. Stimulation of neutrophils with serotonin led to exocytosis of FFN containing granules. This was confirmed by imaging neutrophils with a fluorescent microscope and tracking the FFN filled vesicles (Fig. 1) over time after stimulating neutrophils (Fig. 1.).

2 Results

When comparing the fluorescence decrease after cell stimulation with control groups, the stark decrease in fluorescence of vesicles was attributed to vesicle fusion with plasma membrane and diffusion of FFNs into outside of vesicles. As the fluorescence of FFN511 undergoes rapid photobleaching, there was a concern that fluorescence decrease would not be entirely attributed to exocytosis. We also wanted to distinguish extracellular exocytosis of secretory vesicles and simple diffusion of vesicle content inside cytosol. Therefore, we employed FFN102 molecules which are fluorescent in a pH sensitive manner. The fluorescence of FFN102 molecules increases after encountering higher pH of extravesicular medium. By analyzing the fluorescence background of the extracellular medium and observing a stark increase in fluorescence we were able to confirm that FFNs were indeed secreted into extracellular space (Fig. 1., Fig. S2C.).

Next, the signaling pathway through which serotonin induces dopamine release was investigated. Indeed, the whole molecular pathway in neutrophil degranulation is not discovered. However, several studies have confirmed that Ca^{2+} mobilization plays an important role in all types of neutrophil degranulation.³³ Engagement of G protein-coupled receptors (GPCR) in neutrophils propagate a chain of protein phosphorylation events that leads to Ca^{2+} mobilization³⁴ and ultimately vesicle trafficking to plasma membrane, fusion and extracellular release. Therefore, we investigated if serotonin induced an increase in intracellular Ca^{2+} too. We discovered that serotonin through 5HTR-mediated signaling, induced Ca^{2+} mobilization and consecutively dopamine release (Fig. 2). With our unique approach, simultaneous imaging of intracellular Ca^{2+} and exocytosis of dopamine was carried out which confirmed a direct link between Ca^{2+} signaling and dopamine exocytosis (Fig. 2). Another interesting finding was that dopamine exocytosis required specific 5HTR engagement as 5HTR antagonists blocked serotonin induced dopamine release (Fig. 4). Interestingly, inducing Ca^{2+} increase with a Ca^{2+} ionophore did not induce dopamine release from neutrophils treated with 5HTR antagonists, indicating that dopamine release at least requires specific 5HTR engagement and the signaling pathway does not necessarily follow the same molecular pathway as other types of neutrophil granules (Fig. 4).

Our novel nanosensor, as a powerful tool, provides high spatio-temporal resolution for direct imaging of dopamine. To our knowledge, this platform is the only platform that can

2 Results

directly image catecholamine release. FFNs are indirect labels as they substitute the catecholamines. They also suffer from rapid bleaching which complicates dynamic imaging. The nanosensors however are resistant to bleaching and blinking. Other promising platforms such as optogenetic sensors³⁵, require extensive genetic manipulation. conventional methods, mainly electrochemical methods, such as voltammetry and amperometry have suitable temporal resolution (comparable to the biological time-scale of release events). However, the spatial resolution of these systems is largely limited by the electrodes used. As a result, release events can only be recorded in the vicinity of an electrode. This limits the spatial resolution to single cells. This nanosensor tool affords imaging of multiple cells at the same time (only limited by the field of view of the microscope). And within each cell, theoretically the resolution can be increased up to single nanosensors. Each nanosensor is approximately 600 nm in length with a diameter of less than 5 nm. When the nanosensors are immobilized on a glass surface, they form a homogenized coverage. In effect, their activity can be imagined as a smart checkered surface over which the cells are adhered. Each square lightens up when they encounter dopamine. In our previous studies, we have extensively studied the kinetics of the nanosensors and their selectivity to dopamine.³⁶ By employing this platform, in addition to showing that serotonin induces dopamine release, we observed directional dopamine release from neutrophils and the exocytosis of dopamine from neutrophils was not homogenous along the cell membrane. intercellular variations in dopamine exocytosis were observed that would be difficult to observe with other platforms. Finally, we investigated the autocrine/paracrine effect of dopamine on neutrophils. Similarly, several studies have investigated the effects of dopamine on other immune cells in an autocrine/paracrine functional loop.³⁷

It has been shown that dopamine regulates cytokine secretion³⁸ by suppressing pro-inflammatory cytokines.³⁹ We speculated that dopamine release from neutrophils regulates the response of neutrophils in a feedback loop by having protective effects on proinflammatory behavior of neutrophils. Whether dopamine assumes a pro-inflammatory or anti-inflammatory role is dependent on many factors but mainly the type and abundance of DRs on the cells. For instance, it was discovered that regulatory T cells (Tregs), released substantial amounts of catecholamines which reduced the inhibitory effect of Tregs over

2 Results

effector T cells.⁴⁰ Similarly, dopamine was investigated in the interaction between dendritic cells (DC) and naïve CD4⁺ T cells. DCs released dopamine upon antigen-specific interaction with naïve CD4⁺ T cells. Through D1-like receptors, dopamine shifted differentiation toward Th2 and blocking dopamine receptors shifted differentiation toward Th1.⁴¹

To investigate the autocrine/paracrine loop effect of dopamine in neutrophils, first, we studied the expression of DRs in neutrophils on the protein level (antibody staining, see Fig. 6. and Fig. S3.). A previous study had reported lower levels of D2-like receptor expression (D3 only 2.4%) and more of D1-like receptors (D5 4.5%).⁵ However, we could mainly observe the expression of D2-like receptors in neutrophils. Then, the effect of dopamine on one of the most important host defense functions of neutrophils which is formation of neutrophil extracellular traps (NETosis) was investigated. The formation of neutrophil extracellular traps (NETs)⁴² as a host defense mechanism was investigated when PMA stimulated neutrophils were treated with different concentrations of dopamine. We discovered that dopamine reduced the rate of NETosis (Fig. 6C.). The protective effects of dopamine on neutrophils was concentration dependent. Also, other catecholamines (norepinephrine and epinephrine) did not produce the same response as dopamine, indicating the effect of dopamine was indeed receptor mediated and not a result of its redox activity.

As discussed earlier, this platform is promising in immune cells studies because we can study the behavior of immune cells with special consideration for their microenvironment as spatial context is extremely important in how immune cells interact with other cells, the inflammatory mediators or blood components. A limitation of this study was that we did not distinguish between subpopulations of neutrophils. despite originally perceiving neutrophils as terminally differentiated and homogenous population, several subpopulations of neutrophils with distinct molecular biomarkers have been discovered.⁴³ It has been shown that circadian rhythm, the circulation time of a neutrophil, mechanical forces, microenvironment, infection and priming can cell reprogramming and phenotypical changes. It is possible that different subtypes of neutrophil have different dopamine content and different level of dopamine release. Also, different subtypes of neutrophils might have

2 Results

different sensitivity to serotonin stimulation. future studies should consider the heterogeneity of neutrophils.

Conclusion

NIRDA is a promising platform in immune cells studies because we can study the behavior immune cells with special consideration for their microenvironment as spatial context is extremely important to how immune cells function. This platform enables investigating intercellular heterogeneity. It is possible to image the kinetics of exocytosis in immune synapses and study receptor-mediated cell-cell interaction with a spatial resolution at subcellular level.

References

1. Cosentino M, Marino F, Bombelli R, Ferrari M, Lecchini S, Frigo G. Endogenous catecholamine synthesis, metabolism, storage and uptake in human neutrophils. *Life Sci.* 1999;64(11):975-981. doi:[https://doi.org/10.1016/S0024-3205\(99\)00023-5](https://doi.org/10.1016/S0024-3205(99)00023-5)
2. Musso NR, Brenci S, Setti M, Indiveri F, Lotti G. Catecholamine content and in vitro catecholamine synthesis in peripheral human lymphocytes. *J Clin Endocrinol Metab.* 1996;81(10):3553-3557.
3. Gaskill PJ, Carvallo L, Eugenin EA, Berman JW. Characterization and function of the human macrophage dopaminergic system: implications for CNS disease and drug abuse. *J Neuroinflammation.* 2012;9(1):203. doi:10.1186/1742-2094-9-203
4. Rönnerberg E, Calounova G, Pejler G. Mast cells express tyrosine hydroxylase and store dopamine in a serglycin-dependent manner. *Biol Chem.* 2012;393(1-2):107-112.
5. McKenna F, McLaughlin PJ, Lewis BJ, et al. Dopamine receptor expression on human T- and B-lymphocytes, monocytes, neutrophils, eosinophils and NK cells: a flow cytometric study. *J Neuroimmunol.* 2002;132(1-2):34-40.
6. Calderon TM, Williams DW, Lopez L, et al. Dopamine Increases CD14+CD16+ Monocyte Transmigration across the Blood Brain Barrier: Implications for Substance Abuse and HIV Neuropathogenesis. *J Neuroimmune Pharmacol.* 2017;12(2):353-370. doi:10.1007/s11481-017-9726-9
7. dos-Santos-Pereira M, Acuña L, Hamadat S, et al. Microglial glutamate release evoked by α -synuclein aggregates is prevented by dopamine. *Glia.* 2018;66(11):2353-2365.
8. Fan Y, Chen Z, Pathak JL, Carneiro A, Chung CY. Differential regulation of adhesion and phagocytosis of resting and activated microglia by dopamine. *Front Cell Neurosci.* 2018;12:309.
9. Gaskill PJ, Yano HH, Kalpana G V, Javitch JA, Berman JW. Dopamine receptor activation increases HIV entry into primary human macrophages. *PLoS One.* 2014;9(9):e108232.
10. Tecchio C, Micheletti A, Cassatella MA. Neutrophil-Derived Cytokines: Facts Beyond Expression. *Front Immunol.* 2014;5:508. <https://www.frontiersin.org/article/10.3389/fimmu.2014.00508>.
11. Rosales C. Neutrophil: A Cell with Many Roles in Inflammation or Several Cell Types? *Front Physiol.* 2018;9:113. doi:10.3389/fphys.2018.00113
12. Flierl MA, Rittirsch D, Nadeau BA, et al. Upregulation of phagocyte-derived catecholamines augments the acute inflammatory response. *PLoS One.* 2009;4(2):e4414. doi:10.1371/journal.pone.0004414
13. Flierl MA, Rittirsch D, Nadeau BA, et al. Phagocyte-derived catecholamines

2 Results

- enhance acute inflammatory injury. *Nature*. 2007;449(7163):721-725. doi:10.1038/nature06185
14. Kruss S, Salem DP, Vuković L, et al. High-resolution imaging of cellular dopamine efflux using a fluorescent nanosensor array. *Proc Natl Acad Sci* . 2017;114(8):1789-1794. doi:10.1073/pnas.1613541114
 15. Dinarvand M, Neubert E, Meyer D, et al. Near-Infrared Imaging of Serotonin Release from Cells with Fluorescent Nanosensors. *Nano Lett*. 2019;19(9):6604-6611. doi:10.1021/acs.nanolett.9b02865
 16. Mammadova-Bach E, Mauler M, Braun A, Duerschmied D. Autocrine and paracrine regulatory functions of platelet serotonin. *Platelets*. 2018;29(6):541-548. doi:10.1080/09537104.2018.1478072
 17. Mauler M, Herr N, Schoenichen C, et al. Platelet serotonin aggravates myocardial ischemia/reperfusion injury via neutrophil degranulation. *Circulation*. 2019;139(7):918-931.
 18. Duerschmied D, Suidan GL, Demers M, et al. Platelet serotonin promotes the recruitment of neutrophils to sites of acute inflammation in mice. *Blood*. 2013;121(6):1008 LP - 1015. doi:10.1182/blood-2012-06-437392
 19. Gershon MD, Tack J. The Serotonin Signaling System: From Basic Understanding To Drug Development for Functional GI Disorders. *Gastroenterology*. 2007;132(1):397-414. doi:https://doi.org/10.1053/j.gastro.2006.11.002
 20. Pereira DB, Schmitz Y, Mészáros J, et al. Fluorescent false neurotransmitter reveals functionally silent dopamine vesicle clusters in the striatum. *Nat Neurosci*. 2016;19(4):578-586. doi:10.1038/nn.4252
 21. Gubernator NG, Zhang H, Staal RGW, et al. Fluorescent false neurotransmitters visualize dopamine release from individual presynaptic terminals. *Science (80-)*. 2009;324(5933):1441-1444. doi:10.1126/science.1172278
 22. Rodriguez PC, Pereira DB, Borgkvist A, et al. Fluorescent dopamine tracer resolves individual dopaminergic synapses and their activity in the brain. *Proc Natl Acad Sci*. 2013;110(3):870-875.
 23. Berridge MJ, Lipp P, Bootman MD. The versatility and universality of calcium signalling. *Nat Rev Mol Cell Biol*. 2000;1(1):11-21. doi:10.1038/35036035
 24. DuPre A, Teitler M. Ketanserin. In: Enna SJ, Bylund DBBTTTCPR, eds. New York: Elsevier; 2007:1-16. doi:https://doi.org/10.1016/B978-008055232-3.61983-X
 25. Henry JP, Gasnier B, Isambert MF, Darchen F, Scherman D. Ketanserin as a Ligand of the Vesicular Monoamine Transporter. In: LANGER SZ, GALZIN AM, COSTENTIN JBT-PR and NT, eds. Pergamon; 1991:147-150. doi:https://doi.org/10.1016/B978-0-08-041165-1.50055-7
 26. Torres KCL, Antonelli LR V, Souza ALS, Teixeira MM, Dutra WO, Gollob KJ.

2 Results

- Norepinephrine, dopamine and dexamethasone modulate discrete leukocyte subpopulations and cytokine profiles from human PBMC. *J Neuroimmunol.* 2005;166(1):144-157. doi:<https://doi.org/10.1016/j.jneuroim.2005.06.006>
27. Yan Y, Jiang W, Liu L, et al. Dopamine Controls Systemic Inflammation through Inhibition of NLRP3 Inflammasome. *Cell.* 2015;160(1):62-73. doi:<https://doi.org/10.1016/j.cell.2014.11.047>
 28. Melnikov M, Belousova O, Murugin V, Pashenkov M, Boyko A. The role of dopamine in modulation of Th-17 immune response in multiple sclerosis. *J Neuroimmunol.* 2016;292:97-101. doi:<https://doi.org/10.1016/j.jneuroim.2016.01.020>
 29. Papa I, Saliba D, Ponzoni M, et al. TFH-derived dopamine accelerates productive synapses in germinal centres. *Nature.* 2017;547(7663):318-323. doi:10.1038/nature23013
 30. Thomas Broome S, Louangaphay K, Keay KA, Leggio GM, Musumeci G, Castorina A. Dopamine: an immune transmitter. *Neural Regen Res.* 2020;15(12):2173-2185. doi:10.4103/1673-5374.284976
 31. Papa I, Saliba D, Ponzoni M, et al. TFH-derived dopamine accelerates productive synapses in germinal centres. *Nature.* 2017;547(7663):318-323. doi:10.1038/nature23013
 32. Anlauf M, Schäfer MK-H, Schwark T, et al. Vesicular Monoamine Transporter 2 (VMAT2) Expression in Hematopoietic Cells and in Patients with Systemic Mastocytosis. *J Histochem Cytochem.* 2006;54(2):201-213. doi:10.1369/jhc.5A6739.2005
 33. Lacy P. Mechanisms of Degranulation in Neutrophils. *Allergy, Asthma Clin Immunol.* 2006;2(3):98. doi:10.1186/1710-1492-2-3-98
 34. Káldi K, Szeberényi J, Rada BK, et al. Contribution of phospholipase D and a brefeldin A-sensitive ARF to chemoattractant-induced superoxide production and secretion of human neutrophils. *J Leukoc Biol.* 2002;71(4):695-700.
 35. Patriarchi T, Cho JR, Merten K, et al. Ultrafast neuronal imaging of dopamine dynamics with designed genetically encoded sensors. *Science (80-).* 2018;360(6396):eaat4422. doi:10.1126/science.aat4422
 36. Mann FA, Herrmann N, Meyer D, Kruss S. Tuning selectivity of fluorescent carbon nanotube-based neurotransmitter sensors. *Sensors (Switzerland).* 2017;17(7):1521. doi:10.3390/s17071521
 37. Sarkar C, Basu B, Chakroborty D, Dasgupta PS, Basu S. The immunoregulatory role of dopamine: an update. *Brain Behav Immun.* 2010;24(4):525-528.
 38. Kawano M, Takagi R, Saika K, Matsui M, Matsushita S. Dopamine regulates cytokine secretion during innate and adaptive immune responses. *Int Immunol.* 2018;30(12):591-606. doi:10.1093/intimm/dxy057

2 Results

39. Shao W, Zhang S, Tang M, et al. Suppression of neuroinflammation by astrocytic dopamine D2 receptors via α B-crystallin. *Nature*. 2013;494(7435):90-94.
40. Cosentino M, Fietta AM, Ferrari M, et al. Human CD4⁺ CD25⁺ regulatory T cells selectively express tyrosine hydroxylase and contain endogenous catecholamines subserving an autocrine/paracrine inhibitory functional loop. *Blood*. 2007;109(2):632-642.
41. Nakano K, Higashi T, Takagi R, Hashimoto K, Tanaka Y, Matsushita S. Dopamine released by dendritic cells polarizes Th2 differentiation. *Int Immunol*. 2009;21(6):645-654. doi:10.1093/intimm/dxp033
42. Yipp BG, Kubes P. NETosis: how vital is it? *Blood*. 2013;122(16):2784-2794. doi:10.1182/blood-2013-04-457671
43. Xie X, Shi Q, Wu P, et al. Single-cell transcriptome profiling reveals neutrophil heterogeneity in homeostasis and infection. *Nat Immunol*. 2020;21(9):1119-1133. doi:10.1038/s41590-020-0736-z

competing interests:

Authors declare that they have no competing interests.

Data and materials availability

All data are available in the main text or the supplementary materials.

2 Results

2.2.2 Supplementary Material

Serotonin Triggers Dopamine Exocytosis by Neutrophils in a Functional Negative Feedback Loop

Meshkat Dinarvand¹, Anne Schmitz², Elsa Neubert², Thea Mara Husar², Antonia Luise Gruhn², Benedetta Fazari³, Magdalena Shumanska⁴, Ivan Bogeski⁴, Joseph P. Huston³, Luise Erpenbeck^{2*}, and Sebastian Kruss^{1,5*}

¹Institute of Physical Chemistry, Göttingen University, Göttingen 37077, Germany

²Department of Dermatology, Venereology, and Allergology, University Medical Center, Göttingen 37075, Germany

³Center for Behavioral Neuroscience, Institute of Experimental Psychology, University of Düsseldorf, Düsseldorf, Germany

⁴Molecular Physiology, Institute of Cardiovascular Physiology, University Medical Center, Göttingen, Germany

⁵Physical Chemistry II, Bochum University, Germany

This manuscript is part of an unpublished work, which includes contributions from multiple collaborators. Human neutrophils were isolated and characterized by M.D. E.N., A.S., T.H., A.G. and L.E. Receptor staining were performed by E.N., T.H. M.D. and L.E. FACS analysis was performed by A.S. and L.E. FFN experiments were performed by M.D. Dopamine imaging experiments, nanosensor preparation and Ca imaging experiments were performed by M.D. Platelet were isolated by M.D. NETosis assays were performed by E.N., A.G. and L.E. HPLC analysis was performed by B.F. and M.D. Data analysis was performed by all authors. Image analysis was performed by M.D. and S.K. The research idea was designed by L.E. and S.K.

Supplementary Materials for
Serotonin Triggers Dopamine Exocytosis by Neutrophils in a Functional
Negative Feedback Loop

Meshkat Dinarvand¹, Anne Schmitz², Elsa Neubert², Thea Mara Husar², Antonia Luise
Gruhn², Benedetta Fazari³, Magdalena Shumanska⁴, Ivan Bogeski⁴, Joseph P. Huston³,
Luise Erpenbeck^{2*}, and Sebastian Kruss^{1,5*}

*Corresponding author

This file includes:

Supplementary Text: Materials and Methods

Tables S1 and S2

Figs. S1 to S4

2 Results

Materials and Methods

Isolation of human neutrophils from whole blood

Neutrophils were isolated from whole blood of healthy donors by density gradient separation method. This study was approved by the ethics committee of the University Medical Center Goettingen. Before donating blood, fully informed consent of each donor was obtained.

Briefly, fresh blood was collected into EDTA blood collection plastic tubes. Whole blood was layered on Histopaque 1119 (Sigma-Aldrich) and centrifuged at $1100 \times g$, for 21 minutes in room temperature with breaks off. The neutrophil layers (third layer mainly containing density gradient and fourth layer mainly containing neutrophils) were collected and diluted in HBSS buffer (without Ca^{2+} and Mg^{2+} , Gibco). The cell suspension was centrifuged at $400 \times g$, for 10 minutes in room temperature. The supernatant was discarded and the cell pellet was resuspended in HBSS buffer (without Ca^{2+} and Mg^{2+}) and layered on top of a 5 step Percoll (GE Healthcare) gradient and centrifuged at $1100 \times g$, for 21 minutes in room temperature with breaks off. The neutrophils were collected from the fourth layer and a bit from the layers above and below the fourth. The neutrophils were diluted in HBSS and centrifuged at $400 \times g$, for 10 minutes in room temperature. The pelleted neutrophils were resuspended in RPMI 1640 cell medium containing 10 mM HEPES and 0.5% fetal calf serum (FCS, heat-inactivated at $56^{\circ}C$ for 30 minutes). We confirmed the purity of neutrophils by cyto-spin assay and Diff-Quik staining. We maintained neutrophil purity $> 95\%$ of total isolated cells (without erythrocytes). Neutrophils were used for experiments immediately after isolation.

Isolation of human platelets from whole blood

Platelets were isolated from whole blood of healthy donors. This study was approved by the ethics committee of the University Medical Center Goettingen. Before donating blood, fully informed consent of each donor was obtained. Whole blood was collected into ACD blood collection tubes and whole blood was centrifuged at $300 \times g$, for 20 minutes with breaks off. Platelet rich plasma (PRP) was separated and incubated at $37^{\circ}C$, 5% CO_2 , for 10 minutes. Before centrifugation, PGE1 (1 μM) was added and centrifuged at $800 \times g$ for

2 Results

15 minutes, breaks off. the pelleted platelets were carefully resuspended in Tyrode's solution pH 6.5 and incubated at 37° C, 5% CO₂, for 10 minutes. Then, PGE1 (1 μM) was added and centrifuged again at 800 × g for 15 minutes, breaks off. The pellet was again resuspended in Tyrode's solution pH 6.5 and incubated at 37° C, 5% CO₂, for 10 minutes. Before centrifugation, PGE1 (1 μM) was added and centrifuged at 800 × g for 15 minutes, breaks off. Platelets were resuspended in Tyrode's solution pH 7.4 and incubated in 37° C, 5% CO₂, for 30 minutes before starting experiments.

Synthesis of Nanosensors

(6,5)-enriched SWCNTs (carbon ≤95%, ≥93% carbon as SWCNT, Signis® SG65i, 0.7–0.9 nm diameter (Sigma-Aldrich, Germany) and (GT)₁₀ oligonucleotide (a ssDNA sequence of 5'-GTGTGTGTGTGTGTGTGTGT-3 synthesized by Sigma-Aldrich, Germany) were mixed in phosphate saline buffer (PBS) with final concentrations of 0.5 mg/mL and 50 μM respectively. The dispersion was tip sonicated (Fisher Scientific Model 120 Sonic Dismembrator) at 30 % amplitude for 20 minutes. The nanosensor suspension was centrifuged (Eppendorf centrifuge 5415 D) at 16000 x g for 30 minutes twice. After each centrifugation, the pellet was discarded and the supernatant was collected for further investigation. The nanosensor suspension was stable in room temperature for several months.

Nanosensor Characterization

Absorption spectra of the NIRDA was collected with a UV–vis–nIR spectrometer (JASCO V-670, Spectra Manager Software). The nanosensors were diluted at the ratio 1:100 in PBS to measure nIR absorbance. The concentrations of NIRDA was calculated by integrating the area under the curve belonging to (6,5) SWCNTs peak and taking extinction coefficient with an estimated length of 600 nm. For all dopamine sensing experiments with neutrophils, the concentration of NIRDA was 4 nM. For acquiring the fluorescence emission spectra of NIRDA in suspension, the concentration was 2 nM.

Fluorescence Spectroscopy of Nanosensors

NIRDA suspension in HBSS (2 nM) was excited with a 561 nm laser coupled with an Olympus IX73 microscope at 1 s integration time. The emission spectra from 800 nm to

2 Results

1300 nm were acquired by an Andor iDus InGaAs 491 array NIR detector attached to a Shamrock 193i spectrograph (Andor Technology Ltd., Belfast, Northern Ireland).

Fluorescence Microscopy of Neutrophils Adhered on Nanosensors

NIRDAs were immobilized on glass surfaces by incubating the surface with 4 nM NIRDA suspension overnight in 4° C. Before measurements, the surfaces were washed with HBSS × 3 and HBSS (with Ca²⁺ and Mg²⁺) was added to the surface. Neutrophils at concentration of 10⁶/mL in HBSS (with Ca²⁺ and Mg²⁺) were seeded on NIRDA immobilized glass bottom chamber slides. The neutrophils were let to adhere for 5 minutes and the medium was aspirated to remove loosely adhered cells. Fresh medium was added to the cells and image acquisition was started, after 20 s, the stimulant was added to the media while image acquisition continued.

For imaging, we employed an Olympus BX53 microscope, a 561 nm laser (Cobolt Jive™ laser, Cobolt AB, Solna, Sweden) and two cameras. An Andor Zyla 5.5 sCMOS camera, (Andor Technology Ltd., Belfast, UK) for visible fluorescence and NIR InGaAs camera for nIR fluorescence.

Images were obtained with a 100x objective lens (UPLSAPO100XS, Olympus, Tokyo, Japan) and recorded with 100 ms exposure time and at 5 frame per second rate. For visible fluorescence, an xCite 120Q fluorescence lamp and an EGFP excitation filter was used. The emission was filtered by a 650 nm short-pass filter, a 561 nm notch filter and 525/50 nm bandpass filter. For nIR fluorescence 561 nm laser was used at 100 mW power. Images were analyzed with ImageJ 1.52n.

Fluorescence Microscopy of FFN Exocytosis from Neutrophils

Neutrophils were adhered on glass chamber slides at 10⁶/mL concentration in HBSS (with Ca²⁺ and Mg²⁺). FFN511 (Abcam, USA) was dissolved in DMSO and added to the cell suspension with the final concentration of 5 μM. Cells were incubated in 37° C, 5% CO₂, for 5 minutes, then media was aspirated and cells were washed 3 times with HBSS and immediately used for experiments. For FFN102, 10 μM concentration and 30 minutes incubation time was used.

2 Results

For image acquisition, an Olympus IX83 microscope was used coupled with CoolLed pE-4000 illumination system. The FFNs were excited with 488 nm channel at 500 ms exposure time. Image sequences were acquired before, during and after the stimulant was added with a pipette to the chamber slide. The images were obtained from Olympus cellSense software and analyzed with ImageJ 1.52n.

Calcium Flux Measurement

Neutrophils at 10^6 /mL concentration in RPMI 1640 (supplemented with 10% FBS) were incubated with Fluo-4, AM (1 μ M) in room temperature for 40 minutes. The cells were washed once and resuspended in HBSS (with Ca^{2+} and Mg^{2+}). Cell suspension were added to glass-bottom, black 96-well plates. CLARIOstar Plus plate reader was employed. Wells were scanned with (excitation 480-14 nm/emission 530-30) 691 times at 0.41 s intervals. At $t = 50$ s and $t = 250$ s an autoinjector pumped 10 μ L of stimulant with 430 μ L/s speed into the well.

Monoamines Analysis by HPLC

The content of dopamine (DA), serotonin (5-HT), epinephrine (EPI) and metabolites was measured via high performance liquid chromatography with electrochemical detection (HPLC-ECD). The mobile phase consisted 150 mM chloroacetic acid (Sigma - Aldrich Chemie GmbH, Steinheim, Germany), 4 mM KCl (GR for analysis, Merck KGaA, Darmstadt, Germany), 0.12 M NaOH (Sodium hydroxide pellets, Mallinckrodt Baker, Griesheim, Germany), 0.86 mM Sodium Octylsulfate (Sigma - Aldrich Chemie GmbH, Steinheim, Germany), 0.67 mM EDTA (Ethylenediaminetetraacetic acid, disodium salt: dehydrate 99+ %, Sigma- Aldrich Chemie GmbH, Steinheim, Germany), 3.5 % Acetonitrile (HPLC gradient grade, VWR Chemicals, Fontenay sous Bois, France), 1.8% Tetrahydrofuran (THF, VWR AnalR NORMAPUR, Fontenay sous Bois, France), adjusted to pH =3.0. On a 125 mm long, analytical column filled with Nucleosil C-18 (reversed-phase with 5- μ m particle size; Macherey & Nagel, Duren, Germany) at flow rate 0.7 ml/min monoamines were separated. The electrochemical detector (Decade II, Antec, The Netherlands) was set at 530mV vs. an ISAAC reference electrode (Antec, Leyden, The Netherlands) at 37-40°C. This setup allowed simultaneous measurements of DA, 5-HT,

2 Results

EPI. 3,4-Dihydroxybenzylamine Hydrobromide (DHBA) (Sigma Aldrich, MO, USA) was used as internal standard. The software used to analyze neurotransmitter content was Chrom Perfect Software (Justice Laboratory Software, Denville, NJ, USA).

Antibody Staining

2×10^5 cells in 500 μ L RPMI (with 10 mM HEPES, 0.5% FCS) were seeded on round glass coverslips and left to adhere for 30 minutes at 37°C, 5% CO₂. They were fixed by adding PFA at a final concentration of 2% for 15 minutes at room temperature. Cells were washed twice with PBS and then permeabilized using PBS with 0.1% Triton X 100 and 0.1% sodium citrate for ten minutes at room temperature. After two further washing steps with PBS, neutrophils were blocked with PBS containing 0.5% BSA for 40 minutes at room temperature. Fixed cells were incubated with primary antibodies (Table S1) in PBS containing 0.5% BSA overnight at 4°C. Cells were washed three times with PBS and subsequently incubated with secondary antibody (Table S1) in PBS containing 0.5% BSA for 1 h at 37°C. After three further washing steps, the samples were stained with Hoechst 33342 for 15 minutes and mounted using Darko Fluorescence Mounting Medium.

Fluorescence-Activated Cell Sorting (FACS)

Neutrophils were incubated in PBS containing 1% BSA and 1.5% Human TruStain FcX™ (Biolegend) for 10 minutes on ice. Cells were then stained with antibodies against CD66b and Siglec-8 to confirm neutrophil identity and antibodies against dopamine receptors or the respective isotype controls (Table S2.) for 30 minutes on ice. PBS with 1% BSA was added, cells were centrifuged at 300 x g and 4°C for 5 minutes and the supernatant discarded. Finally, cells were incubated in PBS containing 1% BSA and 1% 7-AAD (Biolegend). Cells were analyzed using BD FACSCanto II and FACSDiva Software. It was gated for single, living cells expressing CD66b but not Siglec-8.

NETosis Assay

Neutrophils were seeded on glass bottom 96 well-plates (10,000 per well), activated with PMA (100 nM), and incubated at 37 °C, 5% CO₂. At defined time points, the cells were

2 Results

fixed with 2% PFA to stop NET formation and stored over night at 4 °C. Cells were then washed once and the chromatin was stained with Hoechst at room temperature. Cells were imaged with an Axiovert 200 microscope (Zeiss, Germany) using a $\times 16$ objective lens. A CoolSNAP ES camera (Photometrics, USA) and blue channel (Filter set49 DAPI shift free, 488049-9901-000, Zeiss) were used for imaging. Images were acquired with Metamorph 6.3r2 software (Molecular Devices). 5 to 6 images from different regions were collected for each well. For all experiments, the amount of decondensed nuclei and the total cell count was quantified with ImageJ.

Statistics and Data Analysis

Data analysis was carried out with GraphPad Prism 9 (GraphPad Software, Inc.), OriginPro 8.5G (OriginLab Corporation) and Python.

Statistical analysis was performed with GraphPad Prism 9 (GraphPad Software, Inc.), OriginPro 8.5G (OriginLab Corporation). one-tailed/two-tailed t-test was performed to determine statistical significance between means. data are presented as (mean \pm standard deviation (SD) or standard error of the mean (SEM) and significance is reported by asterisks if the p values were the following: * $p < 0.05$; ** $p < 0.01$; *** $p < 0.001$; **** $p < 0.0001$).

Table S1. The full list of antibodies

primary antibody	supplier	concentration
DRD1 Polyclonal antibody	Proteintech	1 µg/mL
Anti-D2 Dopamine Receptor (extracellular)-FITC Antibody	Alomone Labs	10 µg/mL
DRD3 Polyclonal Antibody, ALEXA FLUOR® 488 Conjugated	Bioss	10 µg/mL
DRD4 Polyclonal antibody	Proteintech	2.5 µg/mL
DRD5 Polyclonal antibody	Proteintech	0.75 µg/mL
DAT Polyclonal antibody	Proteintech	1 µg/mL
VMAT2 Polyclonal antibody	Proteintech	1.5 µg/mL
Anti-Myeloperoxidase antibody [2C7]	abcam	4 µg/mL
isotypes		
Recombinant Rabbit IgG, monoclonal [EPR25A] - Isotype Control	abcam	0.75 µg/mL, 1 µg/mL, 1.5 µg/mL, 2.5 µg/mL, 10 µg/mL
Mouse IgG1 Isotype Control	Invitrogen	4 µg/mL
secondary antibody		
Goat anti-Rabbit IgG (H+L) Highly Cross-Adsorbed Secondary Antibody, Alexa Fluor 488	Invitrogen	4 µg/mL
Goat anti-Mouse IgG (H+L) Cross-Adsorbed Secondary Antibody, Alexa Fluor 555	Invitrogen	2 µg/mL

2 Results

Table S2. The full list of antibodies used

antibody	Supplier	concentration
Pacific Blue™ anti-human CD66b Antibody	Biolegend	1.5 µg/mL
Pacific Blue™ Mouse IgM, κ Isotype Ctrl Antibody	Biolegend	1.5 µg/mL
PE/Cyanine7 anti-human Siglec-8 Antibody	Biolegend	2 µg/mL
PE/Cyanine7 Mouse IgG1, κ Isotype Ctrl Antibody	Biolegend	2 µg/mL
PE anti-human Dopamine Receptor D1 Antibody	Biolegend	1 µg/mL
PE Mouse IgG2b, κ Isotype Ctrl Antibody	Biolegend	1 µg/mL
Anti-D2 Dopamine Receptor (extracellular)-FITC Antibody	Alomone Labs	5 µg/mL
Rabbit IgG Isotype Control, FITC, eBioscience™	Invitrogen	5 µg/mL
DRD3 Polyclonal Antibody, ALEXA FLUOR® 488 Conjugated	Bioss	1 µg/mL
Rabbit IgG Isotype Control, ALEXA FLUOR® 488 Conjugated	Bioss	1 µg/mL
Anti-D4DR Antibody (2B9) Alexa Fluor® 647	Santa Cruz	1 µg/mL
normal mouse IgG Alexa Fluor® 647	Santa Cruz	1 µg/mL
Anti-Dopamine Receptor D5 (DRD5) antibody (Alexa Fluor 647)	Antikoerper-online	1 µg/mL
Mouse IgG2A Alexa Fluor® 647-conjugated Isotype Control	R&D Systems	1 µg/mL

2 Results

Fig. S1.

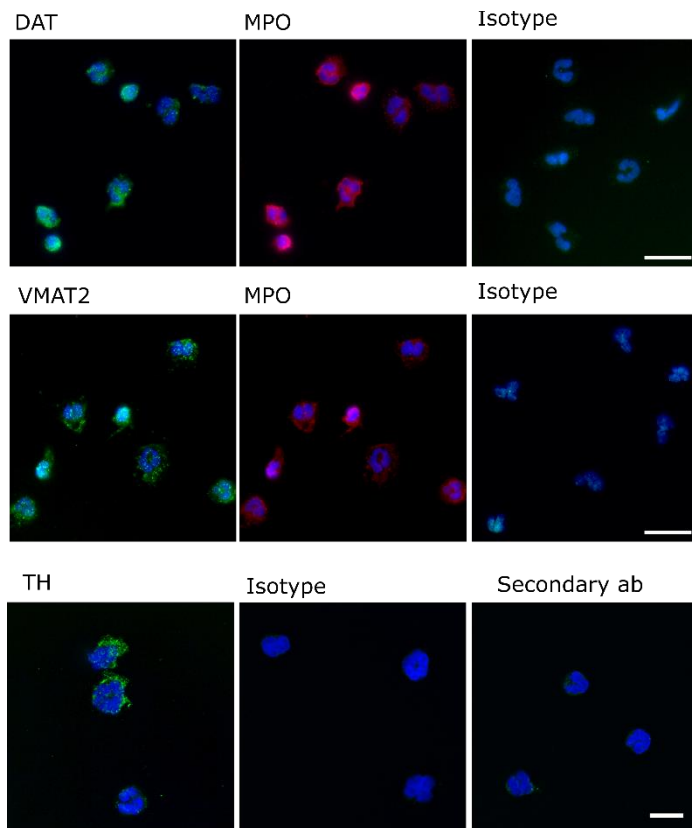


Fig. S1., Double staining of neutrophils with Hoechst (nucleus), MPO and DAT (top), VMAT-2 (middle), along with isotype controls. Scale bar is 20 μm . Antibody staining of neutrophils with TH (bottom) along with isotype and secondary antibody controls. Scale bar is 10 μm .

2 Results

Fig. S2.

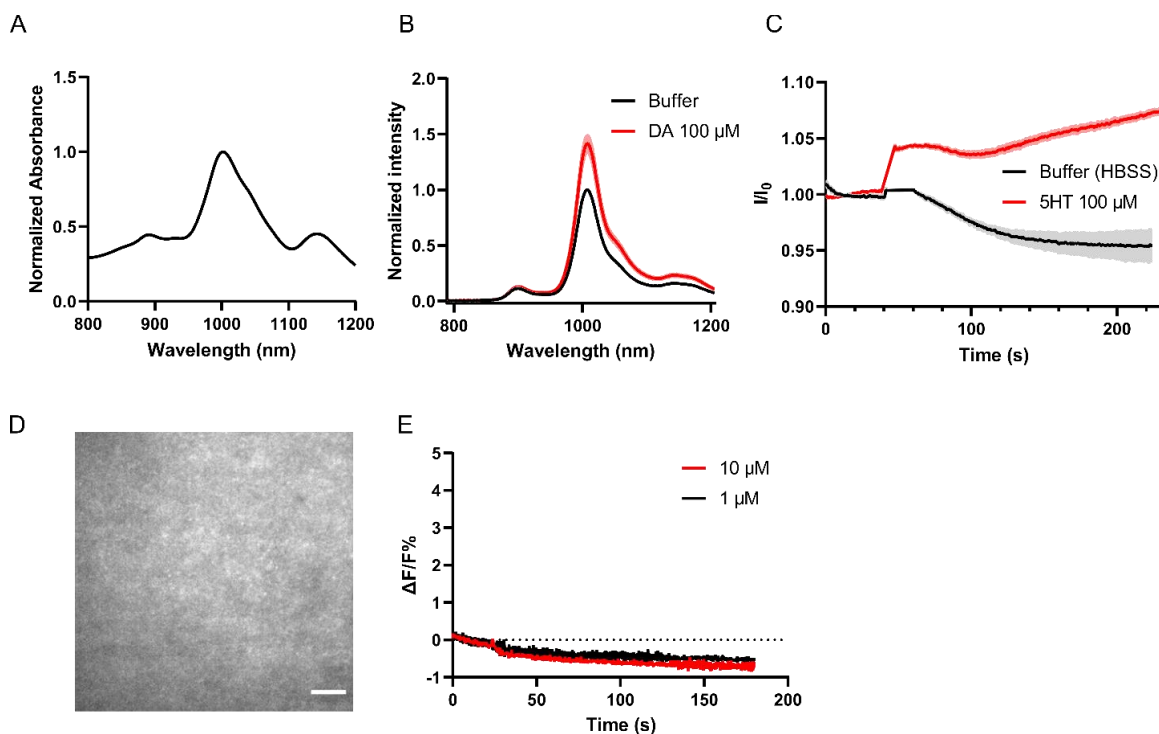


Fig. S2., **A**, The nIR absorbance spectrum of NIRDA suspension. **B**, Normalized fluorescence emission spectra of NIRDA in suspension before and after DA addition. **C**, The fluorescence intensity changes of the extracellular region around cell membrane overtime when cells are stimulated with 5HT compared to control. (cell incubated with FFN102) **D**, NIRDA surface coverage imaged with nIR camera. scale bar in 10 μm . **E**, The fluorescence signal of NIRDA when exposed to H_2O_2 .

2 Results

Fig. S3.

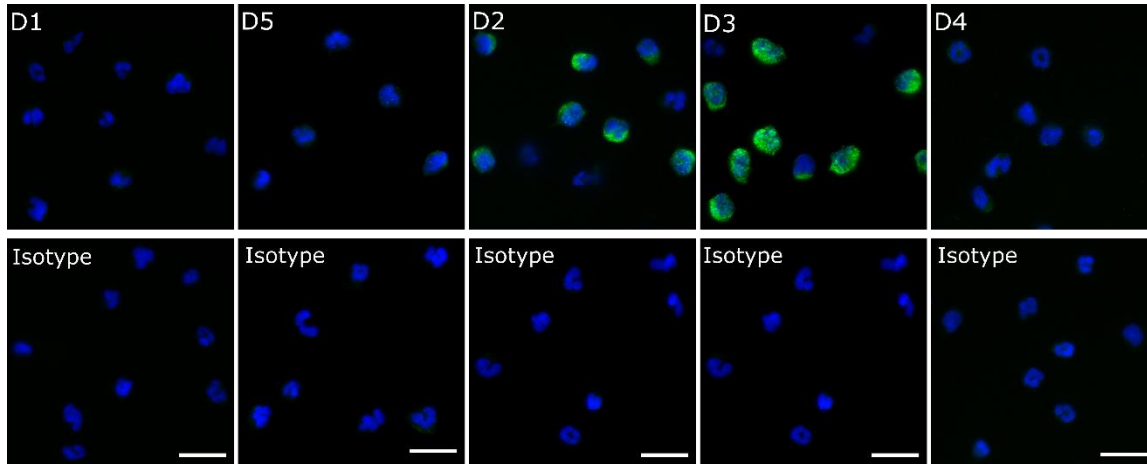


Fig. S3.,

Antibody staining of neutrophils with Hoechst (nucleus), DRs (top), and their isotype controls (bottom). Scale bar is 20 μm .

2 Results

Fig. S4.

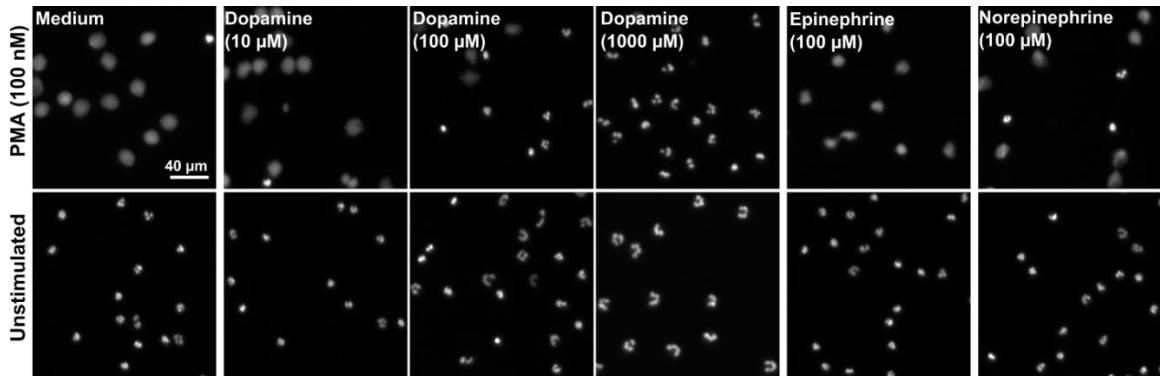


Fig. S4.,

NETosis assay of neutrophils, stimulated with PMA (top) or without PMA (bottom) and treated with different concentrations of catecholamines. The chromatin is stained with Hoechst.

3 Discussion

3.1 Nanosensor Design

Monoamines such as dopamine, norepinephrine, and serotonin are neuromodulators that tune the activity of neurons in a context dependent manner. Monoamines are also important hormones in the endocrine system that control a wide range of physiological responses. More recently, the influence of monoamines in the immune system has been discovered.¹⁴⁶ Studying exocytosis of monoamines is crucial to understand how cells propagate signals and communicate with each other.

As discussed in section 1.6.1, in conventional analytical methods, detection is carried out under static conditions. However, most cellular functions such as cell exocytosis, are highly dynamic. The concentration of the released substance at any location and in any given time is controlled by release parameters (rate of release), diffusion, and re-uptake. As the distance from the release site increases, the role of uptake becomes more prominent. For instance, in the case of dopamine release, at short distances (1–2 μm) from the site of release, only diffusion controlled the concentration of dopamine in the extracellular matrix. In ranges of 5 to 20 μm from the release site, uptake also played a role. In normal circumstances, when each vesicle contained 3000 molecules, dopamine diffused in a range of 12 μm . When DAT (responsible for uptake) were missing (in pathological conditions), the diffusion area increased up to 32 μm .¹⁴⁷ Hence, the concentration of the secreted molecule is time and space dependent. Therefore, conventional methods such as microdialysis and electrochemistry, although valuable tools, lack high resolution in time and space. For instance, microdialysis which affords sampling deep areas of the brain, involves extracting the extracellular matrix with a probe and applying analytical tools to measure the target molecule. As such, the temporal resolution is limited to minutes and the spatial resolution is even lower as the probe occupies a region larger than release sites.¹⁴⁸ Electrochemical methods such as amperometry and fast-scan cyclic voltammetry provide better temporal and spatial resolution. In both techniques, electrodes are inserted close to a cell and the target molecule is detected through its redox activity. The spatial resolution is limited by the diameter of the probe. However, the temporal resolution is within the range

3 Discussion

of exocytosis.¹⁴⁹ Selectivity of this method is reduced in the case of molecules with similar redox potential. Distinguishing sub-cellular sites of exocytosis is severely limited because of the high density of synaptic and extra synaptic release sites and the diameter of the electrodes.

We chose SWCNT nanosensors because they provide high spatio-temporal resolution. (6,5)-SWCNTs fluoresce in the nIR region which falls under the tissue transparency window (>800 nm). The Fluorescence of the SWCNTs can be manipulated by functionalizing them with a wide range of macromolecules. When SWCNTs are coated with macromolecules, a Corona phase is formed around the SWCNT that is sensitive to its microenvironment. The basis of the detection, is a change in the fluorescence emission pattern of SWCNTs after exposure to the target molecule due to spatial changes in its corona phase. This technique is known as Corona phase molecular recognition (CoPhMoRe).¹⁵⁰ We functionalized (6,5)-SWCNTs with specific oligonucleotides to render them sensitive to our target monoamine, (GT)10 oligonucleotide for dopamine nanosensors and a serotonin DNA aptamer (a 57-mer ssDNA) for serotonin nanosensors.¹⁵¹

CoPhMoRe based on oligonucleotides has many advantages. First, oligonucleotides are easier to synthesize compared to antibodies. They are more stable in a wide range of temperatures, pH and reaction conditions. Oligonucleotides can be easily tethered on SWCNTs with non-covalent interactions hence, the 3D structure of the oligonucleotide which is crucial for molecular recognition, is not compromised when the oligonucleotides are bound to SWCNTs. We believe these properties make SWCNT based sensors very attractive in biomedical studies.

The instruments needed for sensing are also easy to operate. The nanosensors were detected with a simple imaging technique. In this technique, nanosensors are immobilized non-covalently on a glass surface and immune cells are adhered on top. While cells undergo exocytosis, we image the surface with a simple microscope. A 561 nm laser is employed to excite the nanosensor surface and the images are acquired with a nIR camera. In theory, when exocytosis happens, each single nanosensor that is exposed to our target molecule will “switch on” and detect the target molecule. As a result, this technique provided high

3 Discussion

parallel spatio-temporal resolution. We achieved sub-micrometer spatial resolution for as many cells that is visible in the field of view of the microscope.

To optimize resolution, a proper sensor must have kinetics that matches that of exocytosis. To study the kinetics of SWCNT sensors, in our lab previously, a simulation was carried out on sensors homogenously immobilized on surface with cell adhered on top. The spatial and temporal resolution was calculated with various binding and unbinding rates. The best results were achieved with sensors with rate constants of $k_{\text{on}} = 10^6 \text{ M}^{-1}\text{s}^{-1}$ and $k_{\text{off}} = 10^2 \text{ M}^{-1}\text{s}^{-1}$. Lower binding affinities (e.g. $K_d = k_{\text{off}}/k_{\text{on}} = 100 \text{ }\mu\text{M}$) provided the best sensing profile.¹⁵² We chose (GT)10 oligonucleotide functionalization for our dopamine nanosensors because they were previously investigated in our lab and were observed to have the highest selectivity and sensitivity for dopamine. Dissociation constant (K_d) of the sensor for dopamine was 9.2 nM.¹⁵³ Since we aimed to study dopamine exocytosis from neutrophils on single cells at near to single SWCNT molecule level, it was important to employ nanosensors with high sensitivity as previous studies had shown that the concentration of endogenous dopamine in lymphocytes was in the range of 10^{-20} - 10^{-17} mol/cell.¹⁵⁴ Our own investigation revealed neutrophil's concentration of dopamine to be $\sim 2 \times 10^{-18}$ mol/cell (section 2.2, Figure 1).

For serotonin nanosensors, the dissociation constant was calculated to be $301 \text{ nM} \pm 138 \text{ nM}$ and the dynamic linear range of the dose-response curve was also in the physiologically relevant region of 100 nM to 1 μM .

The exact mechanism of the sensing is not completely known. However, there are some compelling theories investigated by our lab and several other groups. For instance, SWCNTs were coated with fluorophore labeled (GT)₁₅ oligonucleotides. At first, the fluorophore was quenched due to proximity to SWCNT surface, but when the sensors were exposed to dopamine, the fluorophore regained its fluorescence.¹⁵⁵ This implies that dopamine interacted with DNA in a way that removed the fluorophore label from the proximity of the SWCNT surface. This study confirmed that the sensitivity to dopamine is caused by conformational changes of the oligonucleotide wrapped around the SWCNT which translates to a change in the emission pattern of the SWCNT. This finding is also confirmed by Molecular dynamics (MD) simulation.¹⁵⁶ In the case of (GT)₁₅-SWCNT, MD

3 Discussion

revealed a strong interaction between hydroxyl groups of dopamine and phosphate groups of oligonucleotides. It seems that in the absence of dopamine, phosphate groups affect the exciton diffusion on the surface of SWCNTs, but when hydroxyl groups of dopamine interact with phosphate groups of oligonucleotides, the exciton diffusion pattern changes; as a result, the fluorescence emission pattern also changes.

Interestingly both hydroxyl groups in meta and para positions are necessary for the fluorescence sensitivity of the sensor as tyramine, serotonin, tyrosine and histamine don't affect SWCNT fluorescence.¹⁵⁷ We also dismissed that the fluorescence response of the SWCNT sensor is related to the redox activity of dopamine as compounds with similar redox potential to dopamine did not exert the same effect.¹⁵⁸ In summary the oligonucleotides were stacked on the surface of SWCNT in a semi stable state but changes in their conformation due to interaction with monoamines increased the quantum yield of the SWCNT by affecting the exciton diffusion path. Resulting in an increasing in the intensity of the fluorescence emission which is the basis of the detection strategy.

3.2 Detection of Serotonin Exocytosis from Platelets

Current serotonin sensors lack spatial resolution. When the spatial resolution is increased, typically the detection is limited to a narrower field of view. Compared to analytical methods such as microdialysis, LC-MS, *in situ* sensing affords additional details about the spatial context of the release including heterogeneity in a single cell regarding release hotspots and variations within cells. *In situ* sensing usually requires an external probe that is brought into contact with the cells such as electrochemical sensors. In these systems, the sensing only occurs when an analyte reaches the probe. In order to increase the spatial resolution and parallel sensing of many areas, thinner electrodes and electrode arrays can be designed. but still only regions in close contact to the electrode can be probed. The probes are also prone to fouling.

Amongst the optical sensors, most are indirect detectors. For instance, fluorescent false neurotransmitters (FFNs) are catecholamine analogs with a similar structure to monoamines and therefore, they mimic the behavior of monoamines.¹⁵⁹ By imaging FFNs, one can study the dynamics of monoamine exocytosis in cells indirectly. Although FFNs

3 Discussion

are valuable tools to study neurotransmitters, like most organic fluorophores they suffer from rapid bleaching which makes imaging prolonged release events very challenging.

Here, we took advantage of the optical properties of SWCNTs to design our sensors. Our nanosensor has a stable fluorescence emission with no significant bleaching and blinking during imaging. We synthesized colloidal stable nanosensor suspension with (6,5) enriched SWCNTs functionalized with a 57 oligomer DNA aptamer that detected serotonin with high selectivity and reversibility (NIRSer). Functionalization of SWCNTs with the aptamer did not affect the tertiary structure of the aptamer which is important for efficient aptamer-serotonin binding.

When NIRSer was exposed to serotonin, the intensity of the nIR fluorescence emission increases by 80% (section 2.1.1, Figure 3). We hypothesized a conformational change of the aptamer upon binding to serotonin led to a change in the fluorescence emission pattern of the nanosensors. When we compared the height profile of SWCNTs functionalized with serotonin aptamer (with a strong secondary structure) to SWCNTs functionalized with (GT)₁₀, with atomic force microscopy, we observed heterogeneity in height along the length of the SWCNT, confirming additional features from the secondary tertiary of the aptamer (section 2.1.1, Figure 2).

We confirmed that NIRSer was selective for serotonin by showing that the nanosensor was not sensitive to other molecules with similar structure; such as histamine and tryptophan (section 2.1.1, Figure 3). As discussed in the previous section, NIRSer exhibited linear dynamic range in the dose-response curve for a concentration range from 100 nM and 1 μ M. This concentration range, according to the literature, is relevant to detect serotonin release from platelets.¹⁶⁰

Most DNA-wrapped SWCNTs respond to dopamine with varying sensitivity depending on the DNA sequence. This is due to an interaction with phosphate groups of DNA and hydroxyl groups of dopamine. NIRSer also showed minimal response to dopamine which was significantly lower than serotonin. We believe this minimal response does not affect the overall serotonin sensing because dopaminergic and serotonergic neurons occupy distinct locations in the nervous system. Furthermore, we haven't recognized any cell type that simultaneously synthesizes and releases both serotonin and dopamine.

3 Discussion

We also confirmed that the response to serotonin was due to specific aptamer-serotonin binding as SWCNTs functionalized with scrambled aptamers (aptamer with the same nucleotide composition but scrambled sequence) did not respond to serotonin (section 2.1.2, Figure S5).

The nanosensors were immobilized on glass surface. We observed homogenous coating of the nanosensor on surface. The glass coating is simple and does not require chemical reactions to activate glass surface. Nanosensors exhibited reversible response to serotonin, when they were exposed to alternating flows of serotonin solution and PBS. A reversible “turn-on” switch is more desirable in sensor design compared to “turn-off” switches as the sensor response won’t be conflated with common artefacts such as bleaching, focus drift, and quenching due to aggregation.

We also demonstrated that in the presence of serotonin, the nanosensors responded to increasing concentrations of serotonin in a concentration dependent manner (section 2.1.1, Figure 4). Which means that in the presence of serotonin, nanosensors were able to distinguish different concentrations of serotonin.

As platelet store more than 300 distinct molecules in their secretory granules with some having contradictory effects,¹⁶¹ it is important to record release events in space and time; therefore, to record serotonin release kinetics, we let platelets adhere on NIRSer surfaces. We observed that platelets easily adhered on the nanosensor surface (section 2.1.2, Figure S10). We stimulated platelets with a Ca^{2+} ionophore. As shown in section 2.1 Figure 5, when platelets were activated, we were able to record serotonin release events from single platelets. Furthermore, we were able to pinpoint hot spots on the cell membrane where exocytosis occurred.

We discovered that the increase in fluorescence signal of NIRSers under the cell membrane was not homogenous and hotspots along the cell membrane were observed with significant serotonin release. Since platelet secretion is not entirely discriminatory, other molecules are also released when serotonin is secreted. Therefore, we depleted platelets from serotonin with a VMAT-2 inhibitor and observed that NIRSer did not record serotonin release when these platelets were stimulated.

3 Discussion

The high spatial resolution was only limited to 500 nm by the Abbe limit. This is in the same scale of the size of each NIRSer which had an average length of 600 nm. The high parallel spatial resolution enabled us to investigate multiple cells at the same time which was only limited by the field of view of the microscope. As an example, 10 cells were studied in section 2.1 Figure 5. We were able observe variability between platelets in terms of the time of exocytosis and the amount of serotonin released. In summary we report that this NIRSer tool compared to conventional methods provided additional spatial information on a single cell level in addition to parallel imaging of multiple cells simultaneously.

3.2 Detection of Dopamine Exocytosis from Neutrophils

There is compelling evidence for the existence of catecholamine synthesis in neutrophils as well as a number of other immune cells. Limited studies on this topic have identified the expression of enzymes involved in catecholamine synthesis, storage and metabolism.¹⁴⁰

In this study, we focused on investigating the mechanism of dopamine exocytosis from neutrophils. We were able to identify expression of VMAT-2, DAT and TH proteins in neutrophils by antibody staining. TH expression has previously been identified in neutrophils.¹⁴¹ Direct VMAT-2 expression in neutrophils hasn't been reported before. A previous study on the expression of VMAT-1 and VMAT-2 in leukocytes reported that neither VMATs were expressed in neutrophils.¹⁶² However, an older study had reported that treating neutrophils with VMAT-2 inhibitors, increased the concentration of catecholamines, concluding the VMATs are indeed expressed in neutrophils.¹⁴⁰ Regarding DAT expression, we couldn't find information on DAT expression in neutrophils. Therefore, more studies are needed in this field, to draw conclusive information on the expression of dopaminergic system in neutrophils. However, we could confirm previous findings that neutrophils indeed have a significant concentration of intracellular dopamine by HPLC.

A recent study on the effects of platelet-derived serotonin on neutrophils observed that neutrophils express several serotonin receptors and that serotonin induced neutrophil degranulation. CD11b which is localized to secretory granules and translocated to the

3 Discussion

plasma membrane upon degranulation of secretory granules were identified when neutrophils were stimulated with serotonin.¹⁰³ We investigated whether serotonin induced exocytosis of catecholamine-filled vesicles as well. For this purpose, several FFN exocytosis studies were carried out (section 2.2, Figure 1). For the first time, we observed that indeed FFNs which are stored in VMAT vesicles were secreted after serotonin stimulation of neutrophils. We validated the results by carrying out a conventional analytical tool to quantify the release of dopamine from neutrophils via HPLC and we observed that serotonin treatment indeed led to reduction in the intracellular content of dopamine to a fourth of its original content.

Since, Ca^{2+} mobilization plays a critical role in neutrophil degranulation (section 1.2.1), we investigated the effect of serotonin on Ca^{2+} flux in neutrophils. The exact signaling pathway is not completely known however we speculate that direct engagement of serotonin receptors on neutrophils leads to Ca^{2+} signaling as an important secondary messenger when GPCRs are engaged with agonists. We observed that serotonin stimulation indeed causes an increase in the intracellular Ca^{2+} concentration.

With our unique tool, for the first time, we could directly link Ca^{2+} signaling to dopamine exocytosis. We performed simultaneous imaging of intracellular Ca^{2+} increase with a Ca^{2+} indicator and dopamine with our nanosensor (section 2.2, Figure 2). We observed that upon stimulation of neutrophils, at first, intracellular Ca^{2+} increased and then after ~ 20 s delay, dopamine was released from neutrophils. Dopamine exocytosis was not homogenous along the cell membrane and amongst different cells. There was co-localization between directional intracellular Ca^{2+} increase inside neutrophils and dopamine exocytosis.

After confirming that indeed neutrophils have VMAT vesicles that store dopamine and release them upon serotonin stimulation and Ca^{2+} mobilization, we investigated the kinetics of release with our dopamine sensors (section 2.2, Figure 3). With this powerful tool, we were able to visualize dopamine exocytosis from neutrophils and observe intercellular variability in the amount of dopamine secretion as detected by an increase in the fluorescence intensity of the nanosensors.

We also determined that the signals detected by the nanosensors belonged to dopamine as opposed to unspecific reaction to other secretory molecules or mechanical forces applied

3 Discussion

to the sensor surface by neutrophils upon activation and increased surface adhesion. By depleting the neutrophils of dopamine and substituting FFN102, we recorded exocytosis simultaneously in both FFN visible channel and dopamine NIR channel (section 2.2, Figure 3E). Dopamine exocytosis was not detected in the NIR channel; however, FFN102 exocytosis was recorded by the visible channel.

We also confirmed that serotonin induced exocytosis in a receptor-mediated manner by treating neutrophils to serotonin agonist and antagonist. As predicted, blocking serotonin receptors significantly reduced exocytosis of dopamine. When we stimulated the same cells with ionomycin as a universal Ca^{2+} ionophore, we observed that an increase in intracellular Ca^{2+} did not restore dopamine exocytosis (section 2.2, Figure 4A). This finding indicated that dopamine exocytosis required specific engagement of serotonin receptors.

On the other hand, a serotonin receptor agonist promoted dopamine exocytosis (section 2.2, Figure 4E). In the next step, we investigated platelet-serotonin interactions with our nanosensor tool. We observed that when we stimulated platelets with thrombin to secrete serotonin, neutrophils released dopamine which was recorded by our nanosensors (section 2.2, Figure 5). Figure 7. shows the schematic of the sensing strategy. Simultaneous intracellular Ca^{2+} and dopamine release was visualized. Activated platelets released serotonin which induced neutrophils to release dopamine. The cells are adhered on a smart surface comprised of NIRDA sensors. Each NIRDA switches on when it comes in to contact with dopamine thereby visualizing dopamine release.

Serotonin has been implicated in neutrophil adhesion, recruitment⁷⁸ and degranulation.¹⁰³ Platelet serotonin mediated platelet-neutrophil interaction.¹⁶³ Therefore, serotonin is a propagator of inflammatory response in neutrophils. We speculated that dopamine release from neutrophils upon serotonin-induced neutrophil activation, must act as an autocrine/paracrine modulator to tune down inflammatory response of neutrophils in a feedback loop. There are already studies that indicate dopamine attenuated inflammatory response of neutrophils.¹²⁷ Our study on the effect of dopamine in NETosis also confirms the previous findings.

3 Discussion

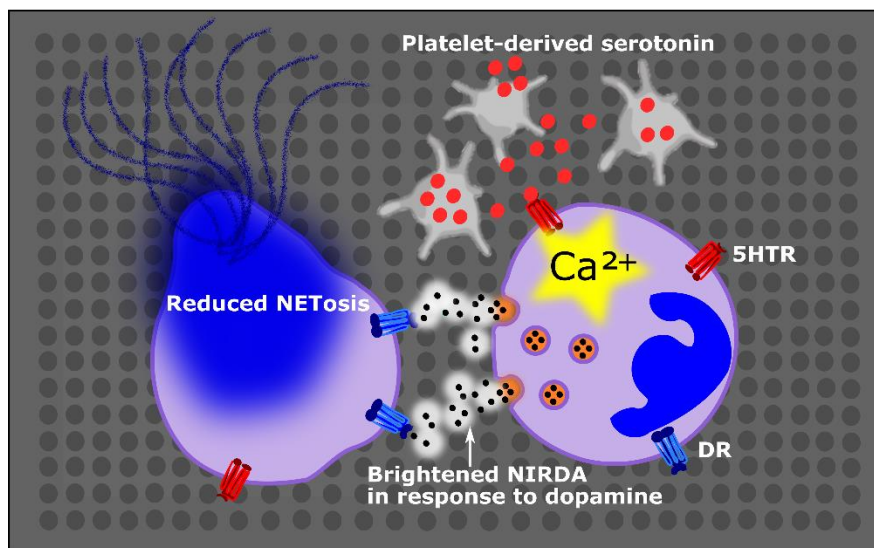


Figure 7. NIRDA detection strategy; When neutrophils and platelets are seeded on NIRDA surface, each NIRDA turns in to a switch on bottom which brightens by binding to dopamine. Therefore, dopamine exocytosis from neutrophils activated by platelet serotonin is visualized.

First, we confirmed the expression of several dopamine receptors (DRs) in neutrophils. There are several studies on the expression of DRs in neutrophils. Again, the results of these studies are not conclusive. For instance, RT-PCR experiments revealed that mRNA of none of the dopamine receptors were present in neutrophils.¹⁶⁴ But another study discovered that all dopamine receptors (D1, D2, D3, D4, D5) were expressed in neutrophils while D2 expression was the lowest of all receptors.¹⁶⁵ Another study also observed that all DRs were expressed in neutrophils with the highest expression belonging to D5 > D3 > D2 > D4.¹⁶⁶ Another study only found D2 and D4 expression.¹⁶⁶ The disparities could be due primer quality, experimental conditions and the degree of purification of the neutrophils. Nevertheless, we mainly observed the expression of D2 and D3 receptors (section 2.21, Figure 6).

After establishing the presence of dopamine receptors, we observed that dopamine reduced the rate of NETosis in PMA treated neutrophils in a concentration dependent manner. We also confirmed that this response was not due to reducing effect of dopamine and its protective effects against production of ROS since other catecholamines such as

3 Discussion

epinephrine and norepinephrine did not produce the same protective effect against NETosis as dopamine (section 2.2, Figure 6).

In summary, in this project, first we established the existence of dopamine synthesis in neutrophils through, antibody staining, FACS, and HPLC. Then, we studied the kinetics of VMAT vesicle exocytosis via FFNs and discovered the stimulatory effect of serotonin on VMAT vesicle exocytosis. We discovered that Ca^{2+} is an important signaling step in serotonin-induced dopamine exocytosis then, we employed our powerful tool to study dopamine exocytosis in neutrophils and visualized serotonin mediated platelet-neutrophil interactions. And finally, we discovered that dopamine is a paracrine immune modulator in neutrophils that reduces the rate of NETosis.

This topic can be explored further in many aspects. Our understanding of neutrophils is growing. Neutrophils were considered permanently differentiated with a homogenous phenotype after they entered the circulation system. However, we know that circulating neutrophils express different markers when they are primed by different agents. A recent study discovered several distinct neutrophil populations with defined molecular signatures.¹⁶⁷ They discovered three subsets of neutrophils from peripheral blood. Several factors can induce neutrophil reprogramming and phenotypical changes during aging,¹⁶⁸ priming, infection and mechanical forces during extravasion. Recent studies show that tumor microenvironment also induces neutrophil reprogramming.¹⁶⁹ A recent study discovered a subpopulation of human T_{FH} cell and not all T cells store and release dopamine in germinal center when forming immune synapses with B cells.¹⁷⁰ So it would be interesting to investigate the heterogeneity in dopamine synthesis and exocytosis amongst distinct neutrophils subpopulations and its implications.

Conclusion and Outlook

In conclusion, designing nIR fluorescent nanosensors provided a powerful tool to study dynamic cellular functions in immune cells. Here, we took advantage of the high parallel spatio-temporal resolution that the sensor afforded to uncover new information regarding exocytosis of monoamines from immune cells. This tool enables researchers to study release dynamics on a subcellular level in many cells simultaneously. Intercellular variations in cellular exocytosis can be studied as different cell subtypes can be marked by labeling agents and the exocytosis can be recorded in all cells simultaneously. As our nanosensor platform employs nIR detection, it can be easily combined with other molecular indicators which are fluorescent predominantly in the visible range to record simultaneous cellular events. Therefore, this nanosensor is a versatile tool for detection of biogenic molecules in real time.

One of the main areas that needs further investigation is increasing the selectivity of the nanosensors to the target molecules. If the molecular recognition is based on oligonucleotide functionalized SWCNTs, and the target molecule is any molecule other than catecholamines, there will always be a background response from the catecholamine. However, depending on the conditions of sensing this issue should be taken into consideration.

Several issues regarding the safety and environmental implications of carbon nanotubes has so far hindered their industrial large-scale use. Carbon nanotubes aren't biodegradable in nature and they aren't biocompatible in the body. However, because of their unique properties such as mechanical strength, electrochemical and optical properties their application cannot be dismissed. There is great need for developing protocols and defining safety risks for carbon nanotubes to facilitate their use in the biomedical field.

References

1. Janeway CA Jr, Travers P, Walport M SM. The components of the immune system. In: *Immunobiology: The Immune System in Health and Disease. 5th Edition*. New York: Garland Science; 2001.
<https://www.ncbi.nlm.nih.gov/books/NBK27092/%0A>.
2. Delves PJ, Roitt IM. The Immune System. *N Engl J Med*. 2000;343(1):37-49.
doi:10.1056/NEJM200007063430107
3. Andersen MH, Schrama D, thor Straten P, Becker JC. Cytotoxic T Cells. *J Invest Dermatol*. 2006;126(1):32-41. doi:<https://doi.org/10.1038/sj.jid.5700001>
4. Luckheeram RV, Zhou R, Verma AD, Xia B. CD4⁺T cells: differentiation and functions. *Clin Dev Immunol*. 2012;2012:925135. doi:10.1155/2012/925135
5. Alberts B, Johnson A, Lewis J et al. B Cells and Antibodies. In: *Molecular Biology of the Cell. 4th Edition*. New York: Garland Science; 2002.
<https://www.ncbi.nlm.nih.gov/books/NBK26884/%0A>.
6. Parkin J, Cohen B. An overview of the immune system. *Lancet*. 2001;357(9270):1777-1789. doi:[https://doi.org/10.1016/S0140-6736\(00\)04904-7](https://doi.org/10.1016/S0140-6736(00)04904-7)
7. Medzhitov R, Janeway C. Innate Immunity. *N Engl J Med*. 2000;343(5):338-344.
doi:10.1056/NEJM200008033430506
8. Nicholson LB. The immune system. *Essays Biochem*. 2016;60(3):275-301.
doi:10.1042/EBC20160017
9. Iwasaki A, Medzhitov R. Regulation of adaptive immunity by the innate immune system. *Science (80-)*. 2010;327(5963):291-295.
10. Lacy P, Stow JL. Cytokine release from innate immune cells: association with diverse membrane trafficking pathways. *Blood*. 2011;118(1):9-18.
doi:10.1182/blood-2010-08-265892
11. Shamri R, Xenakis JJ, Spencer LA. Eosinophils in innate immunity: an evolving story. *Cell Tissue Res*. 2011;343(1):57-83. doi:10.1007/s00441-010-1049-6
12. Yoshimoto T, Yasuda K, Tanaka H, et al. Basophils contribute to TH 2-IgE responses in vivo via IL-4 production and presentation of peptide–MHC class II complexes to CD4⁺ T cells. *Nat Immunol*. 2009;10(7):706-712.
13. Marshall JS. Mast-cell responses to pathogens. *Nat Rev Immunol*. 2004;4(10):787-799.
14. Dale DC, Boxer L, Liles WC. The phagocytes: neutrophils and monocytes. *Blood*. 2008;112(4):935-945. doi:10.1182/blood-2007-12-077917
15. Harizi H, Gualde N. The impact of eicosanoids on the crosstalk between innate and adaptive immunity: the key roles of dendritic cells. *Tissue Antigens*. 2005;65(6):507-514.

References

16. Gabay C, Kushner I. Acute-phase proteins and other systemic responses to inflammation. *N Engl J Med*. 1999;340(6):448-454.
17. Heesterbeek DAC, Angelier ML, Harrison RA, Rooijackers SHM. Complement and Bacterial Infections: From Molecular Mechanisms to Therapeutic Applications. *J Innate Immun*. 2018;10(5-6):455-464. doi:10.1159/000491439
18. Borregaard N. Neutrophils, from Marrow to Microbes. *Immunity*. 2010;33(5):657-670. doi:https://doi.org/10.1016/j.immuni.2010.11.011
19. Silvestre-Roig C, Hidalgo A, Soehnlein O. Neutrophil heterogeneity: implications for homeostasis and pathogenesis. *Blood, J Am Soc Hematol*. 2016;127(18):2173-2181.
20. Lahoz-Beneytez J, Elemans M, Zhang Y, et al. Human neutrophil kinetics: modeling of stable isotope labeling data supports short blood neutrophil half-lives. *Blood, J Am Soc Hematol*. 2016;127(26):3431-3438.
21. Mayadas TN, Cullere X, Lowell CA. The multifaceted functions of neutrophils. *Annu Rev Pathol Mech Dis*. 2014;9:181-218.
22. Evrard M, Kwok IWH, Chong SZ, et al. Developmental Analysis of Bone Marrow Neutrophils Reveals Populations Specialized in Expansion, Trafficking, and Effector Functions. *Immunity*. 2018;48(2):364-379.e8. doi:https://doi.org/10.1016/j.immuni.2018.02.002
23. Rosales C. Neutrophil: A Cell with Many Roles in Inflammation or Several Cell Types? *Front Physiol*. 2018;9:113. doi:10.3389/fphys.2018.00113
24. Kumar V, Sharma A. Neutrophils: Cinderella of innate immune system. *Int Immunopharmacol*. 2010;10(11):1325-1334. doi:https://doi.org/10.1016/j.intimp.2010.08.012
25. Tang D, Kang R, Coyne CB, Zeh HJ, Lotze MT. PAMPs and DAMPs: signal 0s that spur autophagy and immunity. *Immunol Rev*. 2012;249(1):158-175. doi:10.1111/j.1600-065X.2012.01146.x
26. Morikis VA, Simon SI. Neutrophil Mechanosignaling Promotes Integrin Engagement With Endothelial Cells and Motility Within Inflamed Vessels . *Front Immunol* . 2018;9:2774. https://www.frontiersin.org/article/10.3389/fimmu.2018.02774.
27. Wang X, Qiu L, Li Z, Wang X-Y, Yi H. Understanding the multifaceted role of neutrophils in cancer and autoimmune diseases. *Front Immunol*. 2018;9:2456.
28. Cassatella MA. Neutrophil-derived proteins: selling cytokines by the pound. *Adv Immunol*. 1999;73:369-509.
29. Scapini P, Calzetti F, Cassatella MA. On the detection of neutrophil-derived vascular endothelial growth factor (VEGF). *J Immunol Methods*. 1999;232(1-2):121-129.

References

30. Tecchio C, Micheletti A, Cassatella MA. Neutrophil-Derived Cytokines: Facts Beyond Expression . *Front Immunol* . 2014;5:508. <https://www.frontiersin.org/article/10.3389/fimmu.2014.00508>.
31. Charmoy M, Brunner-Agten S, Aebischer D, et al. Neutrophil-derived CCL3 is essential for the rapid recruitment of dendritic cells to the site of *Leishmania major* inoculation in resistant mice. *PLoS Pathog*. 2010;6(2):e1000755.
32. Scapini P, Lapinet-Vera JA, Gasperini S, Calzetti F, Bazzoni F, Cassatella MA. The neutrophil as a cellular source of chemokines. *Immunol Rev*. 2000;177:195-203.
33. Marwick JA, Mills R, Kay O, et al. Neutrophils induce macrophage anti-inflammatory reprogramming by suppressing NF- κ B activation. *Cell Death Dis*. 2018;9(6):665. doi:10.1038/s41419-018-0710-y
34. Bi Y, Zhou J, Yang H, et al. IL-17A produced by neutrophils protects against pneumonic plague through orchestrating IFN- γ -activated macrophage programming. *J Immunol*. 2014;192(2):704-713.
35. Puga I, Cols M, Barra CM, et al. B cell-helper neutrophils stimulate the diversification and production of immunoglobulin in the marginal zone of the spleen. *Nat Immunol*. 2012;13(2):170-180.
36. Coquery CM, Wade NS, Loo WM, et al. Neutrophils contribute to excess serum BAFF levels and promote CD4+ T cell and B cell responses in lupus-prone mice. *PLoS One*. 2014;9(7):e102284.
37. Beauvillain C, Delneste Y, Scotet M, et al. Neutrophils efficiently cross-prime naive T cells in vivo. *Blood, J Am Soc Hematol*. 2007;110(8):2965-2973.
38. Fox S, Leitch AE, Duffin R, Haslett C, Rossi AG. Neutrophil apoptosis: relevance to the innate immune response and inflammatory disease. *J Innate Immun*. 2010;2(3):216-227. doi:10.1159/000284367
39. Lacy P. Mechanisms of Degranulation in Neutrophils. *Allergy, Asthma Clin Immunol*. 2006;2(3):98. doi:10.1186/1710-1492-2-3-98
40. Faurschou M, Borregaard N. Neutrophil granules and secretory vesicles in inflammation. *Microbes Infect*. 2003;5(14):1317-1327.
41. Joiner KA, Ganz T, Albert J, Rotrosen D. The opsonizing ligand on *Salmonella typhimurium* influences incorporation of specific, but not azurophil, granule constituents into neutrophil phagosomes. *J Cell Biol*. 1989;109(6):2771-2782.
42. Sengeløv H, Kjeldsen L, Borregaard N. Control of exocytosis in early neutrophil activation. *J Immunol*. 1993;150(4):1535-1543.
43. Sengeløv H, Kjeldsen L, Diamond MS, Springer TA, Borregaard N. Subcellular localization and dynamics of Mac-1 (alpha m beta 2) in human neutrophils. *J Clin Invest*. 1993;92(3):1467-1476.

References

44. Kjeldsen L, Bjerrum OW, Askaa J, Borregaard N. Subcellular localization and release of human neutrophil gelatinase, confirming the existence of separate gelatinase-containing granules. *Biochem J.* 1992;287(2):603-610.
45. Faurschou M, Sørensen OE, Johnsen AH, Askaa J, Borregaard N. Defensin-rich granules of human neutrophils: characterization of secretory properties. *Biochim Biophys Acta (BBA)-Molecular Cell Res.* 2002;1591(1-3):29-35.
46. Káldi K, Szeberényi J, Rada BK, et al. Contribution of phospholipase D and a brefeldin A-sensitive ARF to chemoattractant-induced superoxide production and secretion of human neutrophils. *J Leukoc Biol.* 2002;71(4):695-700.
47. Barlic J, Andrews JD, Kelvin AA, et al. Regulation of tyrosine kinase activation and granule release through β -arrestin by CXCR1. *Nat Immunol.* 2000;1(3):227-233.
48. Abdel-Latif D, Steward M, Macdonald DL, Francis GA, Dinauer MC, Lacy P. Rac2 is critical for neutrophil primary granule exocytosis. *Blood.* 2004;104(3):832-839.
49. Rothman JE. The protein machinery of vesicle budding and fusion. *Protein Sci.* 1996;5(2):185-194.
50. Martín-Martín B, Nabokina SM, Lazo PA, Mollinedo F. Co-expression of several human syntaxin genes in neutrophils and differentiating HL-60 cells: variant isoforms and detection of syntaxin 1. *J Leukoc Biol.* 1999;65(3):397-406.
51. Martín-Martín B, Nabokina SM, Blasi J, Lazo PA, Mollinedo F. Involvement of SNAP-23 and syntaxin 6 in human neutrophil exocytosis. *Blood, J Am Soc Hematol.* 2000;96(7):2574-2583.
52. Brumell JH, Volchuk A, Sengelov H, et al. Subcellular distribution of docking/fusion proteins in neutrophils, secretory cells with multiple exocytic compartments. *J Immunol.* 1995;155(12):5750-5759.
53. Fasshauer D, Antonin W, Margittai M, Pabst S, Jahn R. Mixed and non-cognate SNARE complexes: characterization of assembly and biophysical properties. *J Biol Chem.* 1999;274(22):15440-15446.
54. El-Benna J, Dang PM-C, Gougerot-Pocidallo M-A. Priming of the neutrophil NADPH oxidase activation: role of p47phox phosphorylation and NOX2 mobilization to the plasma membrane. *Semin Immunopathol.* 2008;30(3):279-289. doi:10.1007/s00281-008-0118-3
55. Lee WL, Harrison RE, Grinstein S. Phagocytosis by neutrophils. *Microbes Infect.* 2003;5(14):1299-1306.
56. McKenzie SE, Schreiber AD. Fc gamma receptors in phagocytes. *Curr Opin Hematol.* 1998;5(1):16-21.
57. Botelho RJ, Teruel M, Dierckman R, et al. Localized biphasic changes in phosphatidylinositol-4, 5-bisphosphate at sites of phagocytosis. *J Cell Biol.*

References

- 2000;151(7):1353-1368.
58. Greenberg S, Grinstein S. Phagocytosis and innate immunity. *Curr Opin Immunol*. 2002;14(1):136-145.
 59. Caron E, Hall A. Identification of two distinct mechanisms of phagocytosis controlled by different Rho GTPases. *Science* (80-). 1998;282(5394):1717-1721.
 60. Cox D, Berg JS, Cammer M, et al. Myosin X is a downstream effector of PI (3) K during phagocytosis. *Nat Cell Biol*. 2002;4(7):469-477.
 61. Korchak HM, Rossi MW, Kilpatrick LE. Selective role for β -protein kinase C in signaling for O⁻ 2 generation but not degranulation or adherence in differentiated HL60 cells. *J Biol Chem*. 1998;273(42):27292-27299.
 62. Möhn H, Le Cabec V, Fischer S, Maridonneau-Parini I. The src-family protein-tyrosine kinase p59hck is located on the secretory granules in human neutrophils and translocates towards the phagosome during cell activation. *Biochem J*. 1995;309(2):657-665.
 63. Branzk N, Papayannopoulos V. Molecular mechanisms regulating NETosis in infection and disease. *Semin Immunopathol*. 2013;35(4):513-530. doi:10.1007/s00281-013-0384-6
 64. Neubert E, Meyer D, Rocca F, et al. Chromatin swelling drives neutrophil extracellular trap release. *Nat Commun*. 2018;9(1):3767. doi:10.1038/s41467-018-06263-5
 65. Yipp BG, Kubes P. NETosis: how vital is it? *Blood*. 2013;122(16):2784-2794. doi:10.1182/blood-2013-04-457671
 66. Berthelot J-M, Le Goff B, Neel A, Maugars Y, Hamidou M. NETosis: at the crossroads of rheumatoid arthritis, lupus, and vasculitis. *Jt Bone Spine*. 2017;84(3):255-262.
 67. Jurk K, Kehrel BE. Platelets: physiology and biochemistry. In: *Seminars in Thrombosis and Hemostasis*. Vol 31. New York: Stratton Intercontinental Medical Book Corporation, c1974-; 2005:381-392.
 68. Fiusa MML, Carvalho-Filho MA, Annichino-Bizzacchi JM, De Paula E V. Causes and consequences of coagulation activation in sepsis: an evolutionary medicine perspective. *BMC Med*. 2015;13(1):1-9.
 69. Alcock J, Brainard AH. Hemostatic containment—An evolutionary hypothesis of injury by innate immune cells. *Med Hypotheses*. 2008;71(6):960-968.
 70. Jenne CN, Urrutia R, Kubes P. Platelets: bridging hemostasis, inflammation, and immunity. *Int J Lab Hematol*. 2013;35(3):254-261.
 71. Li JL, Zarbock A, Hidalgo A. Platelets as autonomous drones for hemostatic and immune surveillance. *J Exp Med*. 2017;214(8):2193-2204.
 72. Rivera J, Lozano ML, Navarro-Núñez L, Vicente V. Platelet receptors and

References

- signaling in the dynamics of thrombus formation. *Haematologica*. 2009;94(5):700.
73. Thon JN, Italiano JE. Platelets: Production, Morphology and Ultrastructure BT - Antiplatelet Agents. In: Gresele P, Born GVR, Patrono C, Page CP, eds. Berlin, Heidelberg: Springer Berlin Heidelberg; 2012:3-22. doi:10.1007/978-3-642-29423-5_1
74. Jones OP. Origin of megakaryocyte granules from Golgi vesicles. *Anat Rec*. 1960;138(2):105-113.
75. Lesurtel M, Graf R, Aleil B, et al. Platelet-Derived Serotonin Mediates Liver Regeneration. *Science (80-)*. 2006;312(5770):104-107. doi:10.1126/science.1123842
76. Savage B, Almus-Jacobs F, Ruggeri ZM. Specific synergy of multiple substrate–receptor interactions in platelet thrombus formation under flow. *Cell*. 1998;94(5):657-666.
77. Coenen DM, Mastenbroek TG, Cosemans JMEM. Platelet interaction with activated endothelium: mechanistic insights from microfluidics. *Blood*. 2017;130(26):2819-2828. doi:10.1182/blood-2017-04-780825
78. Duerschmied D, Suidan GL, Demers M, et al. Platelet serotonin promotes the recruitment of neutrophils to sites of acute inflammation in mice. *Blood*. 2013;121(6):1008 LP - 1015. doi:10.1182/blood-2012-06-437392
79. Parise L V, Smyth SS, Collier BS. Platelet morphology, biochemistry and function. *Williams Hematol*. 2001;7:1597-1645.
80. Zucoloto AZ, Jenne CN. Platelet-neutrophil interplay: insights into neutrophil extracellular trap (NET)-driven coagulation in infection. *Front Cardiovasc Med*. 2019;6:85.
81. Zarbock A, Polanowska-Grabowska RK, Ley K. Platelet-neutrophil-interactions: Linking hemostasis and inflammation. *Blood Rev*. 2007;21(2):99-111. doi:https://doi.org/10.1016/j.blre.2006.06.001
82. Grommes J, Alard J-E, Drechsler M, et al. Disruption of platelet-derived chemokine heteromers prevents neutrophil extravasation in acute lung injury. *Am J Respir Crit Care Med*. 2012;185(6):628-636.
83. Fuchs TA, Brill A, Duerschmied D, et al. Extracellular DNA traps promote thrombosis. *Proc Natl Acad Sci*. 2010;107(36):15880-15885.
84. McDonald B, Davis RP, Kim S-J, et al. Platelets and neutrophil extracellular traps collaborate to promote intravascular coagulation during sepsis in mice. *Blood, J Am Soc Hematol*. 2017;129(10):1357-1367.
85. Semeraro F, Ammollo CT, Morrissey JH, et al. Extracellular histones promote thrombin generation through platelet-dependent mechanisms: involvement of platelet TLR2 and TLR4. *Blood, J Am Soc Hematol*. 2011;118(7):1952-1961.

References

86. Jacobs BL, Azmitia EC. Structure and function of the brain serotonin system. *Physiol Rev.* 1992;72(1):165-229.
87. Lucki I. The spectrum of behaviors influenced by serotonin. *Biol Psychiatry.* 1998;44(3):151-162. doi:10.1016/S0006-3223(98)00139-5
88. Gershon MD, Tack J. The Serotonin Signaling System: From Basic Understanding To Drug Development for Functional GI Disorders. *Gastroenterology.* 2007;132(1):397-414. doi:https://doi.org/10.1053/j.gastro.2006.11.002
89. Darmon MC, Guibert B, Levieil V, Ehret M, Maitre M, Mallet J. Sequence of two mRNAs encoding active rat tryptophan hydroxylase. *J Neurochem.* 1988;51(1):312-316.
90. Walther DJ, Peter J-U, Bashammakh S, et al. Synthesis of serotonin by a second tryptophan hydroxylase isoform. *Science (80-).* 2003;299(5603):76.
91. Cesura AM, Bertocci B, Da Prada M. Binding of [3H] dihydrotetrabenazine and [125I] azidoiodoketanserin photoaffinity labeling of the monoamine transporter of platelet 5-HT organelles. *Eur J Pharmacol.* 1990;186(1):95-104.
92. Weihe E, Schäfer MK-H, Erickson JD, Eiden LE. Localization of vesicular monoamine transporter isoforms (VMAT1 and VMAT2) to endocrine cells and neurons in rat. *J Mol Neurosci.* 1994;5(3):149-164.
93. Barnes NM, Sharp T. A review of central 5-HT receptors and their function. *Neuropharmacology.* 1999;38(8):1083-1152. doi:https://doi.org/10.1016/S0028-3908(99)00010-6
94. Stefulj J, Jernej B, Cicin-Sain L, Rinner I, Schauenstein K. mRNA Expression of Serotonin Receptors in Cells of the Immune Tissues of the Rat. *Brain Behav Immun.* 2000;14(3):219-224. doi:https://doi.org/10.1006/brbi.1999.0579
95. Schoeffter P, Ullmer C, Bobirnac I, Gabbiani G, Lübbert H. Functional, endogenously expressed 5-hydroxytryptamine 5-HT₇ receptors in human vascular smooth muscle cells. 1996.
96. Ullmer C, Schmuck K, Kalkman HO, Lübbert H. Expression of serotonin receptor mRNAs in blood vessels. *FEBS Lett.* 1995;370(3):215-221.
97. Mammadova-Bach E, Mauler M, Braun A, Duerschmied D. Autocrine and paracrine regulatory functions of platelet serotonin. *Platelets.* 2018;29(6):541-548. doi:10.1080/09537104.2018.1478072
98. Mammadova-Bach, E., P. Mangin, F. Lanza and FG. Platelets in cancer. *Hamostaseologie.* 2015;35(04):325-336.
99. Pakala R, Willerson JT, Benedict CR. Mitogenic effect of serotonin on vascular endothelial cells. *Circulation.* 1994;90(4):1919-1926. doi:10.1161/01.CIR.90.4.1919
100. Frishman WH, Grewall P. Serotonin and the heart. *Ann Med.* 2000;32(3):195-209.

References

doi:10.3109/07853890008998827

101. Yicong L, Coedy H, Anthonya C, Asli A. Sepsis-induced elevation in plasma serotonin facilitates endothelial hyperpermeability. *Sci Rep.* 9 (6)(2016) 22747.
102. Dees C, Akhmetshina A, Zerr P, et al. Platelet-derived serotonin links vascular disease and tissue fibrosis. *J Exp Med.* 2011;208(5):961-972.
doi:10.1084/jem.20101629
103. Mauler M, Herr N, Schoenichen C, et al. Platelet serotonin aggravates myocardial ischemia/reperfusion injury via neutrophil degranulation. *Circulation.* 2019;139(7):918-931.
104. Sauer WH, Berlin JA, Kimmel SE. Effect of antidepressants and their relative affinity for the serotonin transporter on the risk of myocardial infarction. *Circulation.* 2003;108(1):32-36.
105. Levite M. Dopamine in the Immune System: Dopamine Receptors in Immune Cells, Potent Effects, Endogenous Production and Involvement in Immune and Neuropsychiatric Diseases BT - Nerve-Driven Immunity: Neurotransmitters and Neuropeptides in the Immune System. In: Levite M, ed. Vienna: Springer Vienna; 2012:1-45. doi:10.1007/978-3-7091-0888-8_1
106. McKenna F, McLaughlin PJ, Lewis BJ, et al. Dopamine receptor expression on human T-and B-lymphocytes, monocytes, neutrophils, eosinophils and NK cells: a flow cytometric study. *J Neuroimmunol.* 2002;132(1-2):34-40.
107. Martel JC, Gatti McArthur S. Dopamine Receptor Subtypes, Physiology and Pharmacology: New Ligands and Concepts in Schizophrenia . *Front Pharmacol* . 2020;11:1003. <https://www.frontiersin.org/article/10.3389/fphar.2020.01003>.
108. Calderon TM, Williams DW, Lopez L, et al. Dopamine Increases CD14+CD16+ Monocyte Transmigration across the Blood Brain Barrier: Implications for Substance Abuse and HIV Neuropathogenesis. *J Neuroimmune Pharmacol.* 2017;12(2):353-370. doi:10.1007/s11481-017-9726-9
109. dos-Santos-Pereira M, Acuña L, Hamadat S, et al. Microglial glutamate release evoked by α -synuclein aggregates is prevented by dopamine. *Glia.* 2018;66(11):2353-2365.
110. Fan Y, Chen Z, Pathak JL, Carneiro A, Chung CY. Differential regulation of adhesion and phagocytosis of resting and activated microglia by dopamine. *Front Cell Neurosci.* 2018;12:309.
111. Gaskill PJ, Yano HH, Kalpana G V, Javitch JA, Berman JW. Dopamine receptor activation increases HIV entry into primary human macrophages. *PLoS One.* 2014;9(9):e108232.
112. Kawano M, Takagi R, Saika K, Matsui M, Matsushita S. Dopamine regulates cytokine secretion during innate and adaptive immune responses. *Int Immunol.* 2018;30(12):591-606. doi:10.1093/intimm/dxy057

References

113. Levite M. Neurotransmitters activate T-cells and elicit crucial functions via neurotransmitter receptors. *Curr Opin Pharmacol*. 2008;8(4):460-471.
114. Strell C, Sievers A, Bastian P, et al. Divergent effects of norepinephrine, dopamine and substance P on the activation, differentiation and effector functions of human cytotoxic T lymphocytes. *BMC Immunol*. 2009;10(1):1-15.
115. Bergquist J, Ohlsson B, Tarkowski A. Nuclear Factor- κ B is Involved in the Catecholaminergic Suppression of Immunocompetent Cells. *Ann N Y Acad Sci*. 2000;917(1):281-289.
116. Saha B, Mondal AC, Basu S, Dasgupta PS. Circulating dopamine level, in lung carcinoma patients, inhibits proliferation and cytotoxicity of CD4⁺ and CD8⁺ T cells by D1 dopamine receptors: an in vitro analysis. *Int Immunopharmacol*. 2001;1(7):1363-1374.
117. Saha B, Mondal AC, Majumder J, Basu S, Dasgupta PS. Physiological concentrations of dopamine inhibit the proliferation and cytotoxicity of human CD4⁺ and CD8⁺ T cells in vitro: a receptor-mediated mechanism. *Neuroimmunomodulation*. 2001;9(1):23-33.
118. Ghosh MC, Mondal AC, Basu S, et al. Dopamine inhibits cytokine release and expression of tyrosine kinases, Lck and Fyn in activated T cells. *Int Immunopharmacol*. 2003;3(7):1019-1026.
119. Carr L, Tucker A, Fernandez-Botran R. In vivo administration of L-dopa or dopamine decreases the number of splenic IFN γ -producing cells. *J Neuroimmunol*. 2003;137(1-2):87-93.
120. Huang Y, Qiu A-W, Peng Y-P, Liu Y, Huang H-W, Qiu Y-H. Roles of dopamine receptor subtypes in mediating modulation of T lymphocyte function. *Neuroendocrinol Lett*. 2010;31(6):782.
121. Sarkar C, Das S, Chakroborty D, et al. Cutting edge: stimulation of dopamine D4 receptors induce T cell quiescence by up-regulating Krüppel-like factor-2 expression through Inhibition of ERK1/ERK2 phosphorylation. *J Immunol*. 2006;177(11):7525-7529.
122. Bergquist J, Tarkowski A, Ekman R, Ewing A. Discovery of endogenous catecholamines in lymphocytes and evidence for catecholamine regulation of lymphocyte function via an autocrine loop. *Proc Natl Acad Sci*. 1994;91(26):12912-12916. doi:10.1073/pnas.91.26.12912
123. Watanabe Y, Nakayama T, Nagakubo D, et al. Dopamine selectively induces migration and homing of naive CD8⁺ T cells via dopamine receptor D3. *J Immunol*. 2006;176(2):848-856.
124. Cosentino M, Fietta AM, Ferrari M, et al. Human CD4⁺ CD25⁺ regulatory T cells selectively express tyrosine hydroxylase and contain endogenous catecholamines subserving an autocrine/paracrine inhibitory functional loop. *Blood*. 2007;109(2):632-642.

References

125. Besser MJ, Ganor Y, Levite M. Dopamine by itself activates either D2, D3 or D1/D5 dopaminergic receptors in normal human T-cells and triggers the selective secretion of either IL-10, TNF α or both. *J Neuroimmunol*. 2005;169(1):161-171. doi:<https://doi.org/10.1016/j.jneuroim.2005.07.013>
126. Cosentino M, Rasini E, Colombo C, et al. Dopaminergic modulation of oxidative stress and apoptosis in human peripheral blood lymphocytes: evidence for a D1-like receptor-dependent protective effect. *Free Radic Biol Med*. 2004;36(10):1233-1240.
127. Sookhai S, Wang JH, Winter D, Power C, Kirwan W, Redmond HP. Dopamine attenuates the chemoattractant effect of interleukin-8: a novel role in the systemic inflammatory response syndrome. *Shock*. 2000;14(3):295-299. doi:10.1097/00024382-200014030-00009
128. Minguet S, Huber M, Rosenkranz L, Schamel WWA, Reth M, Brummer T. Adenosine and cAMP are potent inhibitors of the NF- κ B pathway downstream of immunoreceptors. *Eur J Immunol*. 2005;35(1):31-41.
129. Ch Beck G, Brinkkoetter P, Hanusch C, et al. Clinical review: Immunomodulatory effects of dopamine in general inflammation. *Crit Care*. 2004;8(6):485. doi:10.1186/cc2879
130. Hayden MS, Ghosh S. Signaling to NF- κ B. *Genes Dev*. 2004;18(18):2195-2224.
131. Josefsson E, Bergquist J, Ekman R, Tarkowski A. Catecholamines are synthesized by mouse lymphocytes and regulate function of these cells by induction of apoptosis. *Immunology*. 1996;88(1):140-146.
132. Bergquist J, Josefsson E, Tarkowski A, Ekman R, Ewing A. Measurements of catecholamine-mediated apoptosis of immunocompetent cells by capillary electrophoresis. *Electrophoresis*. 1997;18(10):1760-1766.
133. Musso NR, Brenci S, Setti M, Indiveri F, Lotti G. Catecholamine content and in vitro catecholamine synthesis in peripheral human lymphocytes. *J Clin Endocrinol Metab*. 1996;81(10):3553-3557.
134. Musso NR, Brenci S, Indiveri F, Lotti G. L-tyrosine and nicotine induce synthesis of L-Dopa and norepinephrine in human lymphocytes. *J Neuroimmunol*. 1997;74(1-2):117-120.
135. Bergquist J, Silberring J. Identification of catecholamines in the immune system by electrospray ionization mass spectrometry. *Rapid Commun mass Spectrom*. 1998;12(11):683-688.
136. Ferrari M, Cosentino M, Marino F, et al. Dopaminergic D1-like receptor-dependent inhibition of tyrosine hydroxylase mRNA expression and catecholamine production in human lymphocytes. *Biochem Pharmacol*. 2004;67(5):865-873.
137. Basu S, Dasgupta PS. Dopamine, a neurotransmitter, influences the immune system. *J Neuroimmunol*. 2000;102(2):113-124.

References

138. Papa I, Saliba D, Ponzoni M, et al. TFH-derived dopamine accelerates productive synapses in germinal centres. *Nature*. 2017;547(7663):318-323. doi:10.1038/nature23013
139. Nakano K, Higashi T, Takagi R, Hashimoto K, Tanaka Y, Matsushita S. Dopamine released by dendritic cells polarizes Th2 differentiation. *Int Immunol*. 2009;21(6):645-654. doi:10.1093/intimm/dxp033
140. Cosentino M, Marino F, Bombelli R, Ferrari M, Lecchini S, Frigo G. Endogenous catecholamine synthesis, metabolism, storage and uptake in human neutrophils. *Life Sci*. 1999;64(11):975-981. doi:https://doi.org/10.1016/S0024-3205(99)00023-5
141. Flierl MA, Rittirsch D, Nadeau BA, et al. Phagocyte-derived catecholamines enhance acute inflammatory injury. *Nature*. 2007;449(7163):721-725. doi:10.1038/nature06185
142. Flierl MA, Rittirsch D, Nadeau BA, et al. Upregulation of phagocyte-derived catecholamines augments the acute inflammatory response. *PLoS One*. 2009;4(2):e4414. doi:10.1371/journal.pone.0004414
143. Manawi YM, Samara A, Al-Ansari T, Atieh MA. A review of carbon nanomaterials' synthesis via the chemical vapor deposition (CVD) method. *Materials (Basel)*. 2018;11(5):822.
144. Boghossian AA, Zhang J, Barone PW, et al. Near-Infrared Fluorescent Sensors based on Single-Walled Carbon Nanotubes for Life Sciences Applications. *ChemSusChem*. 2011;4(7):848.
145. Smith AM, Mancini MC, Nie S. Bioimaging: second window for in vivo imaging. *Nat Nanotechnol*. 2009;4(11):710-711. doi:10.1038/nnano.2009.326
146. Meredith EJ, Chamba A, Holder MJ, Barnes NM, Gordon J. Close encounters of the monoamine kind: immune cells betray their nervous disposition. *Immunology*. 2005;115(3):289-295. doi:https://doi.org/10.1111/j.1365-2567.2005.02166.x
147. Sulzer D, Cragg SJ, Rice ME. Striatal dopamine neurotransmission: Regulation of release and uptake. *Basal Ganglia*. 2016;6(3):123-148. doi:https://doi.org/10.1016/j.baga.2016.02.001
148. Chefer VI, Thompson AC, Zapata A, Shippenberg TS. Overview of brain microdialysis. *Curr Protoc Neurosci*. 2009;Chapter 7:Unit7.1-Unit7.1. doi:10.1002/0471142301.ns0701s47
149. Wilson GS, Johnson MA. In-Vivo Electrochemistry: What Can We Learn about Living Systems? *Chem Rev*. 2008;108(7):2462-2481. doi:10.1021/cr068082i
150. Zhang J, Landry MP, Barone PW, et al. Molecular recognition using corona phase complexes made of synthetic polymers adsorbed on carbon nanotubes. *Nat Nanotechnol*. 2013;8(12):959-968. doi:10.1038/nnano.2013.236
151. Nakatsuka N, Yang KA, Abendroth JM, et al. Aptamer-field-effect transistors

References

- overcome Debye length limitations for small-molecule sensing. *Science* (80-). 2018;362(6412):319-324. doi:10.1126/science.aao675
152. Meyer D, Hagemann A, Kruss S. Kinetic Requirements for Spatiotemporal Chemical Imaging with Fluorescent Nanosensors. *ACS Nano*. 2017;11(4):4017-4027. doi:10.1021/acsnano.7b00569
153. Mann FA, Herrmann N, Meyer D, Kruss S. Tuning selectivity of fluorescent carbon nanotube-based neurotransmitter sensors. *Sensors (Switzerland)*. 2017;17(7):1521. doi:10.3390/s17071521
154. Bergquist J, Tarkowski A, Ewing A, Ekman R. Catecholaminergic suppression of immunocompetent cells. *Immunol Today*. 1998;19(12):562-567. doi:https://doi.org/10.1016/S0167-5699(98)01367-X
155. Kruss S, Landry MP, Vander Ende E, et al. Neurotransmitter detection using corona phase molecular recognition on fluorescent single-walled carbon nanotube sensors. *J Am Chem Soc*. 2014;136(2):713-724. doi:10.1021/ja410433b
156. Nißler R, Mann FA, Chaturvedi P, et al. Quantification of the Number of Adsorbed DNA Molecules on Single-Walled Carbon Nanotubes. *J Phys Chem C*. 2019;123(8):4837-4847. doi:10.1021/acs.jpcc.8b11058
157. Kruss S, Salem DP, Vuković L, et al. High-resolution imaging of cellular dopamine efflux using a fluorescent nanosensor array. *Proc Natl Acad Sci* . 2017;114(8):1789-1794. doi:10.1073/pnas.1613541114
158. Polo E, Kruss S. Impact of Redox-Active Molecules on the Fluorescence of Polymer-Wrapped Carbon Nanotubes. *J Phys Chem C*. 2016;120(5):3061-3070. doi:10.1021/acs.jpcc.5b12183
159. Pereira DB, Schmitz Y, Mészáros J, et al. Fluorescent false neurotransmitter reveals functionally silent dopamine vesicle clusters in the striatum. *Nat Neurosci*. 2016;19(4):578-586. doi:10.1038/nn.4252
160. Ge S, Woo E, Haynes CL. Quantal regulation and exocytosis of platelet dense-body granules. *Biophys J*. 2011;101(10):2351-2359.
161. Rendu F, Brohard-Bohn B. The platelet release reaction: granules' constituents, secretion and functions. *Platelets*. 2001;12(5):261-273.
162. Anlauf M, Schäfer MK-H, Schwark T, et al. Vesicular Monoamine Transporter 2 (VMAT2) Expression in Hematopoietic Cells and in Patients with Systemic Mastocytosis. *J Histochem Cytochem*. 2006;54(2):201-213. doi:10.1369/jhc.5A6739.2005
163. Cloutier N, Allaeys I, Marcoux G, et al. Platelets release pathogenic serotonin and return to circulation after immune complex-mediated sequestration. *Proc Natl Acad Sci*. 2018;115(7):E1550 LP-E1559. doi:10.1073/pnas.1720553115
164. Boneberg E-M, von Seydlitz E, Pröpster K, Watzl H, Rockstroh B, Illges H. D3 dopamine receptor mRNA is elevated in T cells of schizophrenic patients whereas

References

- D4 dopamine receptor mRNA is reduced in CD4⁺-T cells. *J Neuroimmunol.* 2006;173(1):180-187. doi:<https://doi.org/10.1016/j.jneuroim.2005.11.018>
165. Chen M-L, Wu S, Tsai T-C, Wang L-K, Tsai F-M. Regulation of neutrophil phagocytosis of *Escherichia coli* by antipsychotic drugs. *Int Immunopharmacol.* 2014;23(2):550-557. doi:<https://doi.org/10.1016/j.intimp.2014.09.030>
166. Pereira A, McLaren A, Bell WR, Copolov D, Dean B. Potential clozapine target sites on peripheral hematopoietic cells and stromal cells of the bone marrow. *Pharmacogenomics J.* 2003;3(4):227-234. doi:10.1038/sj.tpj.6500179
167. Xie X, Shi Q, Wu P, et al. Single-cell transcriptome profiling reveals neutrophil heterogeneity in homeostasis and infection. *Nat Immunol.* 2020;21(9):1119-1133. doi:10.1038/s41590-020-0736-z
168. Wang Q, Doerschuk CM. The signaling pathways induced by neutrophil-endothelial cell adhesion. *Antioxidants Redox Signal.* 2002;4(1):39-47.
169. Zilionis R, Engblom C, Pfirschke C, et al. Single-cell transcriptomics of human and mouse lung cancers reveals conserved myeloid populations across individuals and species. *Immunity.* 2019;50(5):1317-1334.
170. Papa I, Saliba D, Ponzoni M, et al. TFH-derived dopamine accelerates productive synapses in germinal centres. *Nature.* 2017;547(7663):318-323. doi:10.1038/nature23013

Acknowledgement

Since I started my PhD in May 2018, I've been surrounded with great people and lots of support. Special thanks to my supervisor Prof. Dr. Sebastian Kruss for his support and invaluable mentorship. Thank you for trusting me with this exciting project and giving me the opportunity to work in your lab! I'd like to acknowledge my great friends and colleagues; Elsa Neubert, Florian Mann, Daniel Meyer, Robert Nißler, Gabriele Selvaggio, Alexander Spreinat and Niklas Hermann, for their support in every step of the way.

Thanks to Prof. Claudia Steinem, Prof. Andreas Janshoff and Dr Tabea Oswald and their working groups for constant advice and support during my studies. I'd like to thank our collaborating partners that made this project possible. Special thanks go to; Sofia Elizarova from the group of Prof. Brose. Prof. Ivan Bogeski and his lab members for advice and support. Prof. Josef Huston and Benedetta Fazari for immense and invaluable cooperation. I would like to acknowledge our close collaborators Dr. Luise Erpenbeck and her group. Without their collaboration this project wouldn't have been realized.

I'm extremely grateful to my thesis advisory committee members Prof. Jörg Enderlein and Prof. Nils Brose because of their support and insightful advice throughout my PhD project. Thank you for always finding time for my meetings despite having a very busy schedule! I also appreciate my examination board members Prof. Dr. Outeiro, Prof. Dr. Betz and Prof. Dr. Rizzoli for taking the time from their busy schedule to review and evaluate my dissertation.

Finally, and above all, to my parents Prof. Atyabi and Prof. Dinarvand; you have my deepest gratitude and most sincere appreciation for always being there for me. I'm beholden to you for this achievement and every other achievement in my life. My amazing brother and best friend, my family and my best friends who were with me through thick and thin, thank you from the bottom of my heart!

تقدیم به مادرم، پدرم و برادرم

مرگ بادا بی‌شما و جان مبادا بی‌شما

گلبن جان‌های ما خندان مبادا بی‌شما

درد ما در جهان درمان مبادا بی‌شما

سینه‌های عاشقان جز از شما روشن مباد